European air quality maps of PM and ozone for 2011 and their uncertainty

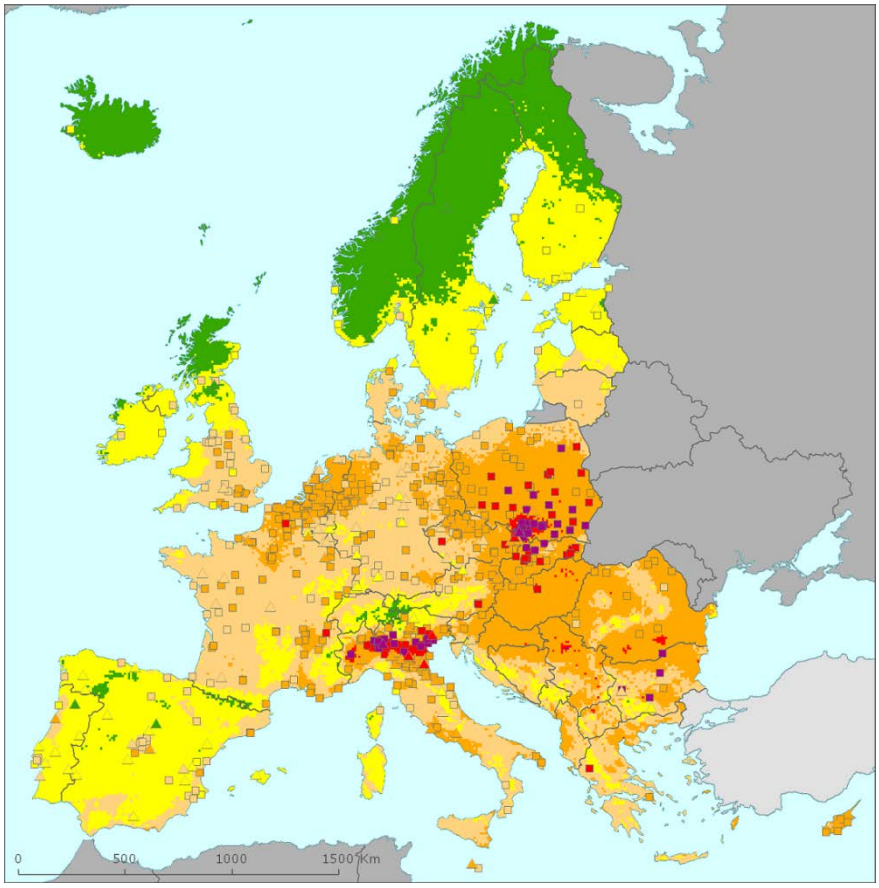

ETC/ACM Technical Paper 2013/13
December 2013

Jan Horálek, Peter de Smet, Pavel Kurfürst,
Frank de Leeuw, Nina Benešová

European Topic Centre
on Air Pollution and
Climate Change Mitigation

The European Topic Centre on Air Pollution and Climate Change Mitigation (ETC/ACM)
is a consortium of European institutes under contract of the European Environment Agency
RIVM UBA-V ÖKO AEAT EMISIA CHMI NILU INERIS PBL CSIC

Front-page picture:
Annual mean PM2.5 concentration in µg.m^{-3} for both rural and urban areas, combined into one final map for the year 2011.Its target value is 25 µg.m^{-3}. (Figure 5.1 of this paper.)

Author affiliation:
Jan Horálek, Pavel Kurfürst, Nina Benešová: Czech Hydrometeorological Institute (CHMI), Prague, Czech Republic
Peter de Smet, Frank de Leeuw: National Institute for Public Health and the Environment (RIVM), Bilthoven, The Netherlands

Refer to this document as:
Horálek J, De Smet P, Kurfürst P, De Leeuw F, Benešová N (2014). European air quality maps of PM and ozone for 2011 and their uncertainty. ETC/ACM Technical paper 2013/13 http://acm.eionet.europa.eu/reports/ETCACM_TP_2013_13_spatAQmaps_2011

DISCLAIMER

ETC/ACM Technical Paper 2013/13
European Topic Centre on Air and Climate Change Mitigation
PO Box 303
3720 AH Bilthoven
The Netherlands
Phone +31 30 2743562
Fax +31 30 2744433
Email etcacm@rivm.nl
Website http://acm.eionet.europa.eu

Contents

1 Introduction

This paper provides an update of European air quality concentrations, probabilities of exceeding relevant thresholds and population exposure estimates for another consecutive year, 2011. The analysis is based on interpolation of annual statistics of observational data from 2011, reported by EEA member and cooperating countries in 2012. The paper presents mapping results and includes an uncertainty analysis of the interpolated maps, adopting the latest methodological developments of Horálek et al. (2007, 2008, 2010, 2013) and De Smet et al. (2009, 2010, 2011, 2012).

We again consider in this paper PM_{10} and ozone as being the most relevant pollutants for annual updating. Additionally and for the second time, $PM_{2.5}$ is presented as a third important policy-relevant pollutant and health-impact indicator based on the mapping methodology developed by Denby et al. (2011b, 2011c).

The analysis method for the year 2011 was similar to that for the year 2010 and 2009. In this paper, we summarise the updates applied to the 2011 data.

The mapping method used is a linear regression model followed by kriging of the residuals produced from that model (residual kriging). In the linear regression model, the measured data are taken as a dependent variable, while a dispersion model's output and other supplementary data (altitude, meteorology) as independent variables.

The maps of health related indicators of PM_{10}, $PM_{2.5}$ and ozone are created for the rural and urban background areas separately on a grid at 10x10 km resolution. Subsequently to this, the rural and urban background maps are merged into one combined air quality indicator map using a population density grid at 1x1 km resolution. For presentational purposes at the European scale, the final merged maps at 1x1 km grid resolution are aggregated into maps at 10x10 km grid resolution. The maps of vegetation related ozone indicators are created on a grid at 2x2 km resolution, based on rural background measurements.

Next to the annual indicator maps, we present in tables the population exposure to PM_{10}, $PM_{2.5}$ and ozone and the exposure of vegetation to ozone. Tables of population exposure are prepared using combined final maps and the population density map of 1x1 km grid resolution. The tables of the exposure of vegetation are prepared with a 2x2 km grid resolution based on the Corine Land Cover 2006 (CLC2006), which is an update of the 2000 version, and primarily attributable to this update delivering less than one per cent difference in the exposure of vegetation.

For all the maps, we include a quantitative estimate of their interpolation uncertainty, using cross-validation parameters and scatter-plots. In addition, the paper contains the maps with probability estimates of limit/target value exceedances.

Chapter 2 describes briefly the used methodology. Chapter 3 documents the updated input data. Chapters 4, 5 and 6 present the calculations, the mapping, the exposure estimates and the uncertainty results for PM_{10}, $PM_{2.5}$ and ozone respectively. Chapter 7 summarizes the conclusions on exposure estimates and their interpolation uncertainties involved with the interpolated mapping of the air pollutant indicators.

2 Used methodology

2.1 Mapping method

Previous technical papers prepared by the ETC/ACM, resp. ETC/ACC (Technical Papers 2012/12, 2011/11, 2011/5, 2010/10, 2010/9, 2009/16, 2009/9, 2008/8, 2007/7, 2006/6, 2005/8 and 2005/7) discuss methodological developments and details on spatial interpolations and their uncertainties. No changes took place in the methodology in comparison with the three preceding reports (Horálek et al., 2013, De Smet et al., 2011, 2012), respectively with the $PM_{2.5}$ mapping methodology paper (Denby et al., 2011c). In this chapter a summary on the currently applied methods is given.

2.1.1 Pseudo $PM_{2.5}$ station data estimation

To supplement measured $PM_{2.5}$ data, in the mapping procedure we also use data from so-called *pseudo $PM_{2.5}$ stations.* These data are the estimates of $PM_{2.5}$ concentrations at the locations of PM_{10} stations with no $PM_{2.5}$ measurement. These estimates are based on measured PM_{10} data and different supplementary data, using linear regression:

$$\hat{Z}_{PM2.5}(s) = c + b.Z_{PM10}(s) + a_1.X_1(s) + ... + a_n.X_n(s) + \varepsilon(s) \quad (2.1)$$

where $\hat{Z}_{PM2.5}(s)$ is the estimated value of $PM_{2.5}$ at the station *s*,

$Z_{PM10}(s)$ is the measured value of PM_{10} at the station *s*,

$X_1(s),\ldots, X_n(s)$ are the values of other supplementary variables at the station *s*,

$c, b, a_1,,\ldots, a_n$ are the parameters of the linear regression model calculated based on the data at the points of measuring stations with both $PM_{2.5}$ and PM_{10} measurements,

n is the number of other supplementary variables used in the linear regression model (apart from PM_{10}).

When applying this estimation method, rural and urban/suburban background stations are handled together. For details, see Denby et al. (2011c).

2.1.2 Interpolation

The mapping method used is a linear regression model followed by kriging of the residuals produced from that model (residual kriging). Interpolation is therefore carried out according to the relation:

$$\hat{Z}(s_0) = c + a_1.X_1(s_0) + a_2.X_2(s_0) + ... + a_n.X_n(s_0) + \eta(s_0) \quad (2.2)$$

where $\hat{Z}(s_0)$ is the estimated value of the air pollution indicator at the point s_o,

$X_1(s_0), X_2(s_0),\ldots, X_n(s_0)$ are the *n* number of individual supplementary variables at the point s_o

$c, a_1, a_2,,\ldots, a_n$ are the *n+1* parameters of the linear regression model calculated based on the data at the points of measurement,

$\eta(s_0)$ is the spatial interpolation of the residuals of the linear regression model at the point s_o calculated based on the residuals at the points of measurement.

For different pollutants and area types (rural, urban), different supplementary data are used, depending on their improvement to the fit of the regression. Ordinary kriging is used to interpolate the residuals:

$$\hat{R}(s_0) = \sum_{i=1}^{N} \lambda_i R(s_i), \ \sum_{i=1}^{N} \lambda_i = 1, \quad (2.3)$$

where $R(s_i)$ are the residuals in the points of the measuring stations s_i,

$\lambda_1, \ldots, \lambda_N$ are the weights estimated based on variogram,

N is the number of the stations used in the interpolation.

The variogram (as a measure of a spatial correlation) is estimated using a spherical function (with parameters *nugget, sill, range*). For details, see Horálek et al. (2007), Section 2.3.5 and Cressie (1993).

For $PM_{2.5}$, both measured data and the estimated data from the pseudo $PM_{2.5}$ stations are used.

For the PM_{10} and $PM_{2.5}$ indicators we apply, prior to linear regression and interpolation, a logarithmic transformation to measurement and EMEP model concentrations. In the case of $PM_{2.5}$ rural map creation, population is also log-transformed. After interpolation, we apply a back-transformation. For details, see De Smet et al. (2011) and Denby et al. (2008). In the case of urban $PM_{2.5}$ map, we do not use any supplementary data – we apply just lognormal kriging.

For the vegetation related indicators (AOT40 for crops and forests) we only construct rural maps based on rural background stations, based on the assumption that no vegetation is located in urban areas. For the health related indicators, we construct the rural and urban background maps separately and then we merge them.

2.1.3 Merging of rural and urban background maps

Health related indicator maps are constructed (using linear regression with kriging of its residuals) for the rural and urban areas separately on a grid at 10x10 km resolution. The rural map is based on rural background stations and the urban map on urban and suburban background stations. Subsequent to this, the rural and urban background maps are merged into one combined air quality indicator map using a European-wide population density grid at 1x1 km resolution. For the 1x1 km grid cells with a population density less than a defined value of α_1, we select the rural map value and for grid cells with a population density greater than a defined value α_2, we select the urban map value. For areas with population density within the interval (α_1, α_2) a weighting function of α_1 and α_2 is applied (for details and the setting of the parameters α_1 and α_2, see Horálek et al., 2010, 2007 and 2005). This applies to the grid cells where the estimated rural value is lower in the case of PM_{10} and $PM_{2.5}$ or higher in the case of ozone, than the estimated urban map value. In the minor areas with grid values for which this criterion does not hold, we apply a joint urban/rural map (created using all background stations regardless their type), as far as its value lies in between the rural and urban map value. For details, see De Smet et al. (2011).

Summarising, the separate rural, urban and joint urban/rural maps are constructed at a resolution of 10x10 km; their merging however takes place on basis of the 1x1 km resolution population density grid, resulting in a final combined pollutant indicator map on this 1x1 km resolution grid. This map is used for the population exposure estimates. At times we specify the applied chain of optimised combinations of spatial resolutions, the process of *interpolation -> merging -> exposure estimate*, as the '10-1-1' (in km). For presentational purposes of European map illustrations, a spatial aggregation to 10x10 km resolution is sufficient and as such applied in this paper.

In all calculations and map presentations the EEA standard projection and datum defined as EEA ETRS89-LAEA5210 is used. The interpolation and mapping domain consists of the areas of all EEA member and cooperating countries, as far as they fall into the EEA map extent *Map_1c* (EEA, 2011).

For further details and discussion on subjects briefly addressed in this section, refer to De Smet et al. (2011), chapter 2.

2.2 Calculation of population and vegetation exposure

Population and vegetation exposure estimates are based on the interpolated concentration maps, population density data and land cover data.

2.2.1 Population exposure

Population exposure for individual countries and for Europe as a whole is calculated from the air quality maps and population density data, both at 1x1 km resolution. For each concentration class, the total population per country as well as the European-wide total is determined. In addition, we express per-country and European-wide exposure as the population-weighted concentration, i.e. the average concentration weighted according to the population in a grid cell:

$$\hat{c} = \frac{\sum_{i=1}^{N} c_i p_i}{\sum_{i=1}^{N} p_i} \tag{2.4}$$

where $\hat{c}$ is the population-weighted average concentration in the country or in the whole Europe,
p_i is the population in the i^{th} grid cell,
c_i is the concentration in the i^{th} grid cell,
N is the number of grid cells in the country or in Europe as a whole.

2.2.2 Vegetation exposure

Vegetation exposure for individual countries and for Europe as a whole is calculated based on the air quality maps and land cover data, both in 2x2 km grid resolution. For each concentration class, the total vegetation area per country as well as European-wide is determined.

2.3 Methods for uncertainty analysis

The uncertainty estimation of the European map is based on cross-validation. The cross-validation method computes the quality of the spatial interpolation for each measurement point from all available information except from the point in question, i.e. it withholds one data point and then makes a prediction at the spatial location of that point. This procedure is repeated for all measurement points in the available set. The predicted and measured values at these points are plotted in the form of a scatter plot. With help of statistical indicators the quality of the predictions is demonstrated objectively. The advantage of the nature of this cross-validation technique is that it enables evaluation of the quality of the predicted values at locations without measurements, as long as they are within the area covered by the measurements.

In addition, we make a simple comparison between the point measurements and interpolated values of the 10x10 km grid (or the 2x2 km grid in the case of AOT40). Where the 10x10 km grid is used, the grid value is the averaged result of the 1x1 km interpolations in each 10 x 10 km grid area. The interpolated value within a grid cell will only approximate the predicted value(s) at the station(s) lying within that cell.

Another method to estimate uncertainties is based on geostatistical theory: together with the prediction, the prediction standard error is computed at all the grid cells, which represents in fact the interpolation uncertainty map (see Cressie, 1993 for a detailed discussion). Based on the concentration and the uncertainty map, the exceedance probability map is created (Section 2.3.3).

2.3.1 Cross-validation

The results of cross-validation are described by the statistical indicators and scatter plots. The main indicator used is root mean squared error (RMSE) and additional is bias or the mean prediction error (MPE):

$$RMSE = \sqrt{\frac{1}{N}\sum_{i=1}^{N}(\hat{Z}(s_i) - Z(s_i))^2} \tag{2.5}$$

$$bias(MPE) = \frac{1}{N}\sum_{i=1}^{N}(\hat{Z}(s_i) - Z(s_i)) \tag{2.6}$$

where $Z(s_i)$ is the measured concentration at the i^{th} point, $i = 1, \ldots, N$,
$\hat{Z}(s_i)$ is the estimated concentration at the i^{th} point using other information, without the measured concentration at the i^{th} point,
N is the number of the measuring points.

RMSE should be as small as possible, bias (MPE) should be as close to zero as possible.

Next to the RMSE expressed in the absolute units, one could express this uncertainty in relative terms by relating the RMSE to the mean air pollution indicator value for all stations:

$$RRMSE = \frac{RMSE}{\overline{Z}}.100 \qquad (2.7)$$

where $RRMSE$ is the relative RMSE, expressed in percents,
$\overline{Z}$ is the arithmetic average of the measured concentrations $Z(s_1), \ldots, Z(s_N)$.

In the cross-validation of $PM_{2.5}$, only stations with measured $PM_{2.5}$ data are used (not the pseudo $PM_{2.5}$ stations).

2.3.2 Comparison of the point measured and interpolated grid values

The comparison of measured and predicted grid values is described by the linear regression equation and its parameters and statistical values. The comparison is executed separately for rural and urban background maps. In the case of $PM_{2.5}$, only the stations with actual measured $PM_{2.5}$ data are used (not the pseudo $PM_{2.5}$ stations).

The point-point cross-validation analysis (Section 2.3.1) describes interpolation performance at point locations when there is no observation (as it follows the leave-one-out approach). In this case the smoothing effect of the interpolation is most prevalent.

The point-grid approach indicates performance of the value for the 10x10 km grid-cell with respect to the observations that are located within that cell. As such, some variability is due to smoothing but it also includes smoothing due to spatial averaging into the 10x10 km cells. Therefore, the point-grid approach tells us how well our interpolated and aggregated values approximate the measurements at the actual stations locations. Whereas, the point-point approach tells us how well our interpolated values estimate the indicator when there are no measurements at a location (under the constrained that it is within the area covered by measurements).

2.3.3 Exceedance probability mapping

The maps with the probability of exceedance (PoE) of a specific threshold value (e.g. limit or target value) are constructed using the concentration and uncertainty maps:

$$PoE(x) = 1 - \Phi\left(\frac{LV - C_c(x)}{\delta_c(x)}\right) \qquad (2.6)$$

where $PoE(x)$ is the probability of limit/target value (LV/TV) exceedance in the grid cell x,
$\Phi(\,)$ is the cumulative distribution function of the normal distribution,
LV is the limit or target value of the relevant indicator,
$C_c(x)$ is the interpolated concentration in the grid cell x,
$\delta_c(x)$ is the standard error of the estimation in the grid cell x.

The standard error of the probability map of the combined (rural and urban background) map is calculated from the standard errors of the separate rural and urban background maps; see Horálek et al. (2008), Section 2.3 and De Smet et al. (2011), Chapter 2. The maps with the probability of threshold value exceedance (PoE) are constructed in 10x10 km grid resolution.

3 Input data

The types of input data in this paper are not different from that of Horálek et al. (2013) and De Smet et al. (2012). The air quality, meteorological and where possible, the supplementary data has been updated. No further changes in selecting and processing of the input data have been implemented. For readability of this paper, we reproduce here the list of the input data. The key data is the air quality measurements at the monitoring stations extracted from AirBase, including geographical coordinates (*latitude*, *longitude*). The supplementary data cover the whole mapping domain and are converted into the EEA reference projection ETRS89-LAEA5210 on a 10x10 km grid resolution. The data for the AOT40 maps, however, we converted – like last year – into a 2x2 km resolution to allow accurate land cover exposure estimates to be prepared for use in Core Set Indicator 005 of the EEA.

3.1 Measured air quality data

Air quality station monitoring data for the relevant year are extracted from the European monitoring database AirBase (Mol et al., 2013). This data set is supplemented by several rural stations from the database EBAS (NILU, 2013) not reported to AirBase. Only data from stations classified by AirBase and/or EBAS of the type *background* for the areas *rural*, *suburban* and *urban* are used. *Industrial* and *traffic* station types are not considered; they represent local scale concentration levels not applicable at the mapping resolution employed. The following substances and their indicators are considered:

PM_{10} – annual average [µg.m^{-3}], year 2011
– 36th highest daily average value [µg.m^{-3}], year 2011

$PM_{2.5}$ – annual average [µg.m^{-3}], year 2011

Ozone – 26th highest daily maximum 8-hour average value [µg.m^{-3}], year 2011
– SOMO35 [µg.m^{-3}.day], year 2011
– AOT40 for crops [µg.m^{-3}.hour], year 2011
– AOT40 for forests [µg.m^{-3}.hour], year 2011

SOMO35 is the annual sum of the differences between maximum daily 8-hour concentrations above 70 µg.m^{-3} (i.e. 35 ppb) and 70 µg.m^{-3}. AOT40 is the sum of the differences between hourly concentrations greater than 80 µg.m^{-3} (i.e. 40 ppb) and 80 µg.m^{-3}, using only observations between 7:00 and 19:00 UTC, calculated over the three months from May to July (AOT40 for crops), respectively over the six months from April to September (AOT40 for forests). Note that the term *vegetation* as used in the ozone directive is not further defined. Comparing the definitions in the Mapping Manual (UNECE, 2004) and those in the ozone directive suggests that we have to interpret the term *vegetation* in the ozone directive as agricultural crops. The exposure of *agricultural crops* has been evaluated here on basis of the AOT40 for vegetation as defined in the ozone directive.

For the indicators relevant to human health (i.e. PM_{10}, $PM_{2.5}$ and for ozone the 26th highest daily maximum 8-hour average and SOMO35) data from *rural*, *urban* and *suburban background* stations are considered. For the indicators relevant to vegetation damage (both AOT40 parameters for ozone) only *rural background* stations are considered.

Only the stations with annual data coverage of at least 75 percent are used. We excluded the stations from French overseas areas (departments), Svalbard, Azores, Madeira and Canary Islands, and also eastern Turkey (which is outside the EEA map extent *Map_1c* (EEA, 2011)). These areas we excluded from the interpolation and mapping domain. To reach a more extended spatial coverage by measurement data we use, in addition to the AirBase data, two additional rural background PM_{10} stations from the EBAS database (NILU, 2013). Table 3.1 shows the number of the measurement stations selected for the individual pollutants and their respective indicators. Compared to 2010, the number of stations selected for 2011 remained approximately the same for PM_{10}, while for $PM_{2.5}$ the number of the stations increased by approximately 16 %, both for rural and urban/suburban background stations. For ozone, the number of the stations increased by approximately 2-3 %, both for rural and urban/suburban background stations.

Table 3.1 Number of stations selected for individual indicators and areas – rural background stations used for rural areas, urban and suburban background stations used for urban areas.

	PM_{10}		$PM_{2.5}$	ozone			
	annual average	36th daily maximum	annual average	26th highest daily max. 8h	SOMO35	AOT40 for crops	AOT40 for forests
rural	331	325	135	509	509	522	519
urban	1126	1121	452	1015	1015		

For $PM_{2.5}$ mapping an additional 212 rural background and 763 urban/suburban background PM_{10} stations (in the places with no $PM_{2.5}$ measurement) were also used for the purpose of calculating the pseudo $PM_{2.5}$ station data.

Due to a lack of rural stations in Turkey for PM_{10}, $PM_{2.5}$ and ozone no proper interpolation results could be presented for this country in a rural map for all the indicators. Therefore, we excluded Turkey also from the production process of the final maps of this paper.

3.2 EMEP MSC-W model output

The chemical dispersion model used was the EMEP MSC-W (formerly called Unified EMEP) model (revision rv4.4), which is an Eulerian model with a resolution of 50x50 km. Information from this model was converted to 10x10 km grid resolution (for health related indicators), resp. into the 2x2 km grid resolution (for vegetation related indicators) for the interpolation process.

As per the previous year, we received the EMEP data in the form of daily means for PM_{10} and $PM_{2.5}$ and hourly means for ozone. We aggregated these primary data according annex B of Mol et al. (2013) to the same set of parameters as we have for the air quality observations:

PM_{10} – annual average [µg.m^{-3}], year 2011 (aggregated from daily values)
– 36th highest daily average value [µg.m^{-3}], year 2011 (aggregated from daily values)

$PM_{2.5}$ – annual average [µg.m^{-3}], year 2011 (aggregated from daily values)

Ozone – 26th highest daily maximum 8-hour average value [µg.m^{-3}], year 2011 (aggregated from hourly values)
– SOMO35 [µg.m^{-3}.day], year 2011 (aggregated from hourly values)
– AOT40 for crops [µg.m^{-3}.hour], year 2011 (aggregated from hourly values)
– AOT40 for forests [µg.m^{-3}.hour], year 2011 (aggregated from hourly values)

Simpson et al. (2012, 2013) and https://wiki.met.no/emep/page1/emepmscw_opensource (web site of Norwegian Meteorological Institute) describe the model in more detail. Emissions for the relevant year (Mareckova et al., 2013) are used and the model is driven by ECMWF meteorology. EMEP (2013) provides details on the EMEP modelling for 2011.

In the original format, a point represents the centre of a grid cell (in 50x50 km resolution). The data are imported into *ArcGIS* as a point shapefile, subsequently converted into a 100x100 m resolution raster grid and spatially aggregated into the reference EEA 10x10 km grid (for health related indicators), resp. into the 2x2 km grid (for vegetation related indicators).

3.3 Altitude

We use the altitude data field (in meters) of GTOPO30 that covers the European continent, with an original grid resolution of 30 x 30 arcseconds. (Source: ESRI, Redlands, California, USA, 2005). The field is converted into a resolution of 200x200 m and spatially aggregated into the reference EEA 10x10 km grid and into the 2x2 km grid. For details, see Horálek et al. (2007).

3.4 Meteorological parameters

Actual meteorological surface layer parameters we extracted from the Meteorological Archival and Retrieval System (MARS) of the ECMWF (European Centre for Medium-range Weather Forecasts). Currently we use the following ECMWF variables (details specified in Horálek et al. 2007, Section 4.5) as supplementary data in the regressions:

Wind speed – annual average [$m.s^{-1}$], year 2011
Surface solar radiation – annual average [$MWs.m^{-2}$], year 2011

The data are imported into *ArcGIS*, subsequently converted into a 100x100 m resolution raster grid and spatially aggregated into the reference EEA 10x10 km grid and into the 2x2 km grid.

3.5 Population density and population totals

Population density (in $inhbs.km^{-2}$, census 2001) is based on JRC data for the majority of countries (JRC, 2009) – source: EEA, pop01clcv5.tif, official version 5, 24 Sep. 2009, resolution 100x100 m.

For countries (Andorra, Albania, Bosnia-Herzegovina, Iceland, Liechtenstein, FYR of Macedonia, Montenegro, Norway, Serbia, Switzerland and Turkey) and regions (Faroe Islands, Jersey, Guernsey, Man and northern part of Cyprus) which are not included in this map we used population density data from an alternative source: ORNL LandScan Global Population Dataset (ORNL, 2008).

The ORNL data is reprojected and converted from its original WGS1984 30x30 arcsec grids into EEA's reference projection ETRS89-LAEA5210 at 1x1 km resolution by EEA (eea_r_3035_1_km_landscan-eurmed_2008, EEA, 2008). The JRC 100x100 m population density data is spatially aggregated into the reference 1x1 km EEA grid; in the areas with the lack of data (see above) it is supplemented with the ORNL data. Thus, the supplemented JRC 1x1 km data covers the entire examined area.

In order to verify the correctness of the merger of JRC and ORNL, we compared ORNL and JRC data for countries covered by both data sources, using the national population totals of the individual countries. Next to this, we compared the national population totals for the JRC gridded data supplemented with the ORNL and the Eurostat national population data for 2011 (Eurostat, 2012). Figure 3.1 presents both these comparisons.

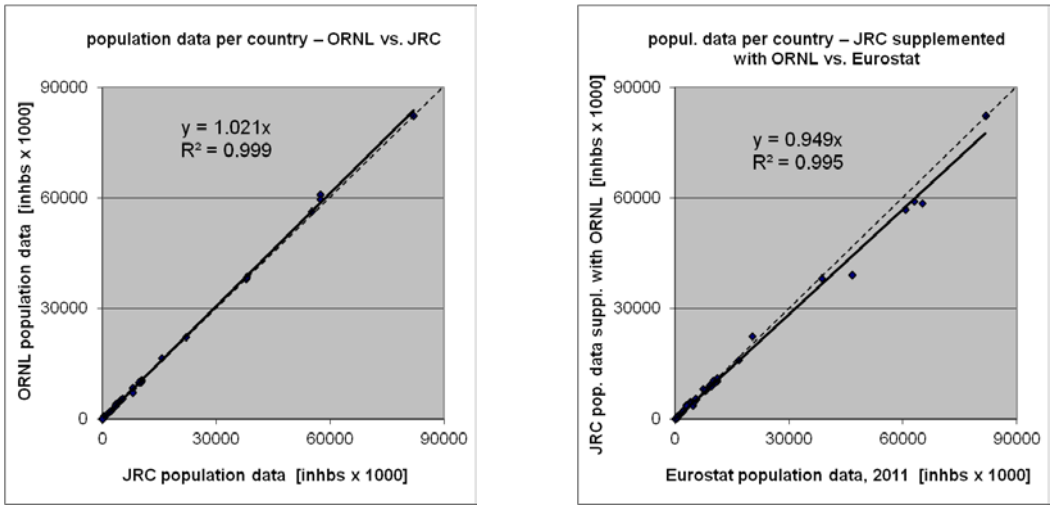

Figure 3.1 Correlation between ORNL (y-axis, left) and JRC (x-axis, left) and between JRC supplemented with ORNL (y-axis, right) and Eurostat 2011 revision (x-axis, right) for national population totals.

From the comparisons, one can see the high correlation of the compared population datasets and the similar level of the JRC and the ORNL population data. Slight underestimation of the supplemented JRC data in comparison with the Eurostat data can be seen, which is caused by the fact

that the Eurostat data is more up-to-date than both JRC and ORNL data. Based on this, the population totals in the report are presented using these actual Eurostat data, see below.

Population density data can be used to classify the spatial distribution of each type of area (rural, urban or mixed population density) in Europe. We use this information to select and weight the air quality value, grid cell by grid cell. Furthermore, we use it to estimate population health exposure and exceedance numbers per country and for Europe as a whole, including involved uncertainties. These activities take place on the 1x1 km resolution grid in accordance with the recommendations of Horálek et al. (2010). The supplemented JRC data (as described above) are used in all the calculations.

Population totals for individual countries presented in exposure tables in Sections 4.1.2, 4.2.2, 5.1.2, 6.1.2 and 6.2.2 are based on Eurostat national population data for 2011 (Eurostat, 2013). For countries (Andorra, Monaco and San Marino) which are not included in the Eurostat database, the population totals are based on UN (2010) for 2010.

3.6 Land cover

CORINE Land Cover 2006 – grid 100 x 100 m, Version 16 (04/2012) is used (CLC2006 – 100m, g100_06.zip; EEA, 2012). The countries missing in this database are Andorra, Greece and Turkey. Greece is missing in the CLC2006 but present in the CLC2000 version that we used in previous mapping years. Therefore, we inserted for Greece the CLC2000 data (grid 100 x 100 m, Version 16, 04/2012). Due to lacking land cover data for Andorra and Turkey, we excluded these countries from the process of exposure estimates related to the vegetation based AOT40 ozone indicators.

The application of CLC2006 versus the previously used CLC2002 on the same spatial air quality data proved to deliver in the exposure of vegetation estimates less than one per cent difference, which is attributable to the difference in the use of this CLC update.

4 PM_{10} maps

This chapter presents the 2011 updates (for the interpolated maps and exposure tables) of the two PM_{10} health related indicators: annual average and 36th highest daily average. The separate urban and rural concentration maps were calculated on the 10x10 km resolution grid and the subsequent combined concentration map was based on the 1x1 km gridded population density map. The population exposure tables were calculated at 1x1 km grid resolution. All maps here are presented using the 10x10 km grid resolution. The standard EEA ETRS89-LAEA5210 coordinate reference system was applied.

4.1 Annual average

4.1.1 Concentration map

Figure 4.1 presents the combined final map for the 2011 PM_{10} annual average as the result of interpolation and merging of the separate maps as described in detail in De Smet et al. (2011) and Horálek et al. (2007). Red and purple areas and stations exceed the limit value (LV) of 40 µg.m^{-3}. Supplementary data in the regression used for rural areas consisted of EMEP model output, altitude, wind speed and surface solar radiation and for urban areas it was EMEP model output only. (The relevant linear regression submodels have been identified earlier in Horálek et al. (2008) and De Smet et al. (2009, 2010, 2011) as P.Eawr and UP.E, respectively.)

As one can observe and like in 2010, in a few areas of the map (e.g. Bulgaria, Poland) the high urban background measurement values do not seem to influence the interpolation results despite their clustering. The main reason is that the map presented here is an aggregation of 1x1 km grid values to a 10x10 km resolution and this aggregation smoothes out the elevated values one would more likely be able to distinguish in the higher resolution map, especially in the case of urban background stations representing the urban areas. (Therefore, the exposure estimates of Table 4.2 are derived just from the 1x1 km grid map). Another less prominent reason is the smoothing effect kriging has in general. However, kriging would in the case of clustering not mask these elevations in the separate 1x1 km urban and rural maps.

Table 4.1 presents the estimated parameters of the linear regression models (c, a_1, a_2,…) and of the residual kriging (*nugget*, *sill*, *range*) and includes the statistical indicators of both the regression and the kriging. The adjusted R^2 and standard error are indicators for the fit of the regression relationship, where the adjusted R^2 should be as close to 1 as possible and the standard error should be as small as possible. The adjusted R^2 was 0.55 for the rural areas and 0.19 for urban areas. The R^2 values show the best fit so far for rural areas compared to its all previous years. For urban areas, the fit is a reasonable fit compared to the years 2005 – 2009, except for 2010. The values of previous years were respectively: 2010 (0.44 and 0.38), 2009 (0.38 and 0.06), 2008 (0.29 and 0.00), 2007 (0.40 and 0.10), 2006 (0.29 and 0.03) and 2005 (0.28 and 0.06) (Horálek et al. 2013, Table 4.1; De Smet et al. 2012, 2011, 2010 and 2009, Table 4.1; Horálek et al. 2008, Tables A.21 and A2.6). The continued better regression fit for urban areas as of 2010 is most likely attributable to improvements of the EMEP model since 2010. The reason probably is the improvement of the EMEP model. RMSE and bias are the cross-validation indicators, showing the quality of the resulting map; the bias indicates to what extent the estimation is un-biased. Sections 4.1.2 and 4.1.3 deal with a more detailed analysis and compares with results of 2009, 2008, 2007, 2006 and 2005.

As indicated in Table 4.1, surface solar radiation was, like in 2010 (and in contrast to 2006–2009), found to be statistically non-significant and thus it was not used in 2011 mapping.

In the case of PM_{10}, the linear regression is applied for the logarithmically transformed data of both measured and modelled PM_{10} values. Thus, in Table 4.1 the standard error and variogram parameters refer to these transformed data, whereas RMSE and bias refer to the interpolation after the back-transformation.

Table 4.1 Parameters of the linear regression models (Eq. 2.2) and of the ordinary kriging variograms (nugget, sill, range) – and their statistics – of PM_{10} indicator annual average for 2011 in rural (left) and urban (right) areas as used for the combined final map. The linear regression models used are P.Eawr (rural areas) and UP.E (urban areas). Interpolation of regression residuals using ordinary kriging (OK) is indicated by '-a'.

linear regr. model + OK of its residuals	rural areas (lnP.Eawr-a) coeff.	urban areas (lnUP.E-a) coeff.
c (constant)	1.52	1.70
a1 (log. EMEP model 2010)	0.764	0.62
a2 (altitude GTOPO)	-0.00038	
a3 (wind speed 2010)	-0.113	
a4 (s. solar radiation 2010)	n. sign.	
adjusted R^2	**0.55**	**0.19**
standard error [µg.m^{-3}]	**0.27**	**0.33**
nugget	0.033	0.014
sill	0.070	0.061
range [km]	420	670
RMSE [µg.m^{-3}]	**4.14**	**6.14**
bias (MPE) [µg.m^{-3}]	**0.13**	**-0.10**

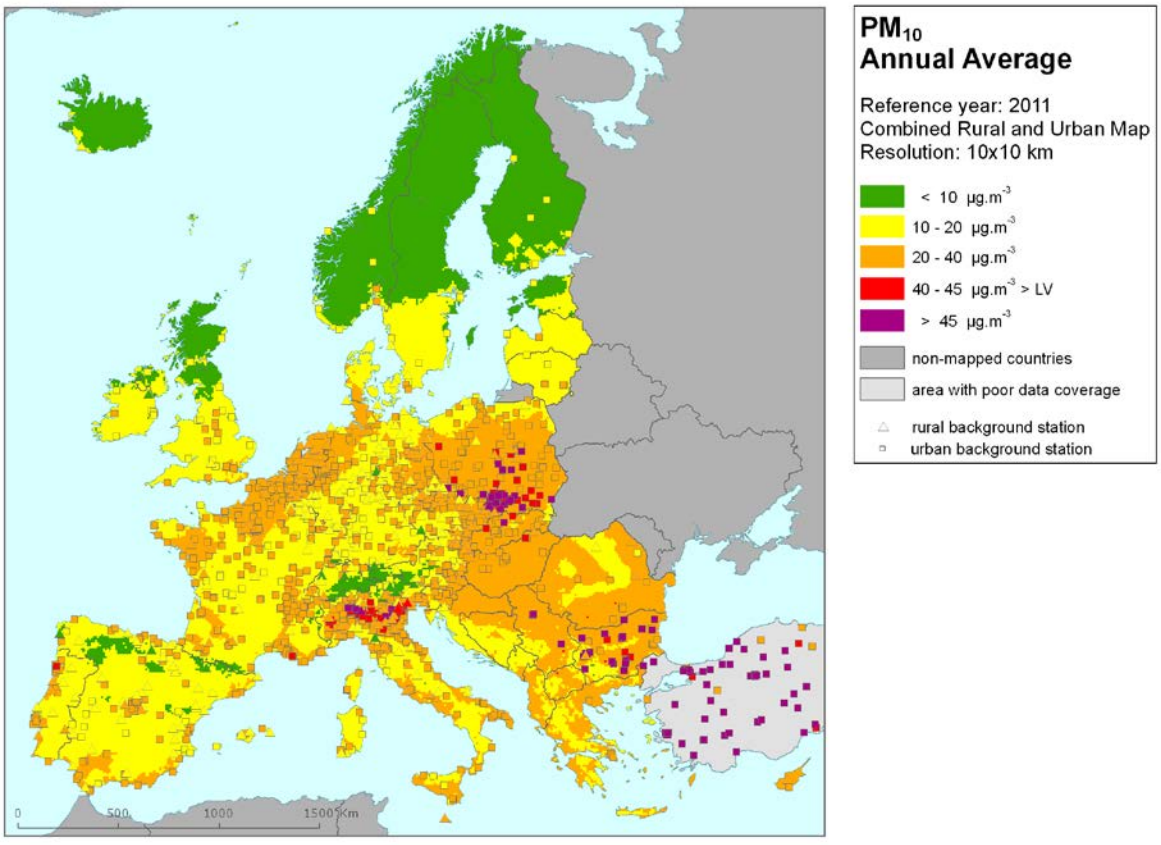

Figure 4.1 Combined rural and urban concentration map of PM_{10} – annual average, year 2011. Spatial interpolated concentration field (10x10 km grid resolution, excluding Turkey due to lack of rural air quality data) and the measured values in the measurement points. Units: µg.m^{-3}.

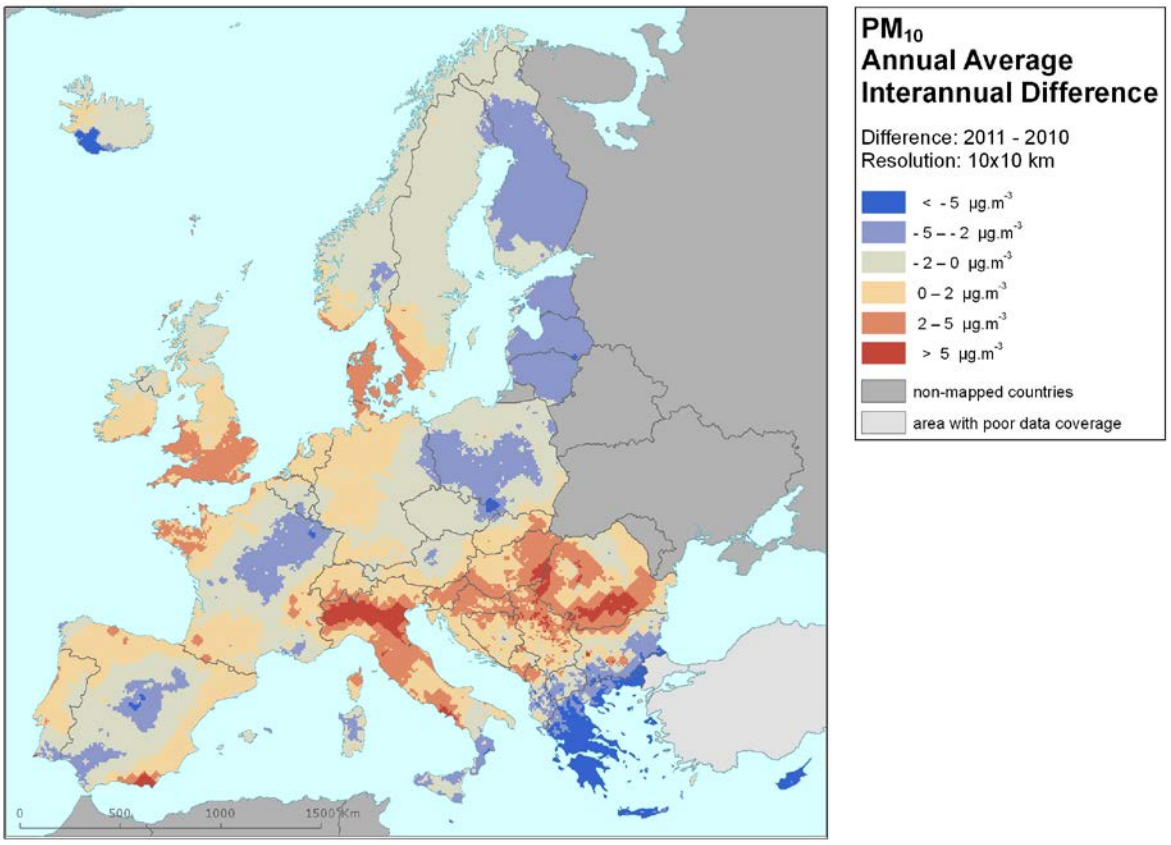

Figure 4.2 Interannual difference between mapped concentrations for 2011 and 2010 – PM_{10}, annual average. Units: $\mu g.m^{-3}$.

Figure 4.2 presents the interannual difference between 2011 and 2010 for annual average PM_{10}. Red areas show an increase of PM_{10} concentration, while blue areas show a decrease. The highest increases can be seen in the Po Valley, central Italy and the Naples area, some areas in the eastern European countries, Denmark and southern UK. Some of these areas showed for the '2010 - 2009' difference the opposite effect. In inversed order such shifts are observed for areas in southern Poland, Finland, Estonia, Latvia, Lithuania, Greece, Crete, Cyprus, Sicily and especially south-eastern Iceland with its steep increased concentration in 2010 due to the volcanic activity of Eyjafjallajökull (De Leeuw, 2012).

4.1.2 Population exposure

Table 4.2 gives the population frequency distribution for a limited number of exposure classes calculated at the 1x1 km grid resolution, as well as the population-weighted concentration for individual countries and for Europe as a whole according to Equation 2.3.

About 40 % of the European population has been exposed to annual average concentrations below 20 $\mu g.m^{-3}$, the WHO (World Health Organization) air quality guideline. EEA (2013) estimates that about 85-88 % of the urban population is exposed to levels above the WHO guideline reference level, i.e. 12-15 % is below the WHO reference level. This lower amount specifically accounts only for the urban population in the larger cities of Europe. It therefore represents areas where, in general, considerably higher PM_{10} concentrations occur throughout the year. The estimate of Table 4.2 (40 %) includes the total European population, including inhabitants in the rural areas, the smaller cities and

the villages that are in general exposed to lower levels of PM_{10} throughout the year. It is important to note that this difference in WHO reference level exposure estimates is explained by the use of different population characteristics and area representation in the calculations. Slightly more than half (57 %) of the European population in 2010 lived in areas where the PM_{10} annual mean concentration was estimated to be between 20 and 40 $\mu g.m^{-3}$. About 2.5 % of the population lived in areas where the PM_{10} annual limit value was exceeded, with Bulgaria, Cyprus, Greece, Italy, Poland and Serbia showing a population-weighted concentration of more than 5 % above the LV. However, as the next Section 4.1.3 discusses, the current mapping methodology tends to underestimate high values. Therefore, the exceedance percentage would most likely be higher and anticipate in exceedances at additional countries, for example Albania.

The evolution of population exposure in the last six years is presented in Table 4.3. It is based on results presented in previous reports (Horálek et al., 2013, De Smet et al., 2012, 2011) for the years 2010 – 2008, based on the recalculated results for 2007 and based on the paper with the tests of new methodology (Horálek et al., 2010) for 2006.

The frequency distribution shows large variability over Europe, with many countries showing exposures above the limit value both in 2010 as well as in 2011, however, for most of them the percentage in exceedance has decreased considerably (e.g. Albania, Poland). Only Italy shows an increase of no exceedance in 2010 to almost 14 % in 2011. In the period 2006 – 2011, the year 2011 appears to show the lowest number of population being exposed to annual averaged concentrations above the limit value. In many cases this reduction occurs for the first time in that period of time. Compared to 2010, an overall reduction of 2.7 % has been realized in 2011.

In a number of countries in northern and north-western Europe, the LV of 40 $\mu g.m^{-3}$ seems to continue not to be exceeded. When comparing between years the total population exposed to the low levels, i.e. below 20 $\mu g.m^{-3}$, it is found that the percentage for 2011 of 40 % is higher than the three previous years 2010 – 2008 (with 29 – 31 %) which on its turn higher is than for the years 2007 with 24 % and 2006 with 20 %. This tendency of reduced exposure of population living in areas with concentrations above the limit value, established in previous years (from 10.3 % in 2006 to 6.8 % in 2007 and 5.8 % in 2008) seems to continue with values of 5.2 % in 2010 and 2.5 % in 2011. The tendency comes with a degree of uncertainty however, as an increase in 2009 (6.0 %) occurred.

Table 4.2 Population exposure and population-weighted concentration – PM_{10}, annual average, year 2011. Resolution: 1x1 km.

Country		Population [inhbs . 1000]	PM_{10} annual average, exposed population [%]					Population weighted conc. [µg.m^{-3}]
			< LV			> LV		
			< 10 µg.m^{-3}	10 - 20 µg.m^{-3}	20 - 40 µg.m^{-3}	40 - 45 µg.m^{-3}	> 45 µg.m^{-3}	
Albania	AL	2 832		14.8	84.3	0.9		26.5
Andorra	AD	85	18.1	0.1	81.8			18.0
Austria	AT	8 404	2.8	44.3	52.8			20.8
Belgium	BE	11 001		6.8	93.2			24.8
Bosnia & Herzegovina	BA	3 843		43.4	56.0	0.7		22.3
Bulgaria	BG	7 369	0.0	10.6	82.0	1.0	6.4	27.3
Croatia	HR	4 290		22.9	77.1			25.0
Cyprus	CY	840			87.2	12.8		31.1
Czech Republic	CZ	10 487		23.9	75.2	0.9		23.7
Denmark	DK	5 561	0.0	85.1	14.8			18.4
Estonia	EE	1 336	65.8	34.2				9.8
Finland	FI	5 375	68.7	31.3				9.5
France	FR	64 995	0.0	36.1	63.9			21.8
Germany	DE	81 752	0.0	54.3	45.7			19.6
Greece	GR	11 123		9.4	84.9	5.7	0.0	24.6
Hungary	HU	9 986		0.0	100.0			29.1
Iceland	IS	318	63.9	36.1				9.3
Ireland	IE	4 571	3.3	96.7				12.8
Italy	IT	60 626	0.4	17.3	68.6	12.1	1.7	27.7
Latvia	LV	2 075		77.6	22.0			14.6
Liechtenstein	LI	36	1.5	98.5				11.3
Lithuania	LT	3 053		95.7	4.3			14.8
Luxembourg	LU	512		100.0				16.4
Macedonia, FYR of	MK	2 057		31.4	66.3	0.1	2.2	23.0
Malta	MT	415			100			27.8
Monaco	MC	35			100			22.8
Montenegro	ME	620	0.0	47.0	52.9			21.5
Netherlands	NL	16 656		0.4	99.6			25.1
Norway	NO	4 920	67.1	31.0	1.9			9.3
Poland	PL	38 530		13.1	81.7	1.7	3.5	27.2
Portugal	PT	10 573	0.1	41.5	58.3			20.8
Romania	RO	20 199		10.4	88.7	0.7	0.2	27.2
San Marino	SM	32			100			20.9
Serbia (incl. Kosovo)	RS	9 046		5.8	80.8	0.8	12.6	30.1
Slovakia	SK	5 392		2.0	97.9	0.1		27.4
Slovenia	SI	2 050		10.2	89.8			25.4
Spain	ES	46 667	0.8	59.2	39.9			18.8
Sweden	SE	9 416	25.4	74.6	0.0			12.3
Switzerland	CH	7 870	4.6	59.7	35.7			17.7
United Kingdom	UK	63 024	5.9	68.1	25.9			17.5
Total		**537 972**	**2.9**	**37.4**	**57.3**	**1.7**	**0.8**	**22.1**
			40.2			**2.5**		

Note1: Turkey is not included in the calculation due to lacking air quality data in rural areas.
Note2: The percentage value "0.0" indicates an exposured population exists, but is small and estimated less than 0.05 %.
Empty cells mean: no population in exposure.

Table 4.3 Evolution of percentage population living in above limit value (left) and population-weighted concentration (right) in the years 2006-2011 – PM_{10}, annual average. Resolution: 1x1 km.

Country		Population above LV 40 µg.m^{-3} [%]							Population-weighted conc. [µg.m^{-3}]						
		2006	2007	2008	2009	2010	2011	diff. '11 - '10	2006	2007	2008	2009	2010	2011	diff. '11 - '10
Albania	AL	3.1	0.1	6.5	52.1	62.6	0.9	-61.7	31.8	31.6	33.3	35.3	45.5	26.5	-19.0
Andorra	AD	0	0	0	0	0	0	0	22.5	20.5	18.7	17.7	17.9	18.0	0.1
Austria	AT	0	0	0	0	0	0	0	26.0	22.1	21.3	21.6	22.7	20.8	-1.9
Belgium	BE	0	0	0	0	0	0	0	31.3	24.8	23.9	26.5	25.7	24.8	-0.9
Bosnia-Herzegovina	BA	6.9	3.3	0.0	51.6	17.2	0.7	-16.5	33.1	32.4	29.3	37.2	30.8	22.3	-8.6
Bulgaria	BG	49.9	42.1	62.1	53.8	49.0	7.4	-41.7	41.6	40.2	44.2	39.8	38.0	27.3	-10.6
Croatia	HR	0.1	0	0	3.0	0	0	0	31.5	30.0	28.1	29.0	27.3	25.0	-2.2
Cyprus	CY	0	0	87.0	73.0	82.7	12.8	-69.9	35.4	33.9	76.1	41.0	50.2	31.1	-19.1
Czech Republic	CZ	13.8	1.8	1.7	3.3	9.4	0.9	-8.5	33.5	25.6	24.2	25.3	28.3	23.7	-4.6
Denmark	DK	0	0	0	0	0	0	0	23.5	20.8	18.8	16.3	15.7	18.4	2.7
Estonia	EE	0	0	0	0	0	0	0	19.7	15.7	12.9	13.4	14.1	9.8	-4.3
Finland	FI	0	0	0	0	0	0	0	17.0	13.7	12.5	11.7	12.2	9.5	-2.7
France	FR	0	0	0	0	0	0	0	20.4	24.6	22.6	24.0	23.0	21.8	-1.2
Germany	DE	0	0	0	0	0	0	0	24.2	20.7	19.6	20.7	21.2	19.6	-1.7
Greece	GR	3.6	1.5	37.0	23.4	20.9	5.7	-15.2	33.6	33.5	39.7	35.3	37.3	24.6	-12.6
Hungary	HU	2.2	0	0	0	0	0	0	32.9	28.7	26.8	27.6	28.1	29.1	1.0
Iceland	IS	0	0	0	0	0.1	0	-0.1	17.4	12.2	15.2	9.0	10.7	9.3	-1.4
Ireland	IE	0	0	0	0	0	0	0	14.9	14.7	15.4	12.8	13.7	12.8	-0.9
Italy	IT	24.2	19.8	2.7	8.8	0	13.7	13.7	33.9	33.2	30.1	28.7	26.4	27.7	1.3
Latvia	LV	0	0	0	0	0	0	0	21.9	17.8	19.1	18.8	21.5	14.6	-6.9
Liechtenstein	LI	0	0	0	0	0	0	0	24.9	20.7	20.6	18.3	17.3	11.3	-6.0
Lithuania	LT	0	0	0	0	0	0	0	22.5	18.5	17.3	19.0	22.0	14.8	-7.2
Luxembourg	LU	0	0	0	0	0	0	0	20.8	19.5	18.2	21.0	19.4	16.4	-3.0
Macedonia, FYR of	MK	61.3	52.1	67.8	74.5	70.0	2.3	-67.7	39.3	38.5	41.6	45.4	43.9	23.0	-20.9
Malta	MT	0	0	0	0	0	0	0	29.4	27.0	27.5	27.2	32.5	27.8	-4.7
Monaco	MC	0	0	0	0	0	0	0	36.7	34.5	29.5	26.8	24.0	22.8	-1.2
Montenegro	ME	9.7	1.3	38.7	61.1	42.1	0	-42.1	33.1	33.1	33.6	35.0	32.8	21.5	-11.2
Netherlands	NL	0	0	0	0	0	0	0	29.1	25.8	24.0	24.3	24.3	25.1	0.8
Norway	NO	0	0	0	0	0	0	0	19.6	15.6	15.7	14.1	14.7	9.3	-5.4
Poland	PL	28.5	13.4	12.4	14.7	30.0	5.2	-24.8	37.0	28.8	28.3	30.8	35.2	27.2	-7.9
Portugal	PT	0	0	0	0	0	0	0	28.4	27.0	21.8	22.9	21.7	20.8	-0.9
Romania	RO	47.0	32.0	19.6	4.0	2.0	0.9	-1.1	39.1	35.0	30.8	28.9	25.2	27.2	2.0
San Marino	SM	0	0	0	0	0	0	0	33.9	31.2	29.6	26.0	25.0	20.9	-4.1
Serbia (incl. Kosovo)	RS	66.0	59.1	61.8	55.5	20.7	13.4	-7.4	41.8	39.4	40.1	39.5	33.1	30.1	-3.1
Slovakia	SK	16.3	2.4	1.7	1.2	3.0	0.1	-2.8	33.8	29.1	26.7	26.9	30.2	27.4	-2.8
Slovenia	SI	0	0	0	0	0	0	0	29.0	27.2	25.0	25.2	26.0	25.4	-0.6
Spain	ES	7.5	2.6	1.3	0	0	0	0	31.4	29.6	25.2	23.7	21.4	18.8	-2.7
Sweden	SE	0	0	0	0	0	0	0	19.0	15.7	16.3	13.8	12.8	12.3	-0.5
Switzerland	CH	0.9	0	0	0	0	0	0	23.2	21.4	20.5	21.0	19.8	17.7	-2.1
United Kingdom	UK	0	0	0	0	0	0	0	23.2	21.6	19.5	18.4	18.2	17.5	-0.7
Total		**10.3**	**6.8**	**5.8**	**6.0**	**5.2**	**2.5**	**-2.7**	**28.5**	**26.2**	**24.8**	**24.6**	**24.3**	**22.1**	**-2.2**
EU-28		**9.3**	**5.9**	**4.4**	**4.1**	**4.1**	**2.4**	**-1.8**	**28.3**	**26.0**	**24.4**	**24.2**	**24.0**	**22.1**	**-1.9**

Considering the average for the whole of Europe in Table 4.3, the overall population-weighted annual mean PM_{10} concentration in 2011 was 22.1 µg.m^{-3}. This is again somewhat lower than in previous years. One may observe a steady reduction of the population-weighted concentration over the period of time 2006 – 2011.

4.1.3 Uncertainties

Uncertainty estimated by cross-validation

Using RMSE as the most common indicator, the *absolute mean uncertainty* of the combined final map at areas 'in between' the station measurements can be expressed in µg.m^{-3}. Table 4.1 shows that the absolute mean uncertainty of the combined final map of PM_{10} annual average expressed by RMSE is 4.1 µg.m^{-3} for the rural areas and 6.1 µg.m^{-3} for the urban areas. That is the lowest absolute uncertainty for rural areas but a more often obtained value for the urban areas of the years 2005 – 2011. Alternatively, one could express this uncertainty in relative terms by relating the absolute RMSE uncertainty to the mean air pollution indicator value for all stations. This *relative mean uncertainty* (RRMSE) of the combined final map of PM_{10} annual average is 21.1 % for rural areas and 20.7 % for urban areas. This is, for rural areas, the lowest of all in the period 2005 – 2011. The somewhat higher uncertainty levels for urban areas in the years 2008 – 2011, compared to the years 2005 – 2007, are caused specifically by addition of Turkish urban background stations reported only since 2008. (Turkish urban stations show high concentrations, uncertainty statistics are sensitive to such values.) These data have been used in the calculations since 2008 (although the interpolation result for Turkey is not present in the map due to lack of rural air quality data for Turkey). These relative uncertainty values fulfil the data quality objectives for models as set in Annex I of the air quality Directive 2008/50/EC (EC, 2008). Table 7.5 summarises both the absolute and relative uncertainties over these past seven years.

Figure 4.3 shows the cross-validation scatter plots, obtained according Section 2.3, for both rural and urban areas. The R^2 indicates that for the rural areas about 68 % and for the urban areas about 77 % of the variability is attributable to the interpolation. Corresponding values of the map of 2005 (52 % and 71 %), 2006 (52 % and 69 %), 2007 (59 % and 66 %), 2008 (48 % and 82 %), 2009 (54% and 73%) and 2010 (62 % and 75 %) help illustrate that for 2011 interpolation performance at both the rural and urban locations is slightly above the average of the earlier six years.

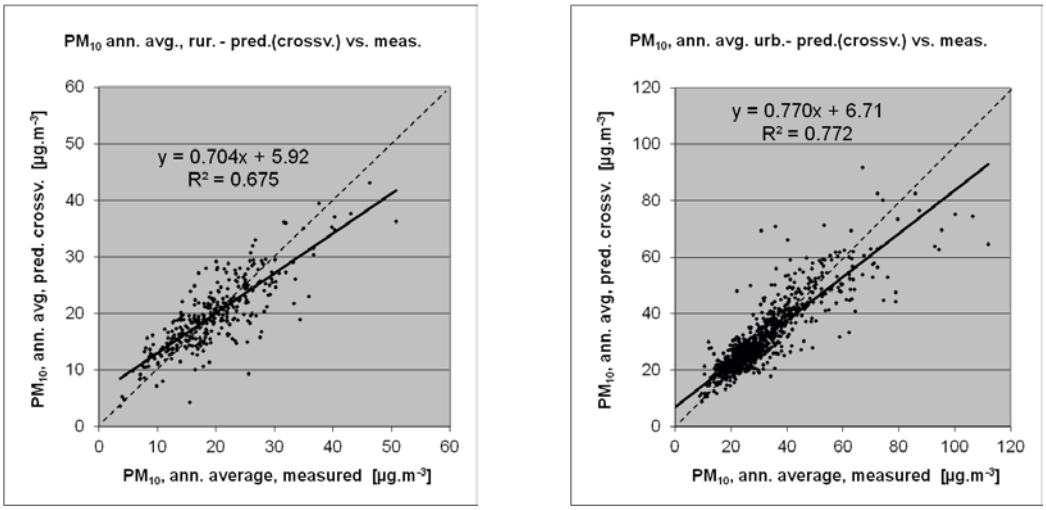

Figure 4.3 Correlation between cross-validation predicted values (y-axis) and measurements (x-axis) for the PM_{10} annual average for 2011 for rural (left) and urban (right) areas. R^2 and the slope a (from the linear regression equation $y = a \cdot x + c$) should be as close 1 as possible, the intercept c should be as close 0 as possible

The scatter plots indicate that in areas with high concentrations the interpolation methods tend to underestimate the levels. For example, in rural areas an observed value of 40 µg.m^{-3} is estimated in the interpolations to be about 34 µg.m^{-3}, about 15 % too low. This underestimation at high values is natural to all spatial interpolations. It can be reduced by either using a higher number of the stations at improved spatial distribution, or introducing a closer regression by using other supplementary data.

Comparison of point measurement values with the predicted grid value

In addition to the point observation – point prediction cross-validation discussed in the previous subsection, a simple comparison has been made between the point observation values and interpolated prediction values averaged at 10x10 km grid resolution for the separate rural and urban background maps. This *point-grid* comparison indicates to what extent the predicted value of a grid cell represents the corresponding measured values at stations located in that cell. The results of the point observation – point prediction cross-validation of Figure 4.3 compared to those of the point-grid validation are summarised in Table 4.4. The table shows a better correlated relation between station measurements and the interpolated values of the corresponding grid cells (i.e. higher R^2, smaller intercept and slope closer to 1) at both rural and urban map areas than it does at the point cross-validation predictions. That is because the simple comparison between point measurements and the gridded interpolated values shows the uncertainty at the actual station locations (points), while the point observation – point prediction cross-validation simulates the behaviour of the interpolation at positions without an actual measurement. The uncertainty at measurement locations is caused partly by the smoothing effect of the interpolation and partly by the spatial averaging of the values in the 10x10 km grid cells. The level of the smoothing effect leading to underestimation at areas with high values is there smaller than it is in situations where no measurement is represented in such areas. For example, in urban areas the predicted interpolation gridded value will be about 59 $\mu g.m^{-3}$ at the corresponding station point with the measured value of 65 $\mu g.m^{-3}$, i.e. an underestimation of about 9 %. This is less than the underestimation of 13 % for such a location without a measurement value, discussed in the previous subsection.

Table 4.4 Linear regression equation and coefficient of determination R^2 from the scatter plots of (i) the predicted point values based on cross-validation and (ii) the aggregated predictions into 10x10 km grid cells versus the measured point values for PM_{10} indicator annual average for rural and urban areas of 2011.

	rural areas		urban areas	
	equation	R^2	equation	R^2
i) cross-validation prediction (Fig 4.3)	y = 0.704x + 5.92	0.675	y = 0.770x + 6.71	0.772
ii) 10x10 km grid prediction	y = 0.770x + 4.22	0.824	y = 0.831x + 4.66	0.894

Probability of Limit Value exceedance map

Next to the point cross-validation analysis, we constructed the map of probability of limit value exceedance. For this purpose, we aggregated the 1x1 km gridded combined final concentration map into a 10x10 km grid resolution map. Then we derived, with support of the 10x10 km uncertainty map and the limit value (40 $\mu g.m^{-3}$), the probability of exceedance (PoE) map at that same resolution (Figure 4.4). It is important to emphasize that the exceedance of the spatial average of a 10x10 km grid cell can show low probability even though some smaller (e.g. urban) areas inside such a grid cell show high probability of exceedance (using finer grid cell resolution). Next to this – keeping in mind that the interpolated maps refer to the rural or (sub)urban *background* situations only, it cannot be excluded that exceedances of limit values may occur at different *hotspot* and traffic locations.

The map demonstrates areas with a probability of limit value exceedance above 75 % marked in red (*high* probability) and areas below 25 % in green (*low* probability). Red indicates areas for which exceedance is *very likely* to occur due to either high concentrations close to or already above the LV accompanied with such uncertainty that exceedance is very likely, or areas with lower concentrations accompanied with high uncertainty levels reaching above the LV that excess is very likely. Vice versa, in the green areas it is *not likely* to have predicted concentrations and accompanying uncertainties at levels that do reach above the LV.

In the probability maps, the areas with 25-50 % and 50-75 % probability of LV exceedance are marked in yellow and orange respectively. The yellow colour indicates the areas with the estimated concentrations below limit value, but for which there exists a *modest* probability of exceeding the limit. On the contrary, the orange areas have estimated concentrations above the limit value, but with a

chance of non-exceedance caused by its accompanying uncertainty. Table 4.5 summarises the classes and terminology for probability (i.e. likelihood) that are distinguished in this paper.

Table 4.5 Probability mapping classes and terminology use in this paper.

Map class colour	Percentage probability of threshold exceedance	Degree of probability (or likelihood) of exceedance	Likelihood of exceedance
Green	0 – 25	Low/ Little	Not likely
Yellow	25 – 50	Modest	Somewhat likely
Orange	50 – 75	Moderate	Rather Likely
Red	75 – 100	High / Large	Very likely

The patterns in the spatial distribution of the different PoE classes over Europe differ in 2011 somewhat from those of 2010. The region of southern Poland – north-eastern Czech Republic with the industrial zones of Krakow, Katowice (PL) and Ostrava (CZ) shows a smaller area with the highest probability of exceedance (75-100 %) in comparison with 2010. Contrary to that, the Po Valley in Italy shows a higher probability of exceedance, in comparison with 2010. In both the areas, the PoE map turned back to the levels of 2009. In south-eastern Europe, where relatively few measurement stations are located, especially at some larger cities with mostly high traffic density and heavy industry, elevated PoE do show up. In comparison with 2010, more (and larger) such areas occur in Romania, Bulgaria and Serbia, while less (and smaller) or none occur in Cyprus and Greece. In other parts of Europe there exists just little likelihood of exceedance. In general, it can be concluded that the likelihood of exceedance in 2011 quite similar, but sometimes in different areas when compared to the levels of 2010.

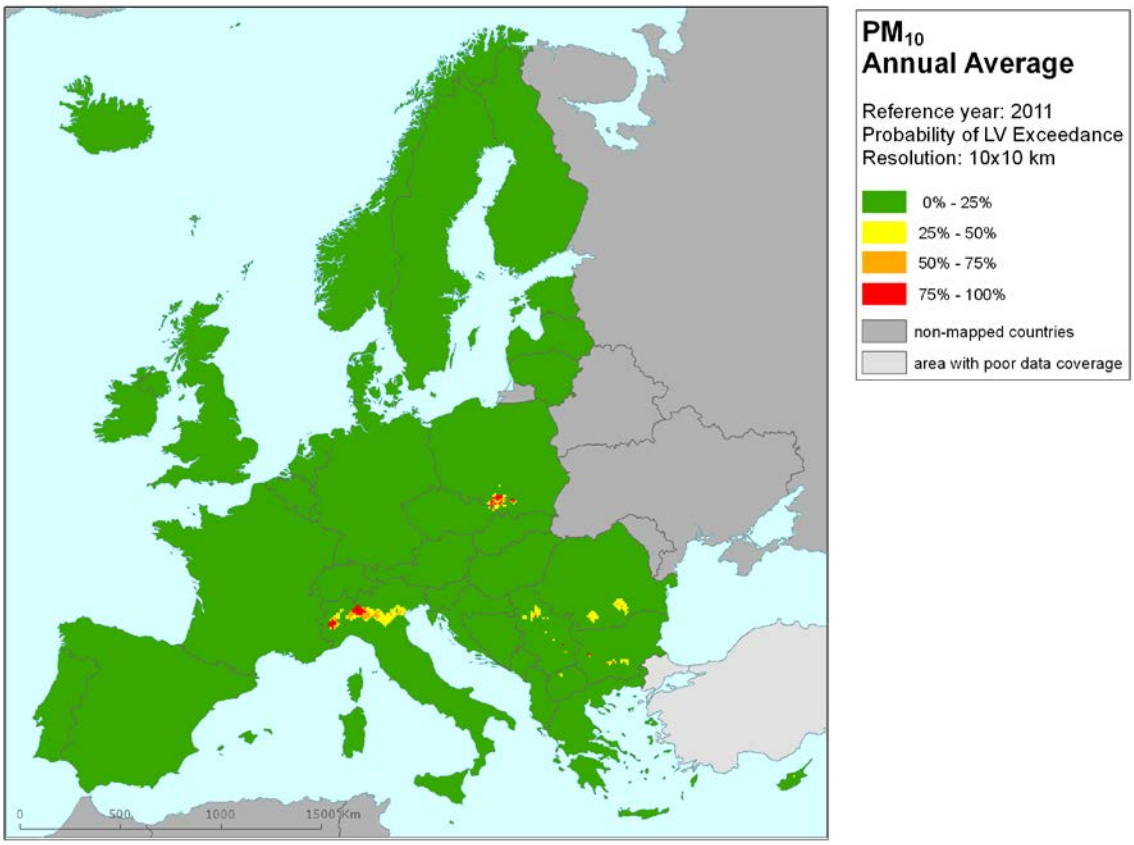

Figure 4.4 Map with the probability of the limit value exceedance for PM_{10} annual average ($\mu g.m^{-3}$) for 2011 on European scale calculated on the 10 x 10 km grid resolution. Interpolation uncertainty is considered only, no other sources of uncertainty.

4.2 36^{th} highest daily average

4.2.1 Concentration map

Similar to the PM_{10} annual average map, the combined final map of 36^{th} highest daily value has been derived from the separate rural, urban and joint rural/urban maps, using the same set of supplementary data parameters (Section 4.1.1) in the regression models and interpolation of residuals. Table 4.6 presents the estimated parameters of the linear regression models and of the residual kriging, including their statistical indicators. As in the case of annual average mapping, surface solar radiation was this year found to be statistically non-significant and thus it was not used in 2011 mapping.

Like in the case of annual average, the linear regression is applied for the logarithmically transformed data of both measured and modelled PM_{10} values. Thus, in Table 4.6 the standard error and variogram parameters refer to these transformed data, whereas RMSE and bias refer to the interpolation after the back-transformation.

Table 4.6 Parameters of the linear regression models (Eq.2.1) and of the ordinary kriging variograms (nugget, sill, range) - and their statistics - of PM_{10} indicator 36^{th} highest daily mean for 2011 in the rural (left) and urban (right) areas as used for final mapping, i.e. rural linear regression model P.Eawr (left), resp. urban UP.E (right), followed by the interpolation on its regression residuals using ordinary kriging (OK, coded with 'a').

linear regr. model + OK on its residuals	rural areas (lnP.Eawr-a) coeff.	urban areas (lnUP.E-a) coeff.
c (constant)	1.60	1.88
a1 (lnEMEP model 2011)	0.774	0.63
a2 (altitude GTOPO)	-0.00038	
a3 (wind speed 2011)	-0.112	
a4 (s. solar radiation 2011)	n. sign.	
adjusted R^2	**0.52**	**0.17**
standard error [µg.m^{-3}]	**0.29**	**0.37**
nugget	0.037	0.012
sill	0.081	0.083
range [km]	390	660
RMSE [µg.m^{-3}]	**8.38**	**13.00**
bias (MPE) [µg.m^{-3}]	**0.26**	**-0.41**

The regressions on the 2011 data have an adjusted R^2 of 0.52 for rural areas and 0.17 for urban areas. Such a fit for rural areas is better than all previous years: 2009 (0.40), 2007 (0.41), 2008 (0.26), 2006 (0.27) and 2005 (0.29). In urban areas the fit was less than for 2010 (0.34) but much better than for the preceding years – 2005, 0.0; 2006, 0.02; 2007, 0.09; 2008, 0.06 (De Smet et al. 2012, 2011, 2010, 2009 and Horálek et al. 2013, 2008). RMSE and bias are the cross-validation indicators for the quality of the resulting map. Section 4.2.3 discusses in more detail the RMSE analysis and the comparison with 2005 – 2010.

Figure 4.5 presents the combined final map, where areas and stations exceeding the limit value (LV) of 50 µg.m^{-3} on more than 35 days are coloured red and purple.

As one can observe in a few areas of the map, the high urban background measurement values do not seem to influence the interpolation results despite their clustering (e.g. in Bulgaria). The main reason is that the map presented here is an aggregation of 1x1 km grid values to a 10x10 km resolution and this aggregation smoothes out the elevated values one would more likely be able to distinguish in the higher resolution map, especially in the case of urban background stations representing the urban areas. Another less prominent reason is the smoothing effect kriging has in general. However, kriging would in the case of clustering, not mask these elevations in the separate 1x1 km urban and rural maps.

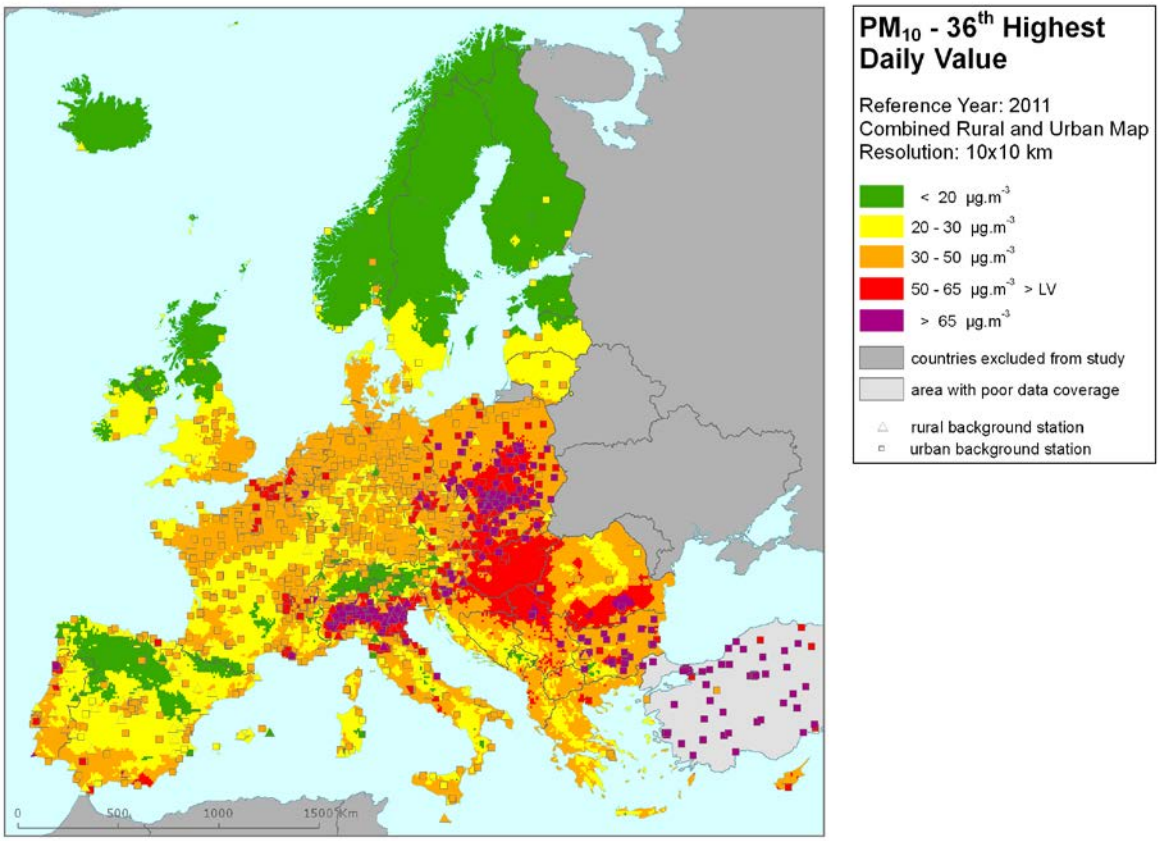

Figure 4.5 Combined rural and urban concentration map of PM_{10} – 36th highest daily average value, year 2011. Spatial interpolated concentration field (10x10 km grid resolution, excluding Turkey due to lack of rural air quality data) and the measured values in the measuring points. Units: µg.m^{-3}.

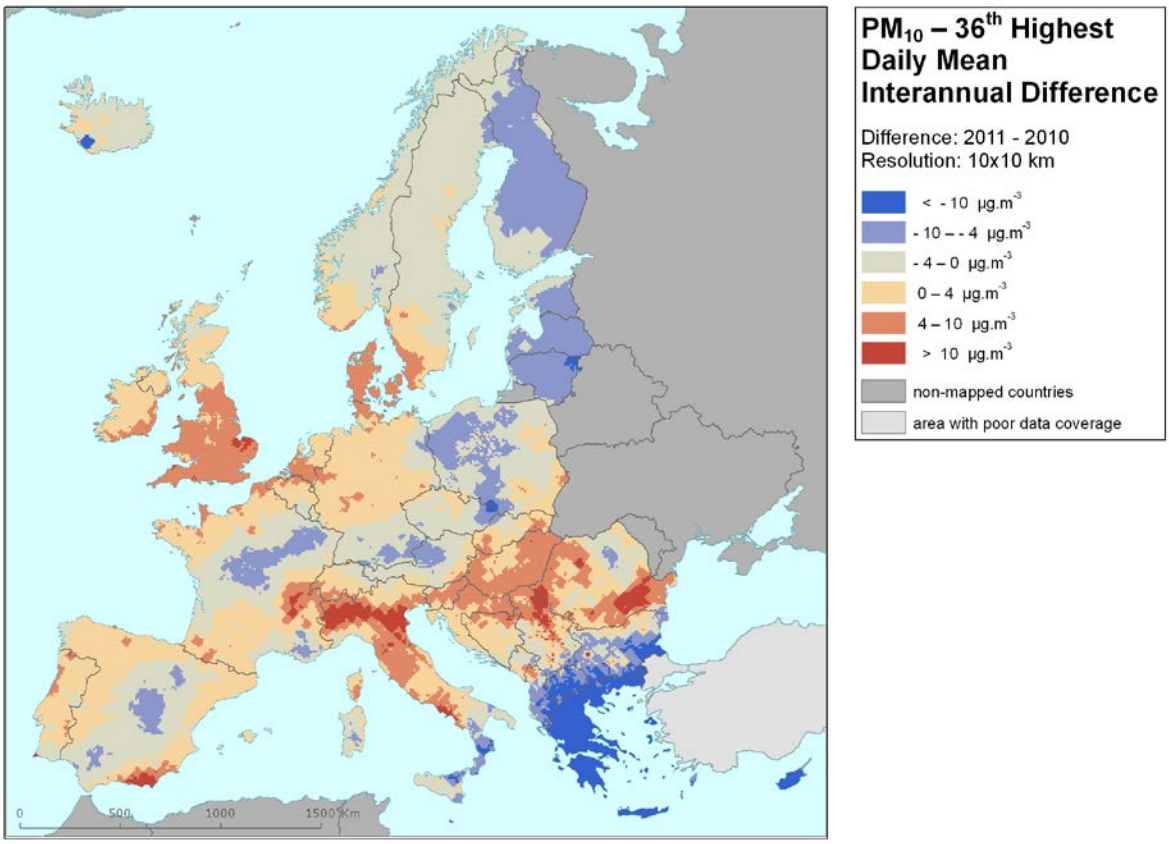

Figure 4.6 Interannual difference between mapped concentrations for 2011 and 2010 – PM_{10}, 36th highest daily average value. Units: µg.m^{-3}. Resolution: 10x10 km.

Figure 4.6 presents the interannual difference between 2011 and 2010 for 36th highest daily mean. Red areas show an increase of PM_{10} concentration, while blue areas show a decrease. The highest increase can be seen in the Po Valley central Italy and the Naples area, southern UK, Denmark, Hungary, Serbia and Romania. The steepest decrease can be seen in Greece, Bulgaria and Cyprus. The map shows areas with inverse effects compared to the one where the difference for '2010 – 2009' is given. This may indicate that the year 2010 deviates from its surrounding years, perhaps due to meteorological variability over these three years.

4.2.2 Population exposure

Table 4.7 gives the population frequency distribution for a limited number of exposure classes calculated at 1x1 km grid resolution, as well as the population-weighted concentration for individual countries and for Europe as a whole. Table 4.8 shows the evolution of the population exposure in the last five years.

Table 4.7 Population exposure and population-weighted concentration – PM_{10}, 36th highest daily average value, year 2011. Resolution: 1x1 km.

Country		Population	PM_{10}, 36th highest d. a., exposed population [%]					Pop. weighted conc.
			< LV			> LV		
			< 20	20 - 30	30 - 50	50 - 65	> 65	
		[inhbs . 1000]	µg.m^{-3}	µg.m^{-3}	µg.m^{-3}	µg.m^{-3}	µg.m^{-3}	[µg.m^{-3}]
Albania	AL	2 832	0.0	7.6	71.2	19.5	1.6	42.8
Andorra	AD	85	18.2		81.8			29.2
Austria	AT	8 404	6.3	15.8	55.2	22.8		38.7
Belgium	BE	11 001		2.2	90.8	7.0		45.1
Bosnia & Herzegovina	BA	3 843	0.1	17.0	63.7	11.2	7.9	40.8
Bulgaria	BG	7 369	0.2	5.8	73.2	11.2	9.5	46.6
Croatia	HR	4 290	0.0	13.1	49.3	29.6	8.0	46.6
Cyprus	CY	840			87.1	12.9		46.2
Czech Republic	CZ	10 487		3.3	65.7	23.9	7.0	46.2
Denmark	DK	5 561	0.4	20.4	79.2			31.6
Estonia	EE	1 336	99.0	1.0				17.6
Finland	FI	5 375	78.3	21.7				16.9
France	FR	64 995	0.3	22.3	74.2	3.2		36.6
Germany	DE	81 752	0.2	19.1	80.2	0.5		35.7
Greece	GR	11 123	0.0	9.9	82.6	1.7	5.7	37.6
Hungary	HU	9 986			7.9	91.1	1.0	55.4
Iceland	IS	318	99.1	0.9	0.0			15.8
Ireland	IE	4 571	19.6	75.1	5.2			23.2
Italy	IT	60 626	0.6	11.1	48.7	16.7	22.8	48.6
Latvia	LV	2 075	10.6	67.2	22.3			26.7
Liechtenstein	LI	36	1.5	98.5				21.3
Lithuania	LT	3 053		90.8	9.2			26.6
Luxembourg	LU	512		60.4	39.6			29.4
Macedonia, FYR of	MK	2 057	0.1	12.0	84.4	0.7	2.8	37.9
Malta	MT	415			100			39.7
Monaco	MC	35			100			37.0
Montenegro	ME	620	4.0	38.9	44.8	11.0	1.4	36.2
Netherlands	NL	16 656			100			44.0
Norway	NO	4 920	81.2	14.5	4.2			16.3
Poland	PL	38 530		0.3	58.4	21.0	20.3	51.4
Portugal	PT	10 573	1.0	20.1	74.0	4.8	0.1	35.4
Romania	RO	20 199		4.3	52.3	29.0	14.4	48.1
San Marino	SM	32			100			35.9
Serbia (incl. Kosovo)	RS	9 046	0.0	3.5	43.6	38.2	14.7	54.6
Slovakia	SK	5 392		0.2	37.5	57.7	4.7	51.5
Slovenia	SI	2 050		1.4	59.5	36.4	2.7	48.1
Spain	ES	46 667	7.1	37.1	54.7	1.0	0.1	30.5
Sweden	SE	9 416	46.1	43.7	10.2			21.1
Switzerland	CH	7 870	5.3	31.4	62.0	1.3		33.0
United Kingdom	UK	63 024	8.1	35.9	56.0			30.3
Total		**537 972**	**4.6**	**18.7**	**60.9**	**10.2**	**5.5**	**39.0**
			84.2			**15.8**		

Note1: Turkey is not included in the calculation due to lacking air quality data in rural areas.
Note2: The percentage value "0.0" indicates an exposured population exists, but is small and estimated less than 0.05 %.
Empty cells mean: no population in exposure.

Table 4.8 Evolution of percentage population living in above limit value (left) and population-weighted concentration (right) in the years 2006-2011 – PM_{10}, 36th highest daily average value. Resolution: 1x1 km.

Country		Population above LV 40 µg.m^{-3} [%]							Population-weighted conc. [µg.m^{-3}]						
		2006	2007	2008	2009	2010	2011	diff. '11 - '10	2006	2007	2008	2009	2010	2011	diff. '11 - '10
Albania	AL	70.6	74.5	76.6	62.4	78.4	21.2	-57.3	54.0	53.3	55.7	51.3	69.5	42.8	-26.7
Andorra	AD	0	0	0	0	0	0	0	35.7	32.1	29.3	29.4	28.5	29.2	0.7
Austria	AT	43.9	3.4	0	0	23.8	22.8	-1.0	47.1	39.9	36.9	36.7	42.8	38.7	-4.1
Belgium	BE	73.1	4.2	0	3.3	0	7.0	7.0	51.3	43.5	38.4	45.8	42.7	45.1	2.4
Bosnia-Herzegovina	BA	80.0	68.8	68.0	65.7	64.9	19.1	-45.8	57.4	52.7	50.6	57.8	53.7	40.8	-12.9
Bulgaria	BG	81.8	76.6	75.4	73.4	80.2	20.8	-59.4	74.2	67.5	78.2	70.3	69.2	46.6	-22.5
Croatia	HR	80.2	46.2	35.0	27.7	58.6	37.6	-21.0	53.7	49.6	48.6	46.9	50.5	46.6	-3.9
Cyprus	CY	81.5	91.8	98.3	80.6	99.0	12.9	-86.1	58.2	54.4	130.7	68.6	74.5	46.2	-28.2
Czech Republic	CZ	76.6	20.9	13.1	14.7	47.2	31.0	-16.2	57.5	46.2	42.5	43.6	53.7	46.2	-7.5
Denmark	DK	0	0	0	0	0	0	0	37.0	32.5	29.0	26.0	25.5	31.6	6.1
Estonia	EE	0	0	0	0	0	0	0	34.1	28.0	22.4	22.4	25.8	17.6	-8.2
Finland	FI	0	0	0	0	0	0	0	29.5	23.9	21.9	19.4	22.7	16.9	-5.9
France	FR	1.7	5.0	0.6	3.0	0	3	3	32.9	41.0	36.3	39.2	37.1	36.6	-0.5
Germany	DE	2.0	0	0	0	0.5	0.5	0.1	41.3	35.7	31.7	34.4	37.2	35.7	-1.5
Greece	GR	78.6	79.5	84.9	38.2	95.7	7.5	-88.3	54.3	53.0	64.9	54.7	64.8	37.6	-27.2
Hungary	HU	96.9	44	35.4	24.4	69.4	92.1	22.7	58.5	48.5	47.5	46.4	52.3	55.4	3.1
Iceland	IS	0.1	0	0	0	0.0	0	0.0	27.2	21.4	25.4	15.8	16.8	15.8	-1.0
Ireland	IE	0	0	0	0	0	0	0	24.1	24.8	25.8	21.7	23.2	23.2	-0.1
Italy	IT	58.4	63.3	46.2	31.9	31.2	39.5	8.3	58.6	57.4	51.7	48.6	45.2	48.6	3.4
Latvia	LV	0	0	0	0	0	0	0	40.0	31.9	32.7	33.4	37.8	26.7	-11.2
Liechtenstein	LI	0	0	0	0	0	0	0	47.5	39.3	38.5	31.5	33.6	21.3	-12.3
Lithuania	LT	0	0	0	0	0	0	0	39.7	33.2	29.5	32.7	39.5	26.6	-12.8
Luxembourg	LU	0	0	0	0	0	0	0	35.9	32.5	29.1	34.3	31.9	29.4	-2.5
Macedonia, FYR of	MK	74.5	78.3	73.8	80.3	87.7	3.5	-84.1	69.9	57.8	71.5	75.6	80.1	37.9	-42.2
Malta	MT	0	0	0	0	3.3	0	-3.3	44.8	42.6	40.3	38.7	49.4	39.7	-9.7
Monaco	MC	100	0	0	0	0	0	0	59.7	46.2	46.0	41.5	36.1	37.0	1.0
Montenegro	ME	69.5	71.6	70.8	65.7	66.9	12.3	-54.6	57.9	53.6	56.7	51.8	54.0	36.2	-17.8
Netherlands	NL	3.9	0	0	0	0	0	0	46.1	41.9	37.7	39.0	40.2	44.0	3.8
Norway	NO	0	0	0	0	0	0	0	31.9	26.3	26.1	24.0	25.7	16.3	-9.4
Poland	PL	75.2	47.1	38.3	60.5	71.3	41.3	-30.0	64.0	50.8	48.6	55.4	65.7	51.4	-14.3
Portugal	PT	57.2	24	0	0	0.2	4.9	4.7	48.3	45.0	35.5	38.5	35.6	35.4	-0.2
Romania	RO	91.2	73.0	53.5	39.8	28.2	43.3	15.1	65.4	57.7	53.1	49.0	45.2	48.1	2.9
San Marino	SM	84.8	100	25.9	0	0	0	0	57.4	54.1	48.9	40.6	44.0	35.9	-8.1
Serbia (incl. Kosovo)	RS	87.5	81.5	77.5	77.8	80.5	52.9	-27.6	73.1	61.8	68.6	67.6	60.1	54.6	-5.5
Slovakia	SK	83.8	43.7	38.2	33.5	82.3	62.4	-20.0	58.5	50.5	47.5	46.2	56.0	51.5	-4.5
Slovenia	SI	63.3	40	5.5	0	38.6	39.1	0.5	49.2	46.1	42.7	41.9	47.2	48.1	1.0
Spain	ES	55.6	40.5	12.5	1.0	0.1	1.1	0.9	49.3	46.9	40.1	38.0	33.4	30.5	-3.0
Sweden	SE	0	0	0	0	0	0	0	32.0	25.8	26.4	23.3	22.1	21.1	-1.0
Switzerland	CH	8.3	2.5	1.9	0.9	0	1.3	1.3	43.9	39.9	36.5	37.1	36.3	33.0	-3.3
United Kingdom	UK	0	0	0	0	0	0	0	35.5	34.7	32.1	30.1	28.8	30.3	1.4
Total		**35.7**	**26.2**	**19.4**	**16.5**	**20.6**	**15.8**	**-4.9**	**47.8**	**44.1**	**41.3**	**41.2**	**41.9**	**39.0**	**-2.9**
EU-28		**34.5**	**24.7**	**17.3**	**14.6**	**18.8**	**15.4**	**-3.4**	**47.2**	**43.8**	**40.5**	**40.5**	**41.3**	**39.0**	**-2.3**

It has been estimated that in 2011 almost 16 % of the European population lived in areas where the 36th highest daily mean of PM_{10} exceeded the limit value of 50 µg.m^{-3}. This is less than in its five previous years (4.9 % lower than in 2010, 0.7 % lower than in 2009 and 3.6 % lower than in 2010). In Hungary, Serbia and Slovakia still both the population-weighted indicator concentration and the median were above the LV, implying that in these countries the average concentration exceeded the LV and more than half of the population was exposed to concentrations exceeding the LV. Poland has a population-weighted concentration just above the LV, but its median dropped below the LV to 41 % of the population. In comparison with 2010, a decrease of both population above the LV and

population-weighted concentration occurs in many countries of south-eastern Europe (in Albania, Bosnia-Herzegovina, Bulgaria, Croatia, Cyprus, Greece, Montenegro, FYROM of Macedonia). However, the lack of the rural stations in these countries should be noted, i.e. the decrease is detected especially by the EMEP model. Apart of this area, a decrease of both exposure indicators is detected in Czech Republic, Poland and Slovakia, while an increase in Romania, Hungary and Italy.

In the EU, more than 15 % of the population lived in areas above the limit value. According to EEA (2013), about 33 % of the urban population in the EU was exposed to PM_{10} above the limit value. The difference of the two numbers is caused by the fact that in the EEA estimate only the urban population in the larger cities is taken into account, while in Table 4.8 the total population, including inhabitants in rural areas, smaller cities and villages is considered.

The European-wide population-weighted concentration of the 36th highest daily mean is estimated for the year 2011 at 39.0 µg.m^{-3}, being the lowest in the period of 2006 – 2011.

Comparing observed PM_{10} exceedances in 2011 (annual average of section 4.1.2, with 36th highest daily average in this section) one can conclude that the daily average limit value is the most stringent of the two. This conclusion was also drawn in the earlier reports.

4.2.3 Uncertainties

Uncertainty estimated by cross-validation

Cross-validation analysis determines the uncertainty. For the combined map of PM_{10} indicator 36th highest daily mean in 2010, Table 4.6 shows an absolute mean uncertainty (expressed as the RMSE) of 8.4 µg.m^{-3} for rural areas and 13.0 µg.m^{-3} for urban areas. For previous years, the values were 8.4 µg.m^{-3} and 12.2 µg.m^{-3} (2010), 8.0 µg.m^{-3} and 13.2 µg.m^{-3} (2009), 8.8 and 12.7 µg.m^{-3} (2008), 8.0 and 9.1 µg.m^{-3} (2007), 13.3 and 9.9 µg.m^{-3} (2006) and 9.8 and 11.7 µg.m^{-3} (2005). This indicates that both rural and urban maps may differ from year to year somewhat in their levels of uncertainty. The relative mean uncertainty (absolute RMSE relative to the mean indicator value) of the 2011 map of PM_{10} indicator 36th highest daily mean is 23.5 % for rural areas and 24.3 % for urban areas. The previous years had: 24.4 and 23.7 % (2010), 24.1 and 26.7 % (2009), 28.2 and 24.4 % (2008), 23.5 and 19.6 % (2007), 26.3 and 21.4 % (2006) and 26.6 and 23.5 % (2005). In urban areas the higher uncertainty for 2008 – 2011, compared to its preceding years is caused specifically by Turkish urban background stations reported and used in the calculations as of 2008. (An interpolation result for Turkey is not presented in the map due to lack of population density data). Table 7.5 summarises both the absolute and relative uncertainties over the past six years.

Figure 4.7 shows the cross-validation scatter plots for both rural and urban areas. The R^2 indicates that for rural areas about 66 % and for urban areas about 75 % of the variability is attributable to the interpolation. Corresponding values with those of the 2010 map (64 % and 77 %), 2009 map (56 % and 72 %), 2008 map (52 and 79 %), the 2007 map (60 and 65 %), the 2006 map (56 and 65 %) and the 2005 map (55 and 75 %) show that the fit of 2010 is the best for rural and for urban areas comparable to some of the other years.

The scatter plots indicate that in areas with high concentrations the interpolation methods tend to underestimate the levels. For example, in urban areas (Figure 4.7, right panel) an observed value of 130 µg.m^{-3} would be estimated in the interpolation as about 110 µg.m^{-3}, i.e. about 15 % too low. For rural areas, the underestimation is slightly stronger.

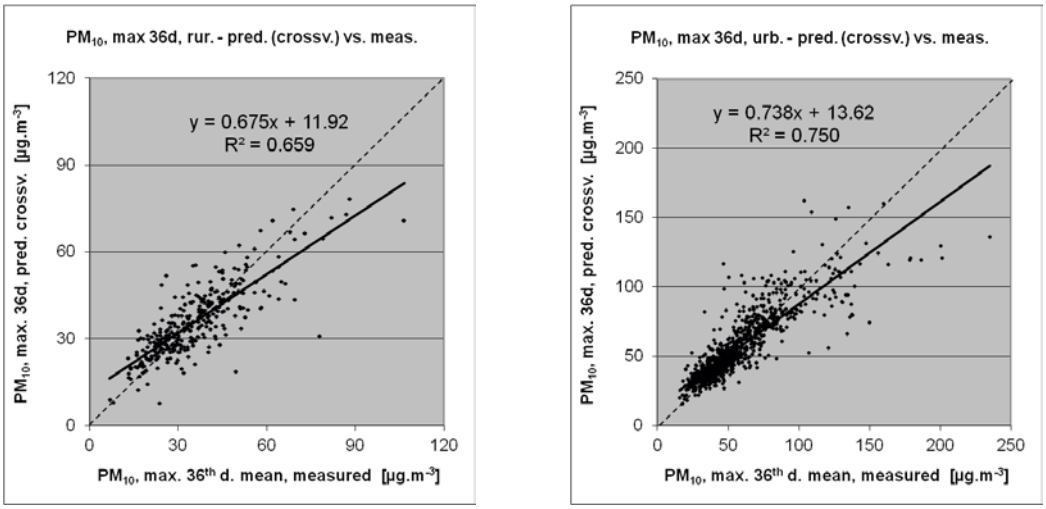

Figure 4.7 Correlation between cross-validation predicted values (y-axis) and measurements (x-axis) for the PM_{10} indicator 36th highest daily mean for 2011 for rural (left) and urban (right) areas. R^2 and the slope a (from the linear regression equation y = a·x + c) should be as close 1 as possible, the intercept c should be as close to 0 as possible.

Comparison of point measurement values with the predicted grid value

In addition to the point observation – point prediction cross-validation, a simple comparison was made between the point observation values and interpolation predicted grid values. The results of the cross-validation compared to the gridded validation are summarised in Table 4.9. The uncertainty at measurement locations is caused partly by the smoothing effect of the interpolation and partly by the spatial averaging of the values in the 10x10 km grid cells. The level of smoothing, which leads to underestimation in areas with high values, is weaker in areas where measurements exist than in areas where a measurement point is not available. For example, in urban areas the predicted interpolation gridded value would be about 115 µg.m^{-3} at a corresponding station point with a measurement value of 130 µg.m^{-3}, i.e. an underestimation of 11 %. This is less than the underestimation of 16 % for such a location without a measurement value, discussed in the previous subsection.

Table 4.9 Linear regression equation and coefficient of determination R^2 from the scatter plots of (i) the predicted point values based on cross-validation and (ii) the aggregation into 10x10 km grid cells versus the measured point values for PM_{10} indicator 36th highest daily mean for rural and urban areas in 2011.

	rural areas		urban areas	
	equation	R^2	equation	R^2
i) cross-validation prediction (Fig 4.6)	y = 0.675x + 11.92	0.659	y = 0.738x + 13.62	0.75
ii) 10x10 km grid prediction	y = 0.751x + 8.31	0.826	y = 0.821x + 8.79	0.900

Probability of Limit Value exceedance map

Again, we constructed the map with the probability of the limit value exceedance (PoE), using an aggregated 10x10 km gridded concentration map (based on the 1x1 km combined final map), the 10x10 km gridded uncertainty map and the limit value (LV, 50 µg.m^{-3}). Figure 4.8 presents the probability of exceedance 10x10 km gridded map classifying the areas with probability of limit value exceedance below 25 % (little PoE) in green, between 25-50 % (modest PoE) in yellow, between 50-75 % (moderate PoE) in orange and above 75 % in red (large PoE). Section 4.1.3 explains in more detail the significance of the colour classes in the map.

Comparing the probabilities of exceedance (PoE) of 2010 (Horálek et al., 2013) and 2009 (see De Smet et al., 2012) with those of 2011, one can conclude that a decrease in the spatial extents and PoE levels in south-eastern Europe occurred in 2011. In particular, large areas of Greece and Cyprus

have decreased PoE, going mostly from red and orange areas in 2010 to yellow and green areas in 2011.

The Po Valley in northern Italy has quite a similar PoE pattern to 2009 and 2010. The areas with the increased PoE levels in southern Poland and north-eastern Czech Republic are smaller than in 2010, but still somewhat larger than in 2009.

Hungary, northern Serbia and eastern and southern Romania show larger areas with high PoE levels, in comparing with 2010 and 2009.

Western Belgium and north-western France have increased levels of PoE, going from green in 2010 back to yellow and orange in 2011 (like in 2009). Increased levels of PoE were detected also in the limited areas in the southern Spain and eastern France and in some French and Italian cities.

A decrease from orange in 2010 back to green (like in 2009) in a limited area of south-west Iceland was related with the decrease of the volcanic activity of Eyjafjallajökull.

It should be noted that the PoE is related to the aggregated 10x10 km grid. Thus, in other different places than shown in this map the PoE levels can be increased at the 1x1 km resolution (namely in some small cities). Next to this – keeping in mind that the interpolated maps refer to the rural or (sub)urban background situations only, it cannot be excluded that exceedances of limit values may occur at the many *hotspot* and traffic locations throughout Europe.

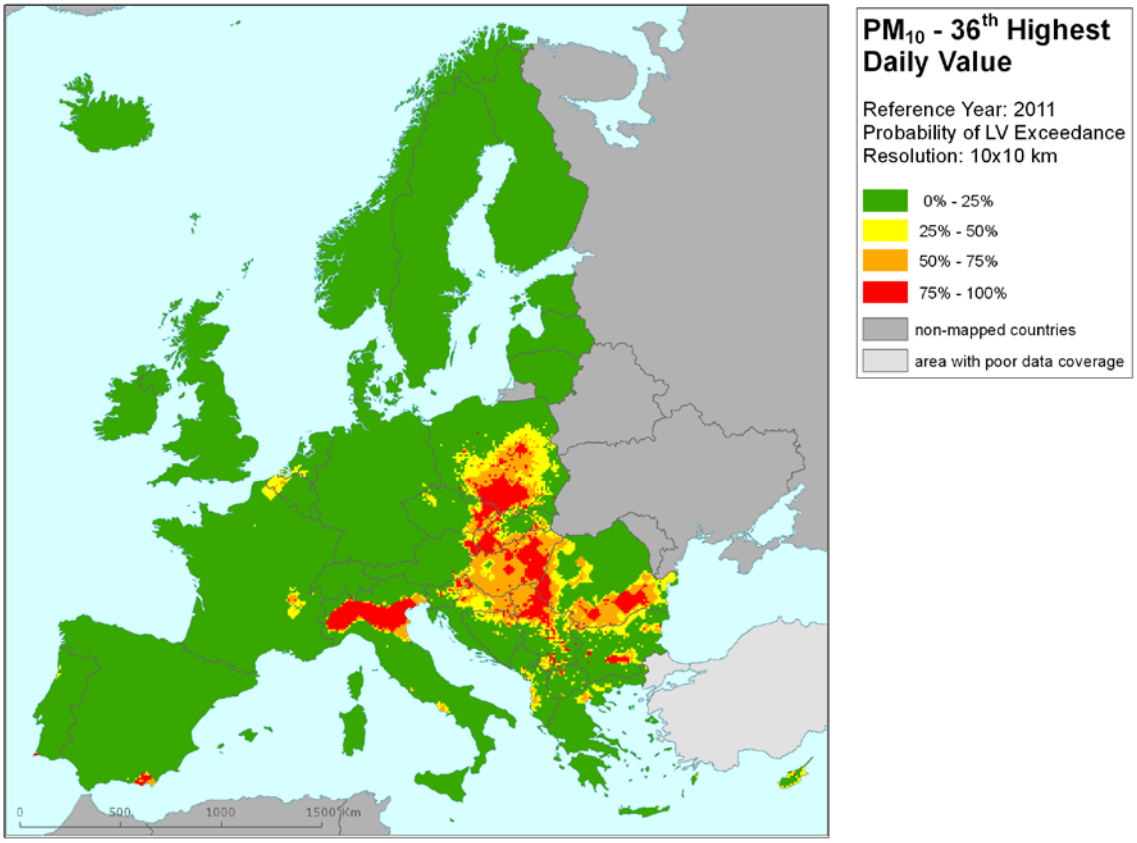

Figure 4.8 Map with the probability of the limit value exceedance for PM_{10} indicators 36th highest daily mean ($\mu g.m^{-3}$) for 2011 on the European scale calculated on the 10 x 10 km grid resolution. Interpolation uncertainty is considered only, no other sources of uncertainty.

5 $PM_{2.5}$ maps

This chapter presents for the second time in this annual report cycle the $PM_{2.5}$ health indicator annual average. The mapping methodology developed in Denby et al. (2011b, 2011c) was used. To increase the spatial coverage of measurements, pseudo $PM_{2.5}$ stations data were used in addition to measured $PM_{2.5}$ data. The separate urban and rural concentration maps were calculated on a grid of 10x10 km resolution and the subsequent combined concentration map was based on the 1x1 km gridded population density map. Population exposure tables are calculated on a grid of 1x1 km resolution. All maps are presented in at 10x10 km resolution. The standard EEA ETRS89-LAEA5210 coordinate reference system was applied.

5.1 Annual average

5.1.1 Concentration map

Figure 5.1 presents the combined final map for the 2011 $PM_{2.5}$ annual average as the result of the interpolation and merging of the separate maps as described in detail in De Smet et al. (2011), using both measured $PM_{2.5}$ and pseudo $PM_{2.5}$ station data, as described in Denby (2011c). The red and purple areas and stations exceed the limit value (LV) of 25 $\mu g.m^{-3}$. Pseudo $PM_{2.5}$ stations data are estimated using PM_{10} measured data, surface solar radiation, latitude and longitude. (Instead of latitude and longitude, the coordinates of ETRS89-LAEA5210 projection could be used alternatively.) Supplementary data in the regression used for rural areas consist of EMEP model output, altitude, wind speed, surface solar radiation and population density. Whereas for urban areas no supplementary data are used. The relevant supplementary data for both pseudo $PM_{2.5}$ station data estimation and the linear regression submodels used in residual kriging were identified earlier in Denby et al. (2011b, 2011c).

As one can observe in a few areas of the map, the high urban background measurement values do not seem to influence the interpolation results despite their clustering. The main reason is that the map presented here is an aggregation of 1x1 km grid values to a 10x10 km resolution and this aggregation smoothes out the elevated values one would more likely be able to distinguish in the higher resolution map, especially in the case of urban stations representing the urban background areas. Another less prominent reason is the smoothing effect kriging has in general. However, kriging would not, in the case of clustering, mask these elevations in the separate 1x1 km urban and rural maps.

Table 5.1 presents the regression coefficients determined for pseudo $PM_{2.5}$ stations data estimation, based on the stations with both $PM_{2.5}$ and PM_{10} measurements (see Section 2.1.1). The number of such stations is 468. The same supplementary data as in Denby (2011c) are used. Nevertheless, population was detected as statistically non-significant (like in 2010). The R^2 values show a weaker fit of the regression than observed in 2010 (0.95), but stronger than observed in the year 2008 (0.84) and similar as observed in the year 2007 (0.89). No $PM_{2.5}$ map was produced for 2009.

Table 5.1 Parameters of the linear regression model (Eq. 2.1) and its statistics for generation of pseudo $PM_{2.5}$ stations data, without regard to the rural or urban/suburban type of the stations, for $PM_{2.5}$ 2011 annual average.

linear regr. model	**both rural and urban areas**
	coeff.
c (constant)	28.81
b (PM_{10} measured data, 2011 annual avg.)	0.675
a1 (population)	n. sign.
a2 (surface solar radiation 2011)	-1.124
a3 (latitude)	-0.349
a4 (longitude)	0.118
adjusted R^2	**0.89**
standard error [$\mu g.m^{-3}$]	**2.62**

Table 5.2 presents the estimated parameters of the linear regression models (c, a_1, a_2,…) and of the residual kriging (*nugget*, *sill*, *range*) and includes the statistical indicators of both the regression and the kriging. The adjusted R^2 and standard error are indicators for the fit of the regression relation, where the adjusted R^2 should be as close to 1 as possible and the standard error should be as small as possible. The adjusted R^2 is 0.60 for the rural areas. The R^2 values show a better fit of the regression than observed at year 2010 (0.49), 2008 (0.44) and 2007 (0.48), while the analysis for 2009 was not conducted (Horálek et al., 2013; Denby et al. 2011c, Table 3). For urban areas, no supplementary data are used, see Denby et al. (2011c).

RMSE and bias are the cross-validation indicators, showing the quality of the resulting map; the bias indicates to what extent the estimation is un-biased. Only stations with measured (not pseudo) $PM_{2.5}$ data are used for calculating RMSE and bias. Section 5.1.3 deals with a more detailed cross-validation analysis.

Like in the case of PM_{10}, the linear regression is applied on the logarithmically transformed data of both measured and modelled $PM_{2.5}$ values. Thus, in Table 5.2 the standard error and variogram parameters refer to these transformed data, whereas RMSE and bias refer to the interpolation after the back-transformation.

As mentioned above, no supplementary data are used for the urban areas. Nevertheless, seeking higher agreement between the measured and modelled data (similar to the case of PM_{10}, Section 4.1) could lead to the decision of using supplementary data in future years. In order to explore this possibility, we examined as test case the use of the linear regression model with EMEP followed by kriging of its residuals in urban areas. The result of this exercise is a value of RMSE equal to 3.15 and a bias equal to 0.05, which is a better result than from the lognormal kriging with no supplementary data used in this year's mapping in Table 5.2. When for the next year's data the test result would be similar as for current 2011 data, we should consider implementing the EMEP model data as a default supplementary data source in the routine mapping of the urban areas from then onward.

Table 5.2 Parameters of the linear regression models (Eq. 2.2) and of the ordinary kriging variograms (nugget, sill, range) – and their statistics – of $PM_{2.5}$ indicator annual average for 2011 in rural areas (left) and urban (middle) areas as used for the combined final map, i.e. linear regression model P.Eawrp followed by interpolation of its regression residuals using ordinary kriging (OK), indicated by 'a' (rural areas, left) and lognormal kriging (LK), indicated by 'b' (urban areas, right). For the urban areas no regression on supplementary data was used (see the text).

linear regr. model + OK on its residuals	**rural areas (lnP.Eawrp-a) coeff.**	**urban areas (b) coeff.**
c (constant)	0.96	
a1 (log. EMEP model 2011)	0.694	
a2 (altitude GTOPO)	-0.00027	
a3 (wind speed 2011)	-0.054	
a4 (s. solar radiation 2011)	n. sign.	
a4 (log. population density)	0.038	
adjusted R^2	**0.60**	
standard error [µg.m^{-3}]	**0.28**	
nugget	0.026	0.019
sill	0.061	0.086
range [km]	240	670
RMSE [µg.m^{-3}]	**2.84**	**3.22**
bias (MPE) [µg.m^{-3}]	**-0.04**	**-0.06**

The merging of the separate rural and urban background maps takes place on the 1x1 km resolution map of population density.

According to Figure 5.1, the most polluted areas seem to be the Katowice (PL) and Ostrava (CZ) industrial region, together with the Po Valley in Northern Italy.

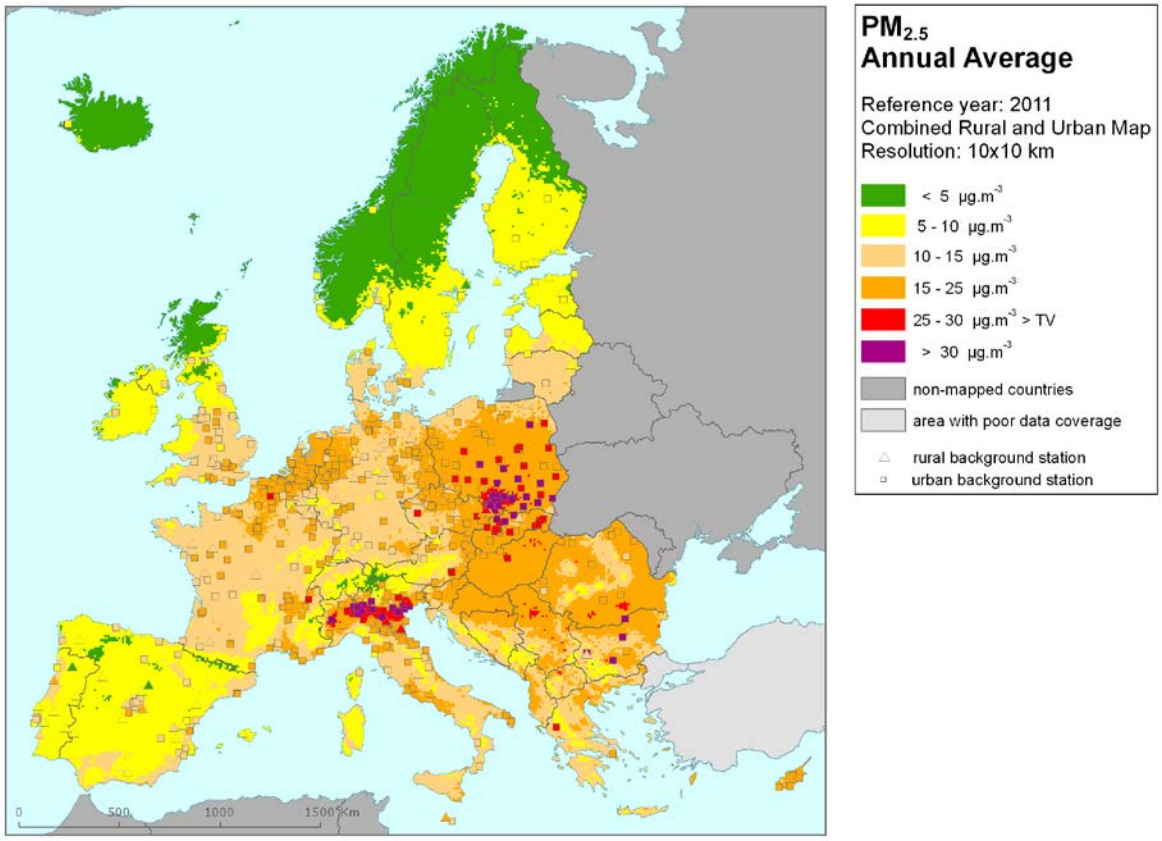

Figure 5.1 Combined rural and urban concentration map of $PM_{2.5}$ – annual average, year 2011. Spatial interpolated concentration field and the measured values in the measuring points. Units: $\mu g.m^{-3}$.

Figure 5.2 presents the interannual difference between 2011 and 2010 for annual average $PM_{2.5}$. Red areas show an increase of PM_{10} concentration, while blue areas show a decrease. The highest increases can be seen in the Po Valley, central Italy and large areas in the central and eastern European countries. Considerable decrease is observed for areas in southern and western Poland, eastern France, southern Spain and especially south-eastern Iceland with its steep increased concentration in 2010 due to the volcanic activity of Eyjafjallajökull (De Leeuw, 2012).

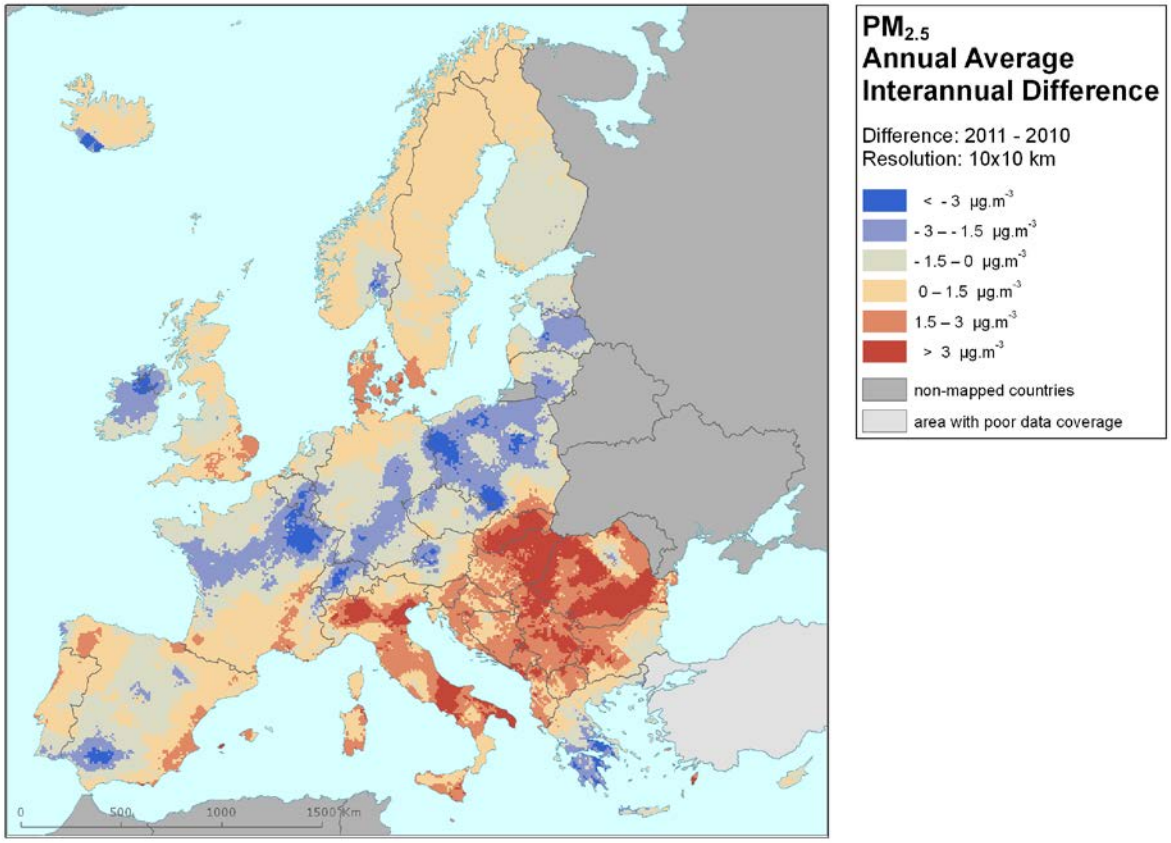

Figure 5.2 Interannual difference between mapped concentrations for 2011 and 2010 – $PM_{2.5}$, annual average. Units: µg.m^{-3}. Resolution: 10x10 km.

5.1.2 Population exposure

Table 5.3 gives the population frequency distribution for a limited number of exposure classes calculated on a grid of 1x1 km resolution, as well as the population-weighted concentration for individual countries and for Europe as a whole according to Equation 2.3.

Only 11 % of the European population in 2011 has been exposed to $PM_{2.5}$ annual mean concentrations below 10 µg.m^{-3}, the WHO (World Health Organization) air quality guideline (WHO, 2005). More than one third (38 %) of the population lived in areas where the $PM_{2.5}$ annual mean concentration is estimated to be between 10 and 15 µg.m^{-3}, while almost half (45 %) of the population lived in areas with $PM_{2.5}$ values between 15 and 25 µg.m^{-3}. About 6 % of the population lived in areas where the $PM_{2.5}$ annual target value (TV) is exceeded in 2011, with no country showing either a population-weighted concentration or a median above the target value. However, as the next section discusses, the current mapping methodology tends to underestimate high values. Therefore, the exceedance percentage will most likely be higher.

According to EEA (2013), about 15 % of the urban population in the EU and EEA-32 was exposed to $PM_{2.5}$ above the target value threshold in 2011. The difference with the estimated 6 % in Table 5.4 is caused by the different population taken into consideration. In the EEA estimate only the urban population in the larger cities is taken into account, while in Tables 5.3 and 5.4 it concerns the total population, including that of smaller cities, towns, villages and the rural areas.

The comparison of the $PM_{2.5}$ exposures of Table 5.2 with that of the PM_{10} exposure of Table 4.2 shows the $PM_{2.5}/PM_{10}$ ratio of population-weighted concentrations to be about 0.7 or 0.8, for most

countries. The exceptions are Portugal, Spain and Malta (0.5 or 0.6); a plausible cause might be the influence of Saharan dust containing there a relative large fraction of coarse particles. Other exceptions are Iceland (0.5) and Ireland (0.6), where a large fraction of coarse particle may originate from volcanic activity, especially in the case of Iceland.

Table 5.3 Population exposure and population-weighted concentration – $PM_{2.5}$, annual average, year 2011. Resolution: 1x1 km.

Country		Population	$PM_{2.5}$ annual average, exposed population [%]						Population-weighted conc.
			< TV				> TV		
			< 5	5 - 10	10 - 15	15 - 25	25 - 30	> 30	
		x 1000	µg.m^{-3}	µg.m^{-3}	µg.m^{-3}	µg.m^{-3}	µg.m^{-3}	µg.m^{-3}	[µg.m^{-3}]
Albania	AL	2 832		0.8	28.6	69.0	1.6		17.2
Andorra	AD	85	11.3	6.9		81.8			13.7
Austria	AT	8 404	0.6	10.6	29.2	59.5			16.3
Belgium	BE	11 001		0.6	13.3	86.1			17.3
Bosnia & Herzegovina	BA	3 843		3.2	37.4	51.2	8.2		17.2
Bulgaria	BG	7 369		3.0	35.0	53.5	1.3	7.1	18.3
Croatia	HR	4 290		0.5	21.8	75.5	2.2		19.6
Cyprus	CY	840			1.4	97.9	0.8		21.0
Czech Republic	CZ	10 487		0.3	17.5	72.0	5.1	5.0	18.8
Denmark	DK	5 561	0.8	6.2	84.8	8.2			12.5
Estonia	EE	1 336	0.0	100.0					8.0
Finland	FI	5 375	1.6	98.4					7.4
France	FR	64 995	0.0	3.8	45.6	50.6			15.3
Germany	DE	81 752	0.0	2.0	51.2	46.8			14.8
Greece	GR	11 123		0.8	35.9	56.3	6.8	0.2	16.8
Hungary	HU	9 986			0.0	77.8	22.2		23.1
Iceland	IS	318	61.1	38.9					4.6
Ireland	IE	4 571	0.7	93.1	6.2				7.9
Italy	IT	60 626	0.0	3.0	27.3	47.9	12.0	9.7	19.8
Latvia	LV	2 075		35.1	64.9				11.1
Liechtenstein	LI	36		93.6	6.4				8.5
Lithuania	LT	3 053		0.9	95.0	4.1			12.7
Luxembourg	LU	512		1.7	98.3				13.3
Macedonia, FYR of	MK	2 057		2.2	46.8	48.1	0.3	2.5	15.8
Malta	MT	415		0.0	22.4	77.6			15.6
Monaco	MC	35				100.0			16.4
Montenegro	ME	620		19.0	32.7	43.4	4.9		15.1
Netherlands	NL	16 656		0.0	4.3	95.7			17.1
Norway	NO	4 920	32.0	63.8	4.2				6.3
Poland	PL	38 530		0.0	7.0	68.6	14.3	10.1	21.8
Portugal	PT	10 573	0.0	42.0	58.0				10.5
Romania	RO	20 199		0.1	8.3	77.6	13.8	0.2	20.5
San Marino	SM	32			70.3	29.7			14.7
Serbia (incl. Kosovo)	RS	9 046		0.5	11.2	70.0	5.7	12.6	21.2
Slovakia	SK	5 392			1.3	93.3	4.0	1.4	21.8
Slovenia	SI	2 050		0.1	9.3	90.7			19.4
Spain	ES	46 667	0.2	33.7	59.4	6.7			11.1
Sweden	SE	9 416	6.6	75.2	18.2				8.1
Switzerland	CH	7 870	0.7	17.4	65.0	16.9			12.6
United Kingdom	UK	63 024	0.6	13.2	71.0	15.1			12.4
Total		**537 972**	**0.6**	**10.6**	**37.9**	**44.7**	**3.9**	**2.3**	**15.9**
			11.2				**6.2**		

Note1: Turkey is not included in the calculation due to lacking air quality data.
Note2: The percentage value "0.0" indicates an exposured population exists, but is small and estimated less than 0.05 %.
Empty cells mean: no population in exposure.

Considering the average for the whole of Europe, the overall population-weighted annual mean $PM_{2.5}$ concentration in 2011 was 15.9 µg.m^{-3}. This is slightly different from previous years: 0.9 µg.m^{-3} lower than in 2010 (16.8 µg.m^{-3}) and 0.5 µg.m^{-3} higher than in both 2008 and 2007 (16.3 µg.m^{-3}). The numbers for 2007 and 2008 were calculated using 1x1 km resolution (while preparing the paper Denby et al., 2011c). No numbers exist for 2009, as no map was produced for 2009.

Table 5.4 shows the evolution of the population exposure in the last years. However, only population exposure for 2007, 2008 and 2010 have been earlier calculated, see Horálek et al. (2013), not for 2009. For all the years presented, the same mapping method is used.

Table 5.4 Evolution of percentage population living in above target value (left) and population-weighted concentration (right) in the years 2007-2011 – $PM_{2.5}$, annual average. Resolution: 1x1 km.

Country		Population above TV 25 µg.m^{-3} [%]						Population-weighted conc. [µg.m^{-3}]					
		2007	2008	2009	2010	2011	diff. '11 - '10	2007	2008	2009	2010	2011	diff. '11 - '10
Albania	AL	1.6	1.6		53.4	1.6	-51.8	20.8	19.6		25.1	17.2	-7.9
Andorra	AD	0	0		0	0	0	11.5	11.3		12.4	13.7	1.3
Austria	AT	0	0		0	0	0	16.3	16.4		17.7	16.3	-1.4
Belgium	BE	0	0		0	0	0	16.6	17.1		18.8	17.3	-1.4
Bosnia-Herzegovina	BA	12.8	10.9		47.2	8.2	-39.0	21.7	20.3		22.2	17.2	-5.0
Bulgaria	BG	68.8	68.4		60.9	8.4	-52.4	28.8	28.4		24.5	18.3	-6.1
Croatia	HR	0.2	0		1.0	2.2	1.2	19.5	18.5		20.0	19.6	-0.4
Cyprus	CY	77.6	79.6		0	0.8	0.8	25.0	25.3		21.8	21.0	-0.8
Czech Republic	CZ	8.0	8.3		15.7	10.2	-5.5	17.5	17.7		21.5	18.8	-2.7
Denmark	DK	0	0		0	0	0	11.5	11.1		11.4	12.5	1.1
Estonia	EE	0	0		0	0	0	8.8	8.9		8.9	8.0	-1.0
Finland	FI	0	0		0	0	0	7.7	7.4		7.8	7.4	-0.4
France	FR	0	0		0	0	0	14.9	14.7		16.2	15.3	-0.9
Germany	DE	0	0		0	0	0	14.0	14.1		16.3	14.8	-1.6
Greece	GR	18.5	18.4		6.3	7.0	0.8	22.0	21.7		20.0	16.8	-3.3
Hungary	HU	0	0		6.7	22.2	15.5	19.3	19.4		20.3	23.1	2.9
Iceland	IS	0	0		0	0	0	7.1	7.1		6.9	4.6	-2.3
Ireland	IE	0	0		0	0	0	8.5	9.6		10.3	7.9	-2.4
Italy	IT	12.4	12.3		6.0	21.8	15.8	19.0	19.1		17.5	19.8	2.3
Latvia	LV	0	0	not	0	0	0	15.3	16.4	not	14.7	11.1	-3.6
Liechtenstein	LI	0	0	mapped	0	0	0	15.5	15.5	mapped	15.3	8.5	-6.8
Lithuania	LT	0	0		0	0	0	13.8	15.5		15.6	12.7	-2.9
Luxembourg	LU	0	0		0	0	0	13.9	14.5		15.8	13.3	-2.5
Macedonia, FYR of	MK	61.5	61.0		73.8	2.8	-70.9	24.4	23.6		27.5	15.8	-11.7
Malta	MT	0	0		0	0	0	14.9	14.9		13.8	15.6	1.8
Monaco	MC	0	0		0	0	0	16.5	16.5		14.9	16.4	1.5
Montenegro	ME	12.6	12.6		64.6	4.9	-59.7	21.4	19.9		24.6	15.1	-9.4
Netherlands	NL	0	0		0	0	0	16.9	17.0		17.6	17.1	-0.4
Norway	NO	0	0		0	0	0	8.6	8.2		8.8	6.3	-2.5
Poland	PL	20.6	21.0		53.1	24.4	-28.7	20.8	21.1		26.4	21.8	-4.6
Portugal	PT	0	0		0	0	0	11.5	10.9		10.5	10.5	0.1
Romania	RO	28.5	27.7		7.8	14.0	6.3	22.4	21.8		17.0	20.5	3.5
San Marino	SM	0	0		0	0	0	18.2	18.2		16.3	14.7	-1.7
Serbia (incl. Kosovo)	RS	69.4	64.7		30.6	18.3	-12.3	26.6	25.4		22.7	21.2	-1.4
Slovakia	SK	12.4	11.5		14.3	5.4	-8.9	20.2	20.6		21.3	21.8	0.5
Slovenia	SI	0	0		0	0	0	18.5	18.0		19.0	19.4	0.4
Spain	ES	0	0		0	0	0	14.1	13.6		11.8	11.1	-0.8
Sweden	SE	0	0		0	0	0	9.2	8.8		8.1	8.1	0.0
Switzerland	CH	0	0		0	0	0	14.9	14.8		15.5	12.6	-3.0
United Kingdom	UK	0	0		0	0	0	12.2	12.5		13.0	12.4	-0.6
Total		**7.8**	**7.6**		**8.3**	**6.2**	**-2.1**	**16.3**	**16.3**		**16.8**	**15.9**	**-0.9**
EU-28		**6.4**	**6.3**		**7.1**	**6.2**	**-0.9**	**16.1**	**16.1**		**16.7**	**15.9**	**-0.7**

In comparison with the year 2010, an increase of both population above TV and population-weighted concentration can be observed for Italy, Hungary and Romania, while decreases are observed for Poland, Czech Republic and especially for the different countries of south-eastern Europe (i.e. Albania, Bosnia-Herzegovina, Bulgaria, FYROM of Macedonia, Montenegro, Serbia). The decrease in south-eastern Europe is in contrast with the increase of concentration levels in these areas as described by Figure 5.2. This difference has its cause in the fact that the maps are presented in a 10x10 km grid resolution and as such represent strongly the results of rural mapping that involve decreased concentration levels for the 2010-2011 period. As such, it masks the urban mapping results for these areas that show increased levels for this period of time. Besides, the exposure tables are based on 1x1 km population density map and as such strongly depend on the urban mapping results that involve increased levels for this period. However, the results for this area (and specifically for West-Balkan countries) are strongly influenced by the limited number of measurement stations in this area.

5.1.3 Uncertainties

Uncertainty estimated by cross-validation

Using RMSE as the most common indicator, the *absolute mean uncertainty* of the combined final map at areas 'in between' the station measurements can be expressed in µg.m^{-3}. Table 5.2 shows that the absolute mean uncertainty of the combined final map of $PM_{2.5}$ annual average expressed as RMSE is 2.8 µg.m^{-3} for the rural areas and 3.2 µg.m^{-3} for the urban areas. Alternatively, one can express this uncertainty in relative terms by relating the absolute RMSE uncertainty to the mean air pollution indicator value for all stations. This *relative mean uncertainty* of the combined final map of PM_{10} annual average is 16.8 % for rural areas and 16.7 % for urban areas. These relative uncertainty values fulfil the data quality objectives for models as set in Annex I of the air quality Directive 2008/50/EC (EC, 2008). Table 7.6 summarises both the absolute and relative uncertainties of different years. The decrease of uncertainties in 2011 is probably caused by an increased number of $PM_{2.5}$ stations.

Figure 5.3 shows the cross-validation scatter plots, obtained according to Section 2.3, for both the rural and urban areas. The R^2 indicates that for the rural areas about 82 % and for the urban areas about 80 % of the variability is attributable to the interpolation.

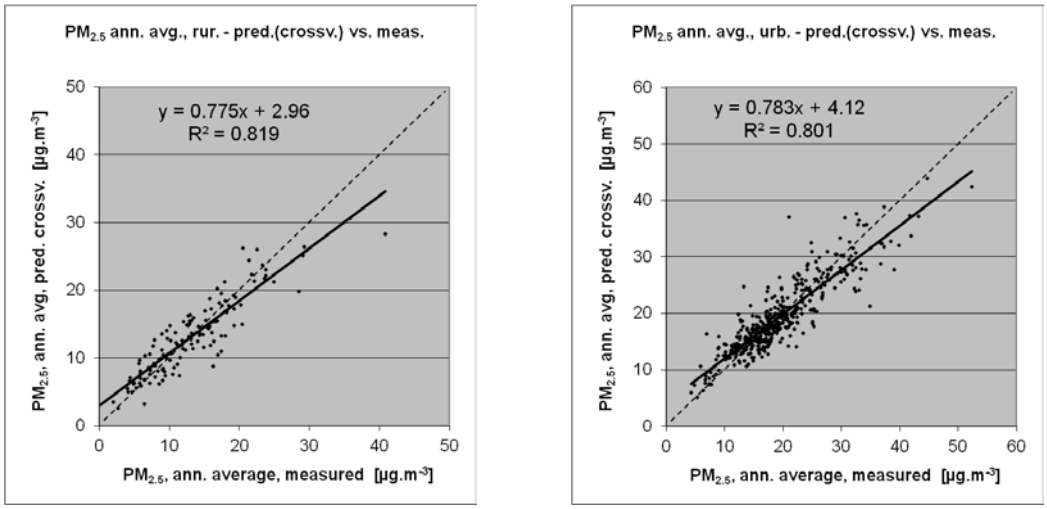

Figure 5.3 Correlation between cross-validation predicted values (y-axis) and measurements (x-axis) for the $PM_{2.5}$ annual average for 2011 for rural (left) and urban (right) areas. R^2 and the slope a (from the linear regression equation $y = a \cdot x + c$) should be as close 1 as possible, the intercept c should be as close 0 as possible

The scatter plots indicate that in areas with high concentrations the interpolation methods tend to underestimate the levels. For example, in rural areas an observed value of 25 µg.m^{-3} is estimated in the interpolations to be about 22 µg.m^{-3}, about 11 % too low. This underestimation at high values is an inherent feature of all spatial interpolations. It can be reduced by either using a higher number of the stations at improved spatial distribution, or introducing a closer regression by using other supplementary data.

Comparison of point measurement values with the predicted grid value

In addition to the above point observation – point prediction cross-validation, a simple comparison has been made between the point observation values and interpolated prediction values averaged in a 10x10 km resolution grid for the separate rural and urban background map. This point-grid comparison indicates to what extent the predicted value of a grid cell represents the corresponding measured values at stations located in that cell. The results of the point observation - point prediction cross-validation of Figure 5.3 compared to those of the point-grid validation are summarised in Table 5.4. The table shows a better correlated relation between station measurements and the interpolated values of the corresponding grid cells (i.e. higher R^2, smaller intercept and slope closer to 1) at both rural and urban map areas than it does at the point cross-validation predictions. That is because the simple comparison between point measurements and the gridded interpolated values shows the uncertainty at the actual station locations (points), while the point observation – point prediction cross-validation simulates the behaviour of the interpolation at positions without actual measurements within the area covered by measurements. The uncertainty at measurement locations is caused partly by the smoothing effect of the interpolation and partly by the spatial averaging of the values in the 10x10 km grid cells. The level of smoothing, which leads to underestimation in areas with high values, is weaker in areas where measurements exist than in areas where a measurement point is not available. For example, in rural areas the predicted interpolation gridded value will be about 23 µg.m^{-3} at the corresponding station point with the measured value of 25 µg.m^{-3}, i.e. an underestimation of about 8 %. This is less than the underestimation of 12 % for such a location without a measurement value, discussed in the previous subsection.

Table 5.4 Linear regression equation and coefficient of determination R^2 from the scatter plots of (i) the predicted point values based on cross-validation and (ii) the aggregated predictions into 10x10 km grid cells versus the measured point values for $PM_{2.5}$ indicator annual average for rural and urban areas of 2011.

	rural areas		urban areas	
	equation	R^2	equation	R^2
i) cross-validation prediction (Fig 5.2)	y =0.775x + 2.96	0.819	y = 0.783x + 4.12	0.801
ii) 10x10 km grid prediction	y = 0.849x + 1.80	0.929	y = 0.837x + 2.86	0.896

Probability of Target Value exceedance map

The probability of target value exceedance map was created for the $PM_{2.5}$ indicator in similar fashion to the PoE maps for PM_{10} indicators. This map at 10x10 km resolution is presented in Figure 5.4, with the Target Value (TV) of 25 µg.m^{-3}.

The areas with the highest probability of TV exceedance include the Po Valley in northern Italy with Turin and Milan, the region of southern Poland – north-eastern Czech Republic with the industrial zones of Krakow, Katowice and Ostrava, and the cities in the central part of Poland. Next to this, increased PoE does occur in south-eastern Europe, where relatively few measurement stations are located (for example, in some urban areas or larger agglomerations with mostly high traffic density and heavy industry). This includes Craiova and Bucharest in Romania. In the other parts of Europe, there exists little likelihood of exceedance.

In comparison with 2010, larger area in the Po Valley with the increased levels of PoE does occur. Next to this, more elevated PoE than in 2010 is visible in larger areas and some agglomerations of

Hungary, Serbia, Romania and Bulgaria (i.e. the shift from green to yellow and from yellow to orange and red). Contrary to that, there is a reduction of the areas with elevated levels of PoE in Poland.

It should be noted that the PoE is related to the aggregated 10x10 km grid. Thus, in other different places than shown in this map the PoE levels can be increased at the 1x1 km resolution (namely in some small cities). Next to this – keeping in mind that the interpolated maps refer to the rural or (sub)urban background situations only, it cannot be excluded that exceedances of limit values may occur at the many *hotspot* and traffic locations throughout Europe.

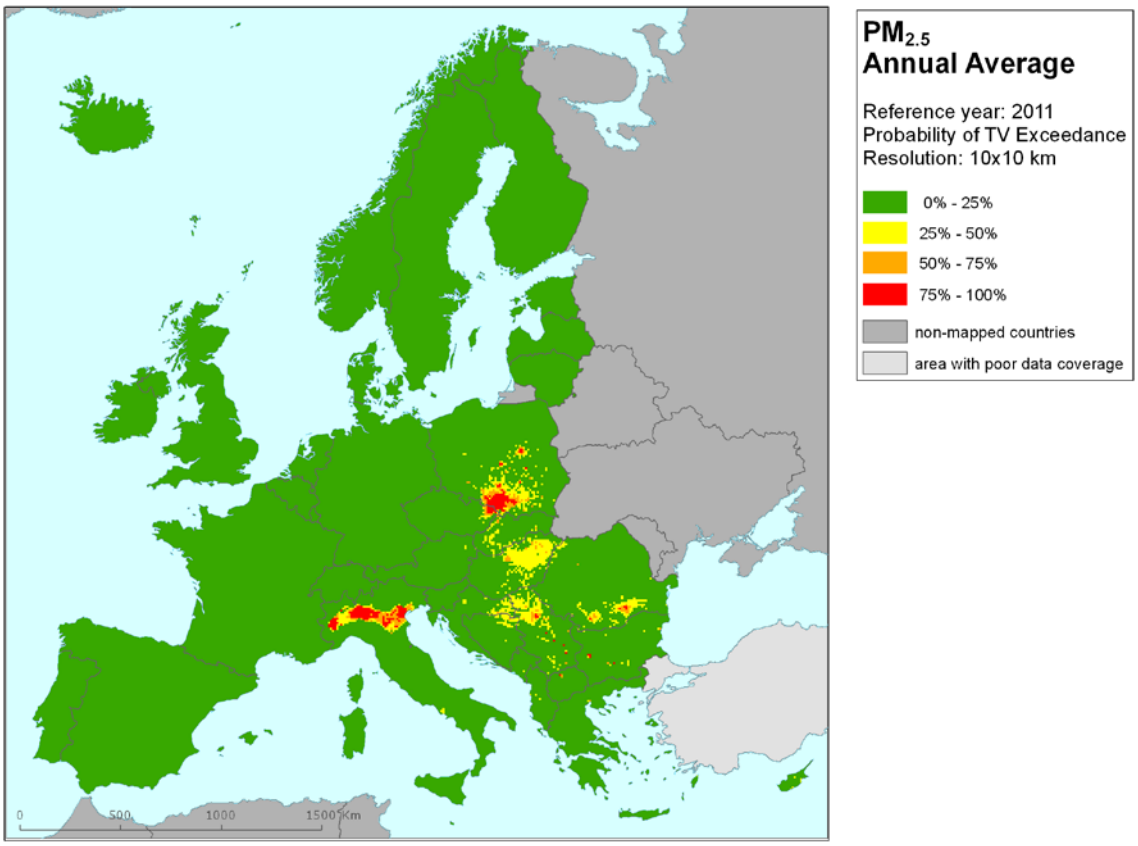

Figure 5.4 Map with the probability of the limit value exceedance for $PM_{2.5}$ annual average ($\mu g.m^{-3}$) for 2011 on European scale calculated on the 10 x 10 km grid resolution. Interpolation uncertainty is considered only.

6 Ozone maps

For ozone, the two health-related indicators (26th highest daily maximum 8-hour running mean and SOMO35) and the two vegetation-related indicators (AOT40 for crops and AOT40 for forests) are considered.

The separate urban and rural health-related indicator fields are calculated at a resolution of 10x10 km. The final health-related indicator maps are then created by combining rural and urban areas based on the 1x1 km resolution gridded population density map, as described in Chapter 2. We present the maps on a 10x10 km grid resolution.

The vegetation-related indicator maps are calculated and presented for rural areas only (assuming urban areas do not cover vegetation) and on a grid of 2x2 km resolution, covering the same mapping domain as at the human health indicators. This resolution serves the needs of the EEA Core Set Indicator 005 on ecosystem exposure to ozone. Map projection is the standard EEA ETRS89-LAEA5210.

During the analysis, it was discovered that in last year's report the maps of the ozone health related indicators (Horálek et al., 2013, Section 6.2 and 6.3) are based on an incorrect temporal aggregation of the EMEP model data. Therefore, the relevant 2010 maps and exposure tables have been recomputed, using the EMEP data correctly aggregated. See the Annex with the corrected maps and tables for the ozone health indicators 26th highest daily maximum 8-hour average and SOMO35. As can be observed, the changes in the corrected version compared to the maps and tables presented in Horálek et al. (2013) are only small. Nevertheless, for consistency we use the results presented in the Annex for 2010 in all the interannual comparisons addressed in this report.

6.1 26th highest daily maximum 8-hour average

6.1.1 Concentration map

Figure 6.1 presents the combined final map for 26th highest daily maximum 8-hour average as a result of combining the separate rural and urban interpolated map following the procedures as described in more detail in De Smet et al. (2011) and Horálek et al. (2007). Both separate maps were created by combining the measured ozone concentrations with supplementary data in a linear regression model, followed by kriging of its residuals. The supplementary data used in the regression model are EMEP model output, altitude and surface solar radiation for rural areas and EMEP model output, wind speed and surface solar radiation for urban areas, respectively. (The relevant linear regression models have been identified in the earlier reports and indicated as O.Ear and UO.Ewr respectively.)

Table 6.1 presents the estimated parameters of the linear regression models and of the residual kriging, including the statistical indicators of both the regression and the kriging. The fit of the 2011 regression relationship, expressed as the adjusted R^2, is 0.59 for rural areas and 0.51 for urban areas. These values are better than in most of the previous years: 2010 (0.56 and 0.51), 2009 (0.59 and 0.54), 2008 (0.41 and 0.43), 2007 (0.51 and 0.48), 2006 (0.40 and 0.43) and 2005 (0.45 and 0.51), see Annex, De Smet et al. (2012, 2011, 2010 and 2009) and Horálek et el. (2008). The numbers show that over the years the fit of the regressions are reasonably of the same order of magnitude at both the rural and the urban areas. RMSE and bias are the cross-validation indicators, showing the quality of the resulting map. Section 5.1.3 discusses in more detail the RMSE analysis and comparison with results of 2005 – 2010.

Table 6.1 Parameters of the linear regression models (Eq. 2.2) and of the ordinary kriging variograms (nugget, sill, range) – and their statistics – of ozone indicator 26th highest daily maximum 8-hour mean for 2011 in the rural (left) and urban (right) areas as used for the combined final map, i.e. linear regression model O.Ear (left), resp. UO.Ewr (right) followed by interpolation of its residuals using ordinary kriging (OK, coded 'a').

linear regr. model + OK on its residuals	rural areas (O.Ear-a) coeff.	urban areas (UO.Ewr-a) coeff.
c (constant)	6.8	23.9
a1 (EMEP model 2011)	0.84	0.75
a2 (altitude GTOPO)	0.0036	
a3 (wind speed 2011)		-2.03
a4 (s. solar radiation 2011)	0.90	0.49
adjusted R^2	**0.59**	**0.51**
standard error [µg.m^{-3}]	**9.36**	**11.01**
nugget	45	50
sill	76	79
range [km]	120	150
RMSE [µg.m^{-3}]	**8.44**	**9.09**
bias (MPE) [µg.m^{-3}]	**0.15**	**0.01**

In the combined final map of Figure 6.1 the red and purple areas and stations do exceed the target value (TV) of 120 µg.m^{-3}. Note that in Directive 2008/50/EC the target value is defined as 120 µg/m^3 not to be exceeded on more than 25 days per calendar year *averaged over three years*.

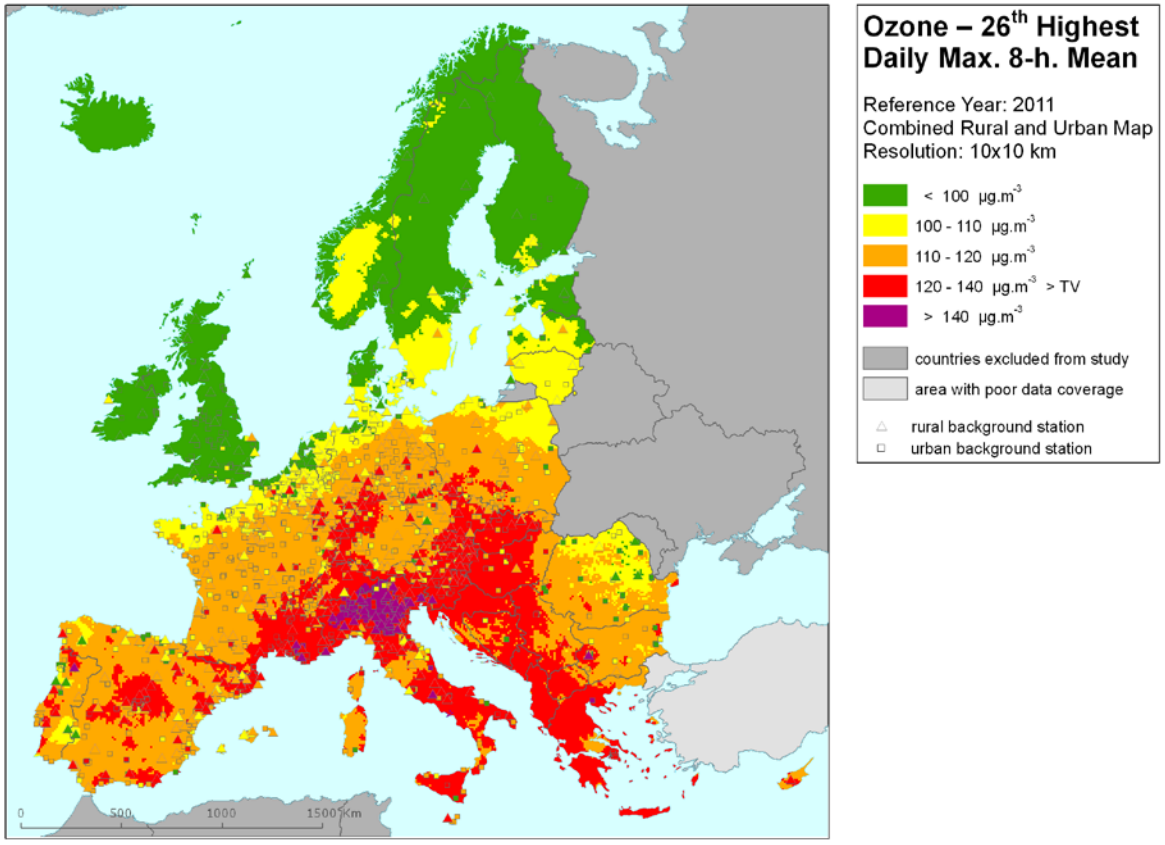

Figure 6.1 Combined rural and urban concentration map of ozone health indicator 26th highest daily maximum 8-hour value in µg.m^{-3} for the year 2011. Its target value is 120 µg.m^{-3}. Resolution: 10x10 km.

As one can observe in a few areas of the map, the high measurement values do not seem to influence the interpolation results despite their clustering. The main reasons are (i) that the map presented here is an aggregation of 1x1 km values to 10x10 km resolution and this aggregation smoothes out the elevated values, and (ii) the smoothing effect kriging has in general.

Figure 6.2 presents the interannual difference between 2011 and 2010 for 26th highest daily maximum 8-hour value. Red areas show an increase of ozone concentration, while blue areas show a decrease. The highest increases can be seen in south-eastern Europe (especially in Romania, Bulgaria, Serbia, FYR of Macedonia and northern Greece), in Belgium and the Netherlands, and in Italy. Considerable decreases are visible in Switzerland, Portugal and southern France. Most of these areas showed for the '2010 - 2009' difference the opposite effect.

The increases (and decreases) in south-eastern Europe are influenced by the limited number of observations in these countries.

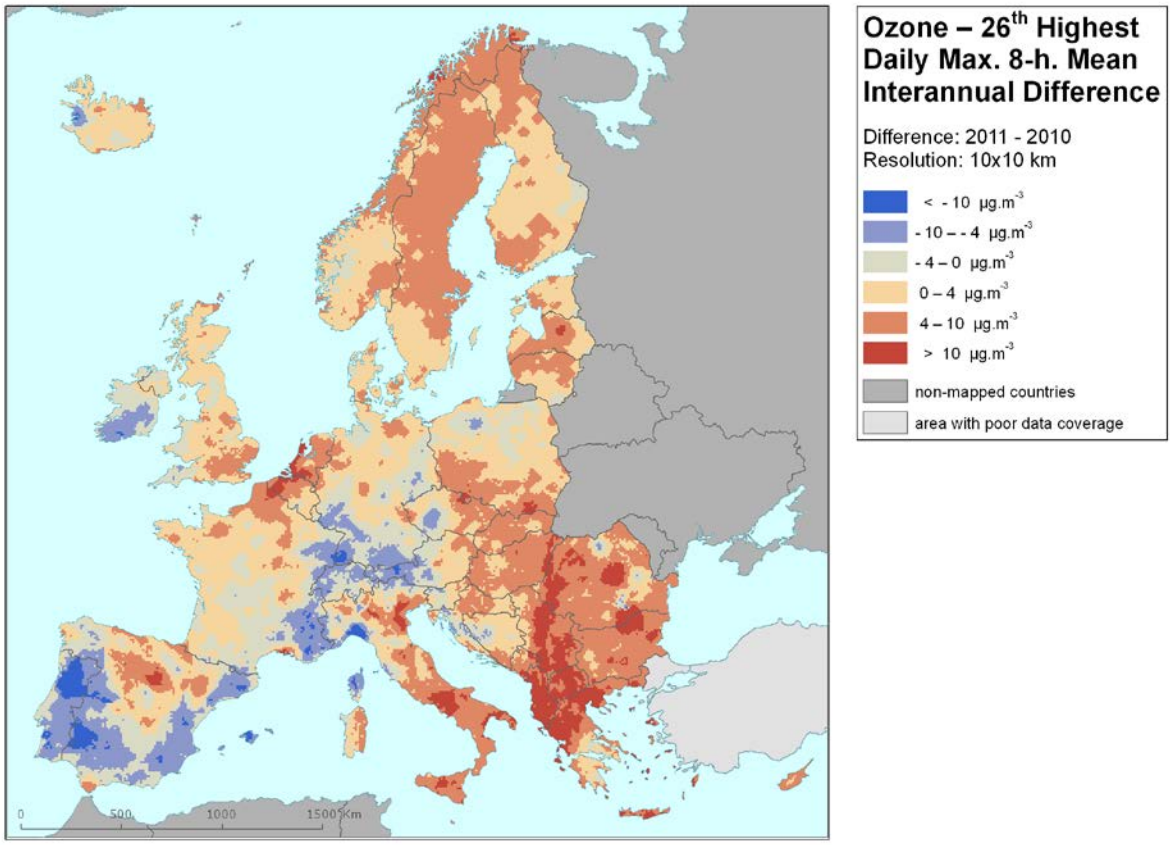

Figure 6.2 Interannual difference between mapped concentrations for 2011 and 2010 – ozone, 26th highest daily maximum 8-hour value. Units: µg.m^{-3}.

6.1.2 Population exposure

Table 6.2 gives, for 26th highest daily maximum 8-hour running mean, the population frequency distribution for a limited number of exposure classes, as well as the population-weighted concentration for individual countries and for Europe as a whole. In Table 6.3 the evolution of population exposure of the last five years is presented.

It has been estimated that in 2011 some 16.5 % of the European population lived in areas where the ozone concentration exceeded the target value (TV of 120 µg.m^{-3}) of the 26th highest daily maximum 8-hour mean. This is a similar level as in 2010 (16.3 %) and a minor increase compared to 2009

(16.0 %) and 2008 (15.0 %). Similar to previous years there are no exceedances in 2011 in Belgium and the Netherlands, Scandinavia and the Baltic countries, the UK, Ireland and Iceland.

Table 6.2 Population exposure and population weighted concentration – ozone, 26th highest daily maximum 8-hour mean for the year 2011.

Country		Population	Ozone, 26th highest dmax. 8-h, exposed population [%]					Population-weighted conc.
			< TV			> TV		
		[inhbs . 1000]	< 100 µg.m-3	100 - 110 µg.m-3	110 - 120 µg.m-3	120 - 140 µg.m-3	> 140 µg.m-3	[µg.m-3]
Albania	AL	2 832		0.0	47.3	52.6		121.1
Andorra	AD	85				100		120.6
Austria	AT	8 404		4.1	50.7	45.2	0.0	118.6
Belgium	BE	11 001	12.0	84.1	3.9			104.4
Bosnia & Herzegovina	BA	3 843	18.8	34.4	22.7	24.1		109.9
Bulgaria	BG	7 369	29.2	41.9	26.6	2.2		105.1
Croatia	HR	4 290		17.6	42.0	40.4		118.3
Cyprus	CY	840		47.4	48.3	4.3		112.0
Czech Republic	CZ	10 487		11.7	77.2	11.1		114.8
Denmark	DK	5 561	88.1	11.9	0.0			96.9
Estonia	EE	1 336	94.8	5.2				94.8
Finland	FI	5 375	98.0	2.0				93.0
France	FR	64 995	1.9	37.6	46.5	14.0	0.0	112.8
Germany	DE	81 752	0.5	34.8	60.8	3.8		111.5
Greece	GR	11 123	0.1	1.7	14.0	84.2		126.5
Hungary	HU	9 986	0.5	8.4	66.8	24.3		117.1
Iceland	IS	318	100					83.6
Ireland	IE	4 571	100					84.4
Italy	IT	60 626		4.0	27.0	46.7	22.2	127.7
Latvia	LV	2 075	76.8	23.2				96.3
Liechtenstein	LI	36			90.5	9.5		116.4
Lithuania	LT	3 053	29.4	70.6	0.0			101.4
Luxembourg	LU	512		54.7	43.5	1.8		110.4
Macedonia, FYR of	MK	2 057		3.4	78.9	17.7		117.4
Malta	MT	415		2.0	94.0	4.0		112.6
Monaco	MC	35				100		126.6
Montenegro	ME	620	2.5	22.8	43.7	31.0		115.1
Netherlands	NL	16 656	58.3	41.7				98.6
Norway	NO	4 920	96.7	3.3				93.7
Poland	PL	38 530	3.8	46.9	46.9	2.4		109.5
Portugal	PT	10 573	4.6	60.9	28.8	5.7		108.4
Romania	RO	20 199	64.4	18.5	16.3	0.7		91.1
San Marino	SM	32			86.2	13.8		117.9
Serbia (incl. Kosovo)	RS	9 046	7.2	27.3	49.0	16.5		112.0
Slovakia	SK	5 392		1.8	69.6	28.7		118.5
Slovenia	SI	2 050			0.5	99.5		125.5
Spain	ES	46 667	8.2	19.2	65.2	7.5		112.1
Sweden	SE	9 416	86.8	13.2				96.1
Switzerland	CH	7 870			59.4	38.3	2.3	120.8
United Kingdom	UK	63 024	99.6	0.4	0.0			87.8
Total		**537 972**	**24.1**	**23.4**	**36.0**	**14.0**	**2.5**	**108.9**
			83.5			**16.5**		

Note1: Turkey is not included in the calculation due to lack of air quality data.
Note2: The percentage value "0.0" indicates an exposured population exists, but is small and estimated less than 0.05 %.
Empty cells mean: no population in exposure.

Countries with a similar percentage in 2011 of inhabitants exposed to concentrations exceeding the target value as in 2009 and 2010 are Bulgaria (2 %), Poland (2 %), Luxemburg (2 %) and the small

states with no or few measurement stations, being San Marino (18 %), Andorra (100 %) and Monaco (100 %).

Table 6.3 Evolution of percentage population living in above target value (left) and population weighted concentration (right) in the years 2006-2011 – O_3, 26th highest daily maximum 8-hour mean. Resolution: 1x1 km.

Country		Population above TV 120 µg.m^{-3} [%]							Population-weighted conc. [µg.m^{-3}]						
		2006	2007	2008	2009	2010	2011	diff. '11 - '10	2006	2007	2008	2009	2010	2011	diff. '11 - '10
Albania	AL	24.9	67.6	6.6	13.2	0.0	52.6	52.6	117.9	126.9	115.3	114.7	109.5	121.1	11.5
Andorra	AD	26.8	18.9	78.2	13.5	100	100	0.0	119.1	118.6	122.0	115.6	122.4	120.6	-1.9
Austria	AT	84.8	67.3	13.7	14.5	26.8	45.2	18.4	124.9	122.8	114.8	116.4	118.4	118.6	0.2
Belgium	BE	94.1	0	0	0	0	0	0	126.0	98.9	103.6	101.5	97.7	104.4	6.6
Bosnia-Herzegovina	BA	34.9	63.8	7.5	25.7	16.5	24.1	7.6	118.1	122.5	113.7	114.5	107.4	109.9	2.5
Bulgaria	BG	0.8	34.2	6.6	16.3	0.3	2.2	1.9	105.0	115.7	114.4	112.0	103.8	105.1	1.3
Croatia	HR	79.6	85.8	8.8	19.2	20.3	40.4	20.1	124.8	124.7	115.5	115.6	114.3	118.3	4.0
Cyprus	CY	1.2	23.8	0.2	50.9	0.0	4.3	4.3	102.1	116.9	115.2	120.8	109.8	112.0	2.2
Czech Republic	CZ	95.6	59.1	6.8	6.6	0.9	11.1	10.2	126.5	121.0	114.6	113.5	114.1	114.8	0.7
Denmark	DK	0	0	0	0	0	0	0	104.9	95.2	102.6	95.5	91.4	96.9	5.5
Estonia	EE	0	0	0	0	0	0	0	105.1	94.1	96.3	90.8	97.2	94.8	-2.4
Finland	FI	0	0	0	0	0	0	0	100.7	89.0	94.3	90.6	92.2	93.0	0.8
France	FR	61.4	14.2	5.6	9.6	22.0	14.0	-8.0	122.0	109.0	107.3	107.3	111.6	112.8	1.3
Germany	DE	88.0	13.1	10.6	2.0	13.0	3.8	-9.2	125.8	113.3	113.5	108.8	112.8	111.5	-1.3
Greece	GR	34.6	76.7	84.5	59.4	43.2	84.2	41.0	115.8	126.5	131.1	122.8	119.4	126.5	7.1
Hungary	HU	69.3	85.9	28.6	85.6	3.5	24.3	20.8	121.7	125.0	117.5	124.2	110.9	117.1	6.2
Iceland	IS	0	0	0	0	0	0	0	93.3	81.1	90.8	81.4	78.3	83.6	5.4
Ireland	IE	0	0	0	0	0	0	0	90.2	84.2	92.1	84.9	85.6	84.4	-1.2
Italy	IT	88.8	71.6	55.2	57.3	48.8	69.0	20.2	135.1	129.5	123.2	125.8	124.3	127.7	3.4
Latvia	LV	0	0	0	0	0	0	0	104.5	95.8	94.9	91.9	93.2	96.3	3.1
Liechtenstein	LI	100	21.8	9.4	17.8	100	9.5	-90.5	127.3	119.9	119.4	118.9	123.3	116.4	-6.8
Lithuania	LT	0	0	0	0	0	0	0	110.1	98.1	102.0	95.8	96.9	101.4	4.5
Luxembourg	LU	100	0	0	0	2.9	1.8	-1.1	130.0	111.7	112.1	108.6	111.4	110.4	-1.0
Macedonia, FYR of	MK	15.0	29.7	78.4	16.6	0.0	17.7	17.7	110.3	121.1	121.0	111.3	109.0	117.4	8.4
Malta	MT	4.9	2.7	1.6	0	0.7	4.0	3.3	115.6	109.1	108.4	107.7	109.4	112.6	3.2
Monaco	MC	100	100	100	100	100	100	0	142.4	127.3	123.1	127.2	124.0	126.6	2.6
Montenegro	ME	23.7	35.4	12.3	14.5	5.3	31.0	25.7	114.3	122.3	118.1	111.7	108.6	115.1	6.4
Netherlands	NL	38.8	0	0	0	0	0	0	116.1	94.1	98.4	94.7	90.7	98.6	7.9
Norway	NO	0	0	0	0	0	0	0	101.7	91.3	99.0	94.0	88.8	93.7	4.9
Poland	PL	53.0	12.3	1.9	0.4	0.0	2.4	2.4	120.4	112.9	109.7	107.8	106.6	109.5	2.9
Portugal	PT	46.5	5.0	0.0	18.5	23.3	5.7	-17.5	119.4	111.0	102.7	112.4	112.0	108.4	-3.7
Romania	RO	0.6	36.7	3.1	8.0	0.0	0.7	0.7	105.7	116.9	110.1	108.8	94.0	91.1	-2.9
San Marino	SM	22.9	100	14.1	13.8	11.6	13.8	2.3	120.8	130.4	119.0	118.1	116.1	117.9	1.7
Serbia (incl. Kosovo)	RS	6.3	62.2	20.2	38.2	4.1	16.5	12.4	108.5	122.5	117.3	115.8	102.5	112.0	9.4
Slovakia	SK	66.5	69.2	24.0	88.3	1.1	28.7	27.5	122.2	122.2	116.4	122.7	112.8	118.5	5.7
Slovenia	SI	100	99.9	22.7	38.2	56.5	99.5	43.0	132.6	126.6	116.9	119.7	122.1	125.5	3.5
Spain	ES	42.5	24.6	16.8	18.1	30.7	7.5	-23.3	116.2	115.4	110.7	113.1	115.4	112.1	-3.3
Sweden	SE	0.1	0	0	0	0	0	0	104.5	93.5	97.6	94.2	91.2	96.1	4.9
Switzerland	CH	100.0	53.6	11.1	15.4	99.5	40.6	-58.9	132.6	120.1	116.8	117.3	124.7	120.8	-3.9
United Kingdom	UK	0.0	0	0	0	0	0	0	98.0	83.3	93.1	86.8	81.6	87.8	6.2
Total		**51.4**	**27.1**	**15.0**	**16.0**	**16.3**	**16.5**	**0.3**	**118.2**	**110.7**	**109.8**	**108.1**	**106.8**	**108.9**	**2.1**
EU-28		**52.4**	**25.6**	**14.3**	**15.7**	**15.5**	**16.8**	**1.3**	**118.3**	**110.2**	**109.5**	**107.8**	**106.8**	**108.7**	**1.9**

Increases in national population exposures are observed for 2011 compared to 2010; they can be categorized into three cases:

- Countries with a minor or small increase (up to 15%) in the population exposed to levels above the TV: Cyprus, Bosnia-Herzegovina, Serbia, and the Czech Republic.
- Countries with population exposures above the TV in 2009 that show a medium increase in 2011 of 15 - 30 %: Austria, Hungary, Slovakia, Italy, Croatia, Montenegro, FYR of Macedonia.
- Countries with remarkably large increases in the percentage of national population exposed: Albania (from 0 % in 2010 to 53 % in 2010), Greece (from 43 % to 84 %) and Slovenia (from 56 to 99 %). Results in these countries might be influenced by the limited number of observations.

For the decreases in national population exposures of 2011 compared to those of 2010, one observes three cases as well:

- Countries showing a small decrease of about 10 %: France, Germany.
- Countries of the Iberian Peninsula, showing a decrease of about 20 %: Spain, Portugal.
- Countries showing a large decrease: Switzerland (from 99 % in 2010 to 41 % in 2011) and Liechtenstein (from 100 % in 2010 to 10 % in 2011).

The population-weighted concentrations of Albania, Andorra, Greece, Italy, Liechtenstein, Monaco, Slovenia and Switzerland have been estimated, for 2011, to be above the TV. This is a similar set of countries as in 2010. About 50 % of the Albanians, 69 % of the Italians, 84 % of the Greeks, more than 99 % of the Slovenian population and all citizens of Andorra and Monaco were exposed to average levels above the TV. Part of the population in Switzerland (2 %) and more substantially in Italy (about 22 %) were estimated to be exposed to ozone levels of more than 140 $\mu g.m^{-3}$. As the current mapping methodology tends to underestimate high values due to interpolation smoothing, these actual numbers will most likely be higher. Most of the countries showed an increase in their population-weighted concentrations in 2011 compared to 2010, however, decreases most obviously occurred in Switzerland, Liechtenstein, Spain, Portugal, Estonia and Romania.

The overall European population-weighted ozone concentration in terms of the 26th highest daily maximum 8-hour mean was estimated for the year 2011 to be 109 $\mu g.m^{-3}$. That is an increase compared to the previous year.

6.1.3 Uncertainties

Uncertainty estimated by cross-validation

The basic uncertainty analysis is provided by cross-validation. Table 6.1 shows RMSE values of 8.4 $\mu g.m^{-3}$ for the rural areas and 9.1 $\mu g.m^{-3}$ for the urban areas of the combined final map. For previous years the values were for rural and urban areas respectively: 8.9 and 9.2 (2010) 8.2 and 9.3 (2009) 8.7 and 8.8 $\mu g.m^{-3}$ (2008), 8.8 and 8.9 $\mu g.m^{-3}$ (2007), 11.2 and 10.2 $\mu g.m^{-3}$ (2006) and 12.3 and 10.0 $\mu g.m^{-3}$ (2005) (Horálek et al. 2013 and 2008, De Smet et al. 2012, 2011, 2010 and 2009). The relative mean uncertainty of the 2011 ozone map is 7.2 % for rural areas and 8.1 % for urban areas. The previous years had for rural and urban areas respectively: 7.7 % and 8.2 % (2010), 7.2 % and 8.4 % (2009), 7.6 % and 7.9 % (2008), 7.5 % and 7.9 % (2007), 8.9% and 8.4 % (2006), 10.3 % and 8.9 % (2005). Table 7.7 summarises both the absolute and relative uncertainties over these past six years.

Figure 6.3 shows the cross-validation scatter plots for both the rural and urban areas of the 2011 map. The R^2, an indicator for the interpolation correlation with the observations, shows that for the rural areas about 67 % and for the urban areas about 66 % of the variability is attributable to the interpolation. Corresponding values for the 2010 map (68 % and 71 %), 2009 map (69 % and 64 %),

2008 map (56 % and 61 %), 2007 map (71 % and 66 %), the 2006 map (49 % and 53 %) and the 2005 map (51 % and 50 %), show a lower urban fit of the 2011 urban interpolations than in 2010. However, a better fit than in 2009, 2008, 2006 and 2005 and the same as in 2007 occurs. The rural interpolations for 2011 are in line with the quality of 2010, 2009 and 2007 and fit better than in the years 2005, 2006 and 2008.

The scatter plots indicate that the higher values are underestimated and the lower values somewhat overestimated by the interpolation method; a typical smoothing effect inherent to interpolation method of the linear regression and its residuals kriging. For example, in rural areas (Figure 6.3, left panel) an observed value of 150 µg.m^{-3} is estimated in the interpolation as 140 µg.m^{-3}, which is 7 % too low.

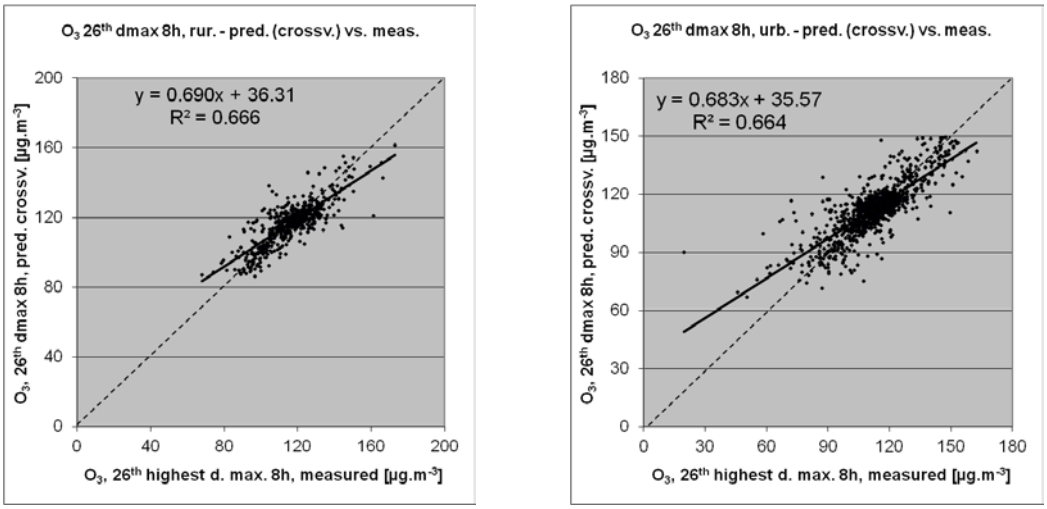

Figure 6.3 Correlation between cross-validation predicted values (y-axis) and measurements (x-axis) for the ozone indicator 26th highest daily maximum 8-hour mean for rural (left) and urban (right) areas in 2011.

Comparison of point measurement values with the predicted grid value

In addition to the point observation – point prediction cross-validation, a simple comparison was made between the point observation values and interpolated predicted grid values. The results of the cross-validation compared to the gridded validation examination are summarised in Table 6.4. The uncertainty at measurement locations is caused partly by the smoothing effect of interpolation and partly by the spatial averaging of the values in the 10x10 km grid cells The level of smoothing, which leads to underestimation in areas with high values, is weaker in areas where measurements exist than in areas where a measurement point is not available. For example, in rural areas the predicted interpolation grid value will be about 138 µg.m^{-3} at the corresponding station point with the observed value of 143 µg.m^{-3}, i.e. an underestimation of about 3.6 %. This is less than the underestimation of 7 % for such a location without a measurement value, discussed in the previous subsection.

Table 6.4 Linear regression equation and coefficient of determination R^2 from the scatter plots of (i) the predicted point values based on cross-validation and (ii) aggregation into 10x10 km grid cells versus the measured point values for the ozone indicator 26th highest daily maximum 8-hour mean for rural and urban areas of 2011.

	rural areas		urban areas	
	equation	R^2	equation	R^2
i) cross-validation prediction (Fig 6.3)	y = 0.690x + 36.31	0.666	y = 0.683x + 35.57	0.664
ii) 10x10 km grid prediction	y = 0.803x + 23.00	0.868	y = 0.767x + 26.20	0.817

Probability of Target Value exceedance map

A gridded map of 10x10 km resolution showing the probability of target value exceedance is in Figure 6.4. It was constructed on the basis of the 10x10 km gridded concentration map (Figure 6.1, derived from the 1x1 km resolution results), the 10x10 km gridded uncertainty map and the target value (TV) of 120 µg.m^{-3}. Section 4.1.3 explains the significance of the colour classes in the map.

The PoE map for 2011 was compared with 2005 – 2010. It becomes evident that after the year 2006 with its temporary increase in PoE to levels above 50 % and even above 75 % in large parts of specifically central Europe, a decrease took place in the levels of PoE in 2007 – 2011, to levels in many areas well below those of 2005. In 2011, most of the red areas (large PoE) in the northern Italy, southern France and Slovenia did not change compared to 2010.

In south-eastern Europe and in southern Italy there were clear increases of the areas with elevated PoE. The small number of rural stations in this area means high sensitivity of the map to the values measured at these relative few stations.

On the Iberian Peninsula we observe reduced areas with large PoE (red). A minor decrease was visible also in some areas of central Europe, changing from yellow to green.

The meteorologically induced variations from year to year, combined with methodological uncertainties and the limited number of years considered here do not allow for conclusions on whether, or not, there is any significant tendency in this ozone indicator. For that purpose, one would need a longer time series and reduced uncertainties.

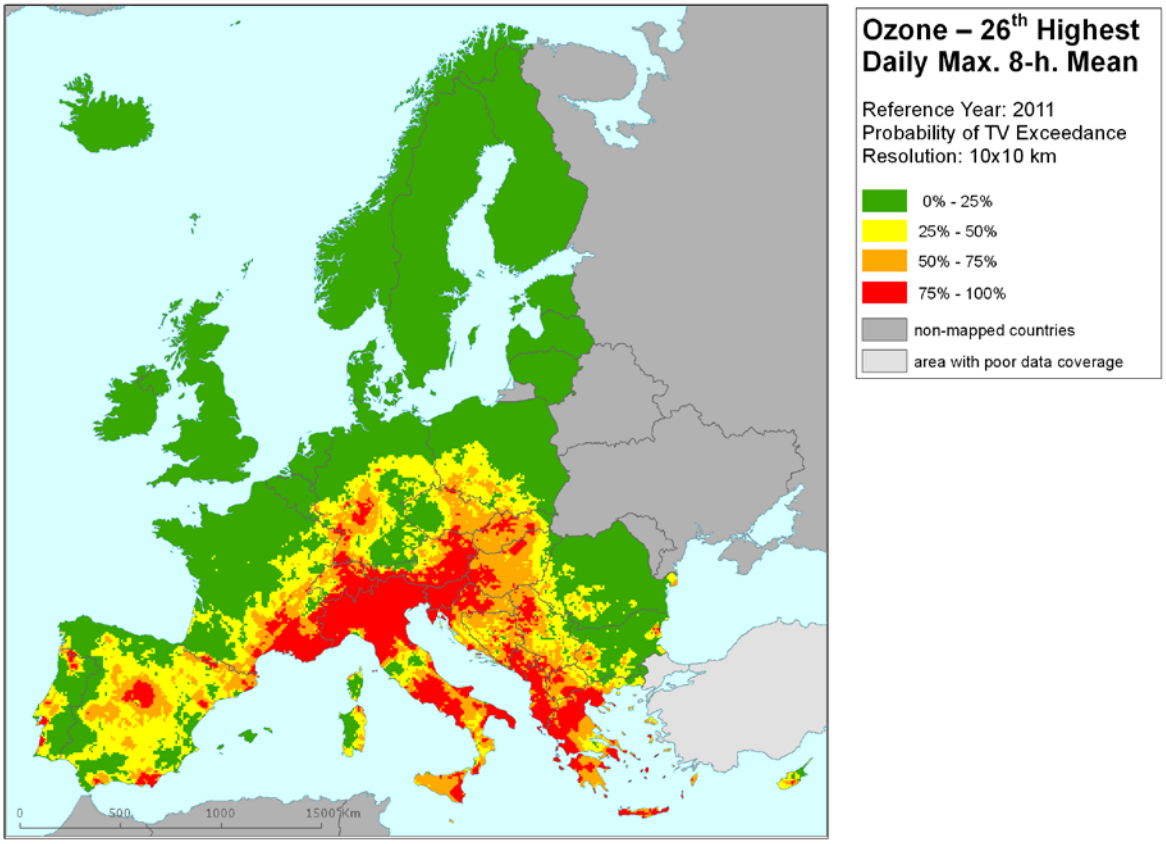

Figure 6.4 Map with the probability of the target value exceedance for ozone indicator 26th highest daily maximum 8-hour average (µg.m^{-3}) for 2011 on European scale calculated on the 10 x 10 km grid resolution. Interpolation uncertainty is considered only, no other sources of uncertainty.

6.2 SOMO35

6.2.1 Concentration map

Figure 6.5 presents the combined final map for SOMO35 as result of combining the separate rural and urban interpolated map following the procedure as described in De Smet et al. (2011) and Horálek et al. (2007).

As one can observe in a few areas of the map, the high or low measurement values do not seem to influence the interpolation results despite their clustering. The main reason is that the map presented here is an aggregation of 1x1 km values to 10x10 km resolution and this aggregation smoothes out the values one would more likely be able to distinguish in the higher resolution map, especially in the case of urban stations representing the urban areas. Another less prominent reason is the smoothing effect kriging has in general.

The supplementary data used in the regression models are the same as for 26th highest daily maximum 8-hour mean, i.e. EMEP model output, altitude and surface solar radiation for rural areas and EMEP model output, wind speed and surface solar radiation for urban areas. (The relevant linear regression models are indicated as O.Ear and UO.Ewr for urban areas.)

Table 6.5 presents the estimated parameters of the linear regression models and of the residual kriging, including the statistical indicators of both the regression and the kriging. The fit of the regression is expressed by the adjusted R^2 and standard error. The adjusted R^2 in 2011 for the rural areas is 0.60 and for the urban areas 0.54. This is quite a similar fit to 2010 (0.59 and 0.54), 2009 (0.60 and 0.53) and 2007 (both 0.58) and somewhat better than in 2008 (0.49 and 0.44), 2006 (0.42 and 0.38) and 2005 (0.51 and 0.49), see Annex, De Smet et al. (2012, 2011, 2010 and 2009) and Horálek et al. (2008). RMSE and bias are the cross-validation indicators showing the quality of the resulting map. Section 6.2.3 discusses in more detail the RMSE analysis and comparison with results of 2005 – 2010.

Table 6.5 Parameters of the linear regression models (Eq. 2.2) and of the ordinary kriging variograms (nugget, sill, range) – and their statistics – of ozone indicator SOMO35 for 2011 in the rural (left) and urban (right) areas as used for final mapping, i.e. rural linear regression model O.Ear (left), resp. UO.Ewr (right) followed by the interpolation on its residuals using ordinary kriging (OK, coded with 'a').

linear regr. model + OK on its residuals	**rural areas (O.Ear-a) coeff.**	**urban areas (UO.Ewr-a) coeff.**
c (constant)	-1519	-833
a1 (EMEP model 2011)	0.61	0.51
a2 (altitude GTOPO)	1.09	
a3 (wind speed 2011)		-127.53
a4 (s. solar radiation 2011)	250.39	204.42
adjusted R^2	**0.60**	**0.54**
standard error [µg.m^{-3}.d]	**1831**	**1597**
nugget	2.4E+06	1.2E+06
sill	3.3E+06	1.8E+06
range [km]	400	160
RMSE [µg.m^{-3}.d]	**1747**	**1374**
bias (MPE) [µg.m^{-3}.d]	**-4**	**5**

SOMO35 is not subject to one of the EU air quality directives and there are no limit or target values defined that might allow for mapping the probability of exceedances.

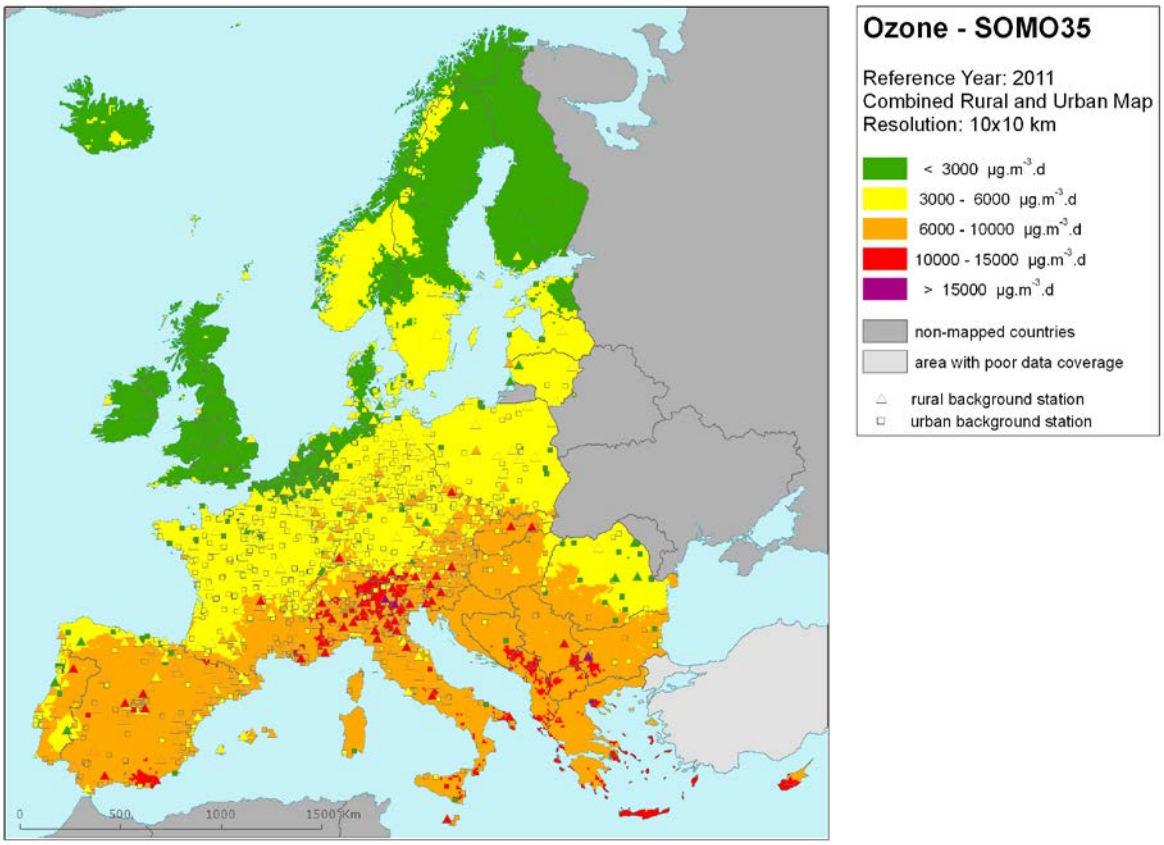

Figure 6.5 Combined rural and urban concentration map of ozone indicator SOMO35 in µg.m^{-3}.days for the year 2011. Resolution: 10x10 km.

Figure 6.6 presents the interannual difference between 2011 and 2010 for SOMO35. Red areas show an increase of ozone concentration, while blue areas show a decrease. A considerable increase is visible in south-eastern Europe – especially in Albania, Bulgaria, Serbia and FYR of Macedonia. The limited number of observations in concerned countries influences this increase.

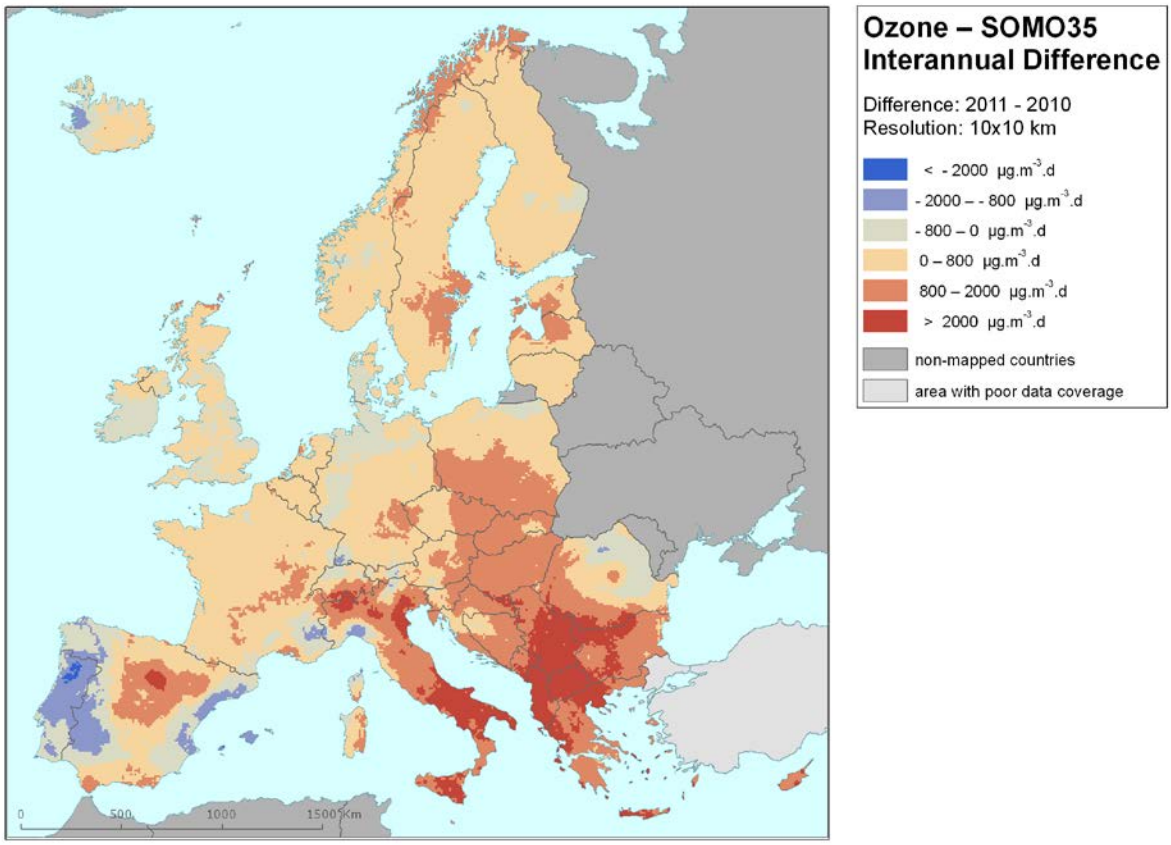

Figure 6.6 Interannual difference between mapped concentrations for 2011 and 2010 – ozone, SOMO35. Units: µg.m^{-3}.days.

6.2.2 Population exposure

Table 6.6 gives for SOMO35 the population frequency distribution for a limited number of exposure classes, as well as the population-weighted concentration for individual countries and for Europe as a whole. In the Table 6.7, the evolution of population exposure in the last five year is presented.

It has been estimated that in 2011 about 24 % of the European population lived in areas with SOMO35 values above 6000 µg.m^{-3}.d [(*)]. This is an increase of 7 % compared to 2010. In 2011, the northern and north-western European countries show no people living in areas above 6000 µg.m^{-3}.d (Figure 6.5), similarly as in the year 2010. Other areas mostly show increases of different extents and ranges, with the exception of Portugal, Spain, Malta and Cyprus (which show a small decrease).

Comparing the national frequency distributions of 2011 with that of 2010, shifts were observed in the percentage of inhabitants per class per country that coincide more or less with shifts in SOMO35 map colours between 2011 and 2010. In most of the countries of central and south-eastern Europe, an increase of the values occurred (such as in FYR of Macedonia, Albania, Slovenia and Slovakia).

(*) Note that the 6 mg.m^{-3}.d does not represent a health-related legally binding 'threshold'. In this and previous papers it concerns a somewhat arbitrarily chosen threshold to facilitate the discussion of the observed distributions of SOMO35 levels in their spatial and temporal context. This choice is based on a comparison of the 26th highest daily max. 8-hour means versus the SOMO35 of the ozone concentration measurements at all background stations in The Netherlands. The SOMO35 is estimated to be about 4 mg.m^{-3}.d when no Dutch population is exposed to ozone concentrations above the target value of the 26th h.d.m.8-hour mean. The Netherlands has in general relative low ozone concentrations compared to most other European countries. Over the years we applied the level of 6 mg.m^{-3}.d in our discussions of the annual results for two reasons: (i) to compensate for a possible underestimation of the SOMO35, and (ii) to match with a class interval limit of the SOMO35 map (Figure 6.5).

We observe in 2011 compared to 2010 a slight European overall increase in population exposed to ozone levels above 10 000 µg.m^{-3}.d. In 2011, some areas in south-eastern Europe, and also in France, Spain and Switzerland exhibited these elevated SOMO35 values (red pixels on the map).

Table 6.6 Population exposure and population-weighted concentration – ozone, SOMO35, year 2011.

Country		Population	Ozone, SOMO35, exposed population [%]					Population-weighted conc.
			< 3000	3000 - 6000	6000 - 10000	10000 - 15000	> 15000	
		[inhbs.1000]	µg.m^{-3}.d	µg.m^{-3}.d	µg.m^{-3}.d	µg.m^{-3}.d	µg.m^{-3}.d	[µg.m^{-3}.d]
Albania	AL	2 832		0.7	94.9	4.3		7 769
Andorra	AD	85			100			7 891
Austria	AT	8 404		78.0	21.9	0.1		5 452
Belgium	BE	11 001	85.1	14.9				2 714
Bosnia & Herzegovina	BA	3 843		61.4	38.0	0.6		5 702
Bulgaria	BG	7 369	3.0	67.4	28.9	0.6		5 215
Croatia	HR	4 290		51.2	48.6	0.2		6 470
Cyprus	CY	840			90.4	9.6		8 773
Czech Republic	CZ	10 487		91.5	8.5			4 743
Denmark	DK	5 561	85.5	14.5				2 752
Estonia	EE	1 336	82.4	17.6				2 516
Finland	FI	5 375	97.7	2.3				2 052
France	FR	64 995	10.0	75.4	14.6	0.0		4 439
Germany	DE	81 752	26.9	72.8	0.4			3 668
Greece	GR	11 123		1.5	90.4	8.1		9 182
Hungary	HU	9 986	0.0	66.3	33.7			5 828
Iceland	IS	318	100.0	0.0				1 094
Ireland	IE	4 571	99.5	0.5				1 353
Italy	IT	60 626		10.1	87.8	2.0		7 532
Latvia	LV	2 075	66.1	33.9				2 708
Liechtenstein	LI	36		87.8	12.2			5 128
Lithuania	LT	3 053	47.5	52.5				3 131
Luxembourg	LU	512		100.0				3 527
Macedonia, FYR of	MK	2 057		8.1	89.9	2.0		7 110
Malta	MT	415			97.1	2.9		7 127
Monaco	MC	35			100			8 354
Montenegro	ME	620		32.6	60.2	7.3		6 970
Netherlands	NL	16 656	98.1	1.9				2 283
Norway	NO	4 920	88.8	11.2				2 395
Poland	PL	38 530	5.1	93.0	1.8			4 065
Portugal	PT	10 573	15.8	66.8	17.4			4 552
Romania	RO	20 199	51.5	39.5	9.0			3 276
San Marino	SM	32		81.6	18.4			6 220
Serbia	RS	9 046	0.0	62.8	36.8	0.3		5 793
Slovakia	SK	5 392		54.1	45.9			6 051
Slovenia	SI	2 050		17.7	82.2	0.0		7 062
Spain	ES	46 667	6.4	46.9	46.4	0.3		5 858
Sweden	SE	9 416	78.7	21.3				2 628
Switzerland	CH	7 870		85.7	13.8	0.5		5 435
United Kingdom	UK	63 024	99.2	0.8	0.0			1 471
Total		**537 972**	**30.6**	**45.9**	**23.0**	**0.5**	**0**	**4 414**
			76.4		**23.6**			

Note1: Turkey is not included in the calculation due to lacking air quality data.
Note2: The percentage value "0.0" indicates an exposured population exists, but is small and estimated less than 0.05 %. Empty cells mean: no population in exposure.

Table 6.7 Evolution of percentage population living in above 6000 µg.m^{-3} (left) and population-weighted concentration (right) in the years 2006-2011 – ozone, SOMO35. Resolution: 1x1 km.

Country		Population above 6000 µg.m^{-3}.d [%]							Population-weighted conc. [µg.m^{-3}.d]						
		2006	2007	2008	2009	2010	2011	diff. '11 - '10	2006	2007	2008	2009	2010	2011	diff. '11 - '10
Albania	AL	75.3	95.8	100	97.6	32.1	99.3	67.2	7193	7817	7668	6754	5617	7769	2153
Andorra	AD	29.3	100	29.6	100	100	100	0	6587	7121	6319	7186	7282	7891	610
Austria	AT	40.1	56.7	12.5	13.4	12.1	22.0	9.9	6237	5874	5099	5050	4969	5452	483
Belgium	BE	0.3	0	0	0	0	0	0	4017	2235	2520	2599	2401	2714	312
Bosnia-Herzegovina	BA	55.5	67.2	37.4	33.8	29.0	38.0	9.0	6571	6938	5972	5536	4879	5702	822
Bulgaria	BG	28.2	39.2	47.7	32.7	8.4	29.6	21.1	4896	6064	5797	5686	4377	5215	838
Croatia	HR	85.7	83.2	35.8	32.5	28.6	48.6	20.0	6928	6756	5899	5491	5419	6470	1051
Cyprus	CY	25.6	98.1	100.0	100	100	90.4	-9.6	5759	7739	8027	8788	7374	8773	1399
Czech Republic	CZ	47.3	11.8	1.7	0.8	0.2	8.5	8.3	6097	5123	4576	4487	4160	4743	583
Denmark	DK	0.0	0	0	0	0	0	0	3578	2440	3080	2440	2245	2752	507
Estonia	EE	0	0	0	0	0	0	0	3594	2061	2363	1762	2646	2516	-130
Finland	FI	0.0	0	0	0	0	0	0	3141	1332	1938	1623	1925	2052	127
France	FR	18.3	12.0	4.7	13.2	13.4	14.6	1.2	4972	3686	3563	4025	4139	4439	300
Germany	DE	8.2	1.1	0.5	0.4	0.3	0.4	0.0	4860	3648	3822	3507	3652	3668	16
Greece	GR	74.6	98.0	99.9	98.8	86.4	98.5	12.1	6657	8330	8969	8330	7483	9182	1699
Hungary	HU	36.3	87.2	25.5	89.9	0.9	33.7	32.8	5738	6547	5751	6631	4408	5828	1421
Iceland	IS	0	0	0	0	0	0	0	2265	1168	2224	833	775	1094	319
Ireland	IE	0	0	0	0	0	0	0	2453	1412	2096	1487	1419	1353	-66
Italy	IT	96.0	86.7	66.1	75.3	61.7	89.9	28.1	8205	7506	6386	6986	6302	7532	1230
Latvia	LV	0	0	0	0	0	0	0	3734	2262	2347	1837	2304	2708	404
Liechtenstein	LI	51.4	9.1	6.4	12.2	10.8	12.2	1.4	6258	4826	4930	5271	5244	5128	-116
Lithuania	LT	0.0	0	0	0	0	0	0	4535	2744	3059	2291	2608	3131	523
Luxembourg	LU	1.2	0	0	0	0	0	0	5090	3424	3557	3500	3505	3527	22
Macedonia, FYR of	MK	32.7	35.6	100	41.5	13.6	89.9	76.3	6297	6690	7133	6229	5081	7110	2028
Malta	MT	100	100	100	100	100	97.1	-2.9	7797	7209	6582	6634	6722	7127	405
Monaco	MC	100	100	100	100	100	100	0	8903	8381	7246	8325	8028	8354	326
Montenegro	ME	35.5	71.8	100	37.1	33.1	60.2	27.0	6554	7379	7120	6237	5653	6970	1317
Netherlands	NL	0	0	0	0	0	0	0	3245	1816	2104	1922	1916	2283	368
Norway	NO	2.9	0.0	0	0	0	0	0	3496	1705	2514	2000	1803	2395	592
Poland	PL	27.3	1.4	0.7	0.5	0.0	1.8	1.8	5416	4179	3951	3747	3278	4065	787
Portugal	PT	24.8	14.8	8.6	28.9	32.4	17.4	-15.0	5257	4863	3851	5003	5133	4552	-581
Romania	RO	19.5	41.4	17.9	28.3	1.1	9.0	7.9	4798	5882	5039	5044	3033	3276	243
San Marino	SM	22.9	100	14.1	15.3	11.6	18.4	6.8	6321	7296	5863	5860	5331	6220	889
Serbia (incl. Kosovo)	RS	27.1	65.1	74.9	60.6	9.4	36.8	27.4	5239	6768	6378	6118	4001	5793	1792
Slovakia	SK	51.9	57.8	19.5	75.6	6.2	45.9	39.7	6261	6098	5455	6348	4748	6051	1303
Slovenia	SI	98.5	68.1	37.2	36.6	37.5	82.3	44.8	7480	6671	5761	5775	5998	7062	1064
Spain	ES	50.6	61.0	32.6	57.7	50.0	46.7	-3.4	5813	5992	5110	5983	6088	5858	-230
Sweden	SE	0.0	0	0	0	0	0	0	3635	1795	2387	2100	2025	2628	603
Switzerland	CH	40.5	12.7	8.6	14.3	12.9	14.3	1.4	6321	5114	4619	5139	5127	5435	307
United Kingdom	UK	0.0	0	0	0	0	0	0	2676	1174	2044	1433	1072	1471	399
Total		**29.5**	**28.1**	**19.6**	**24.6**	**16.6**	**23.6**	**6.9**	**5167**	**4411**	**4275**	**4275**	**3917**	**4414**	**497**
EU28		**29.0**	**26.9**	**17.4**	**23.6**	**16.7**	**23.6**	**6.8**	**5128**	**4319**	**4178**	**4208**	**3888**	**4339**	**451**

The total European population-weighted ozone concentration in terms of SOMO35 was estimated to be 4414 µg.m^{-3}.d, which is more than 2010's value of 3915 µg.m^{-3}.d and than 2009's value of 4275 µg.m^{-3}.d. In most of the countries, the population-weighted concentration increased, in comparison with 2010.

6.2.3 Uncertainties

Uncertainty estimated by cross-validation

The basic uncertainty analysis is given by the cross-validation. In Table 6.5, the absolute mean uncertainty (RMSE) in 2011 was 1747 µg.m^{-3}.d for the rural areas and 1374 µg.m^{-3}.d for the urban areas. The uncertainties at rural and urban areas in previous years were: 1608 and 1278 µg.m^{-3}.d (2010), 1635 and 1475 µg.m^{-3}.d (2009), 1609 and 1293 µg.m^{-3}.d (2008), 1801 and 1260 µg.m^{-3}.d (2007), 2077 and 1472 µg.m^{-3}.d (2006) and 2173 and 1459 µg.m^{-3}.d (2005). The relative mean uncertainty of the 2011 map of SOMO35 is 29.6 % for rural and 29.7 % for urban areas. The previous years had for rural and urban areas respectively: 29.6 % and 29.6 % (2010), 29.7 % and 33.1 % (2009), 30.7 % and 31.3 % (2008), 33.3 % and 29.5 % (2007), 31.6 % and 29.2 % (2006) and 35.5 % and 32 % (2005), meaning that the 2011 relative uncertainties for both rural and urban areas are at the lower end of the range. Table 7.7 summarises both the absolute and the relative uncertainties over these past seven years.

Figure 6.7 shows the cross-validation scatter plots for interpolated values at both rural and urban areas. R^2 for rural areas and urban areas in 2011 indicates that, respectively, about 63 % and 66 % of the variability is attributable to the interpolation. The corresponding values for the 2010 maps (62 % and 65 %), 2009 maps (63 % and 62 %), 2008 maps (63 % and 54 %), 2007 maps (63 % and 67 %), the 2006 maps (47 % and 49 %) and 2005 maps (55 % and 58 %), illustrate a somewhat similar fit for the years 2007 – 2011.

The scatter plots show again that in areas with high concentrations the interpolation methods tend to deliver underestimated predictions, although some overestimation or lower values of urban areas is also likely. For example, in urban areas (Figure 6.7, right panel) an observed value of 10 000 µg.m^{-3}.d is estimated in the interpolation as about 8200 µg.m^{-3}.d. That is 18 % too low, leading in general to considerable underestimations at high SOMO35 values. Vice versa at low values an overestimation will occur, e.g. at a measured 2000 µg.m^{-3}.d the interpolation will predict some 2900 µg.m^{-3}.d, which is about 45 % too high.

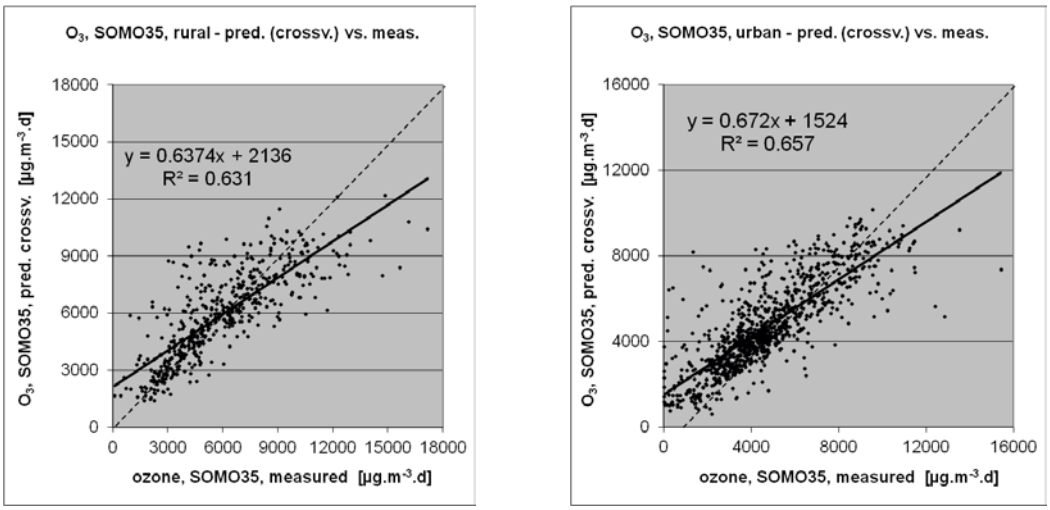

Figure 6.7 Correlation between cross-validation predicted values (y-axis) and measurements (x-axis) for the ozone indicator SOMO35 for rural (left) and urban (right) areas in 2011.

Comparison of point measurement values with the predicted grid value

Additional to the point observation – point prediction cross-validation, a simple comparison was made between the point measurements and interpolated predicted grid values averaged in on a grid of 10x10 km resolution the separate rural and urban background maps. This point-grid comparison indicates to what extent the predicted value of a grid cell represents the corresponding measured values at stations located in that cell. The results of the point observation – point prediction cross-validation of Figure 6.7, compared to those of the point-grid validation are summarised in Table 6.8. The table shows a

better correlated relationship (i.e. higher R^2, smaller intercept, slope closer to 1) between station measurements and the interpolated values of the corresponding grid cells (case ii) at both rural and urban background map areas than it does for the point cross-validation predictions (case i). This is because the simple comparison between point measurements and the gridded interpolated values shows the uncertainty of predictions where there are actual station locations, while the point observation – point prediction cross-validation simulates the behaviour of the interpolation at positions without actual measurements but within the area covered by measurements. The uncertainty at measurement locations is caused partly by the smoothing effect of the interpolation and partly by the spatial averaging of the values into 10x10 km grid cells. The degree of smoothing leading to underestimation in areas with high values is weaker when measurements exist, than when no measurement exists. For example, in urban areas the predicted interpolation grid value will be about 8700 µg.m^{-3}.d at a corresponding station point with an observed value of 10 000 µg.m^{-3}.d, i.e. an underestimation of about 13 %. This underestimation is smaller than the 18%, discussed in the previous subsection, which was simulating the situation where no measurement exists.

Table 6.8 Linear regression equation and coefficient of determination R^2 from the scatter plots of (i) the predicted point values based on cross-validation and (ii) aggregation into 10x10 km grid cells versus the measured point values for the ozone indicator SOMO35 for rural and urban areas of 2011.

	rural areas		urban areas	
	equation	R^2	equation	R^2
i) cross-validation prediction (Fig 6.7)	y = 0.637x + 2136	0.631	y = 0.672x + 1524	0.657
ii) 10x10 km grid prediction	y = 0.696x + 1790	0.740	y = 0.752x + 1156	0.804

No Limit Value or Target Value is set for the WHO recommended ozone health indicator SOMO35, therefore no probability of exceedance map has been prepared.

6.3 AOT40 for crops and for forests

The ecosystem based accumulative ozone indicators described in this section are specifically prepared for calculation of EEA Core Set Indicator 005 (CSI005, http://themes.eea.europa.eu/indicators). For the estimation of the vegetation and forested area exposure to accumulated ozone the maps in this section are created on a grid of 2x2 km resolution, instead of the 10x10 km grid used for the human health indicators. This resolution is selected as a compromise between calculation time and accuracy in the impact assessment done for ozone within CSI005. It serves as a refinement of the exposure frequency distribution outcomes of the overlay with 100x100 m resolution CLC2006 land cover classes.

6.3.1 Concentration maps

The interpolated maps of AOT40 for crops and AOT40 for forests were created for rural areas only, combining AOT40 data derived from rural background station observations with supplementary data sources EMEP model output, altitude and surface solar radiation. The relevant linear regression model is referred to as O.Ear. Note that supplementary data sources are the same as for the human health related ozone indicators.

Table 6.9 presents the estimated parameters of the linear regression models and of the residual kriging, including their statistical indicators of the regression and kriging. The fit of the regression is expressed by adjusted R^2 and the standard error. The adjusted R^2 is in 2011 for AOT40 for crops 0.52 and for AOT40 for forests 0.61, i.e. a slightly worse fit as in 2010 (0.59 and 0.63) and 2009 (0.64 and 0.61), but a better fit than in 2008 (0.40 and 0.49) and in 2007 (0.49 and 0.59) (Horálek et al. 2013, De Smet et al. 2012, 2011 and 2010). RMSE and bias are the cross-validation indicators, showing the quality of the resulting map. Section 5.3.3 discusses in more detail the RMSE analysis and comparison with results of 2005 – 2010.

Table 6.9 Parameters of the linear regression models (Eq2.1) and of the ordinary kriging variograms (nugget, sill, range) - and their statistics - of ozone indicators AOT40 for crops (left) and for forests (right) for 2011 in the rural areas as used for final mapping, i.e. rural linear regression model O.Ear followed by the interpolation on its residuals using ordinary kriging (OK, coded with 'a').

linear regr. model + OK on its residuals	AOT40 for crops (O.Ear-a) coeff.	AOT40 for forests (O.Ear-a) coeff.
c (constant)	-4387	-12094
a1 (EMEP model 2011)	0.54	0.55
a2 (altitude GTOPO)	1.54	3.79
a3 (s. solar radiation 2011)	877.5	1745.9
adjusted R^2	**0.52**	**0.61**
standard error [µg.m^{-3}]	**5917**	**10148**
nugget	1.5E+07	4.6E+07
sill	3.2E+07	9.3E+07
range [km]	120	110
RMSE [µg.m^{-3}]	**5263**	**9341**
bias (MPE) [µg.m^{-3}]	**100**	**43**

Figure 6.8 presents the final map of AOT40 for crops. The areas and stations in the map that exceed the target value (TV) of 18 mg.m^{-3}.h are marked in red and purple. It is applicable to rural areas only, as it is based on rural background station observations. It represents the indicator for vegetation exposure to ozone while assuming there is no relevant vegetation in urban areas. The map was compared to the one of 2010 and in general a slight decrease in the extent of areas with the highest AOT40 levels (red and purple) was found specifically in the central and south-western regions of Europe. Some increase occurred in southern Italy, the Balkan regions and Greece.

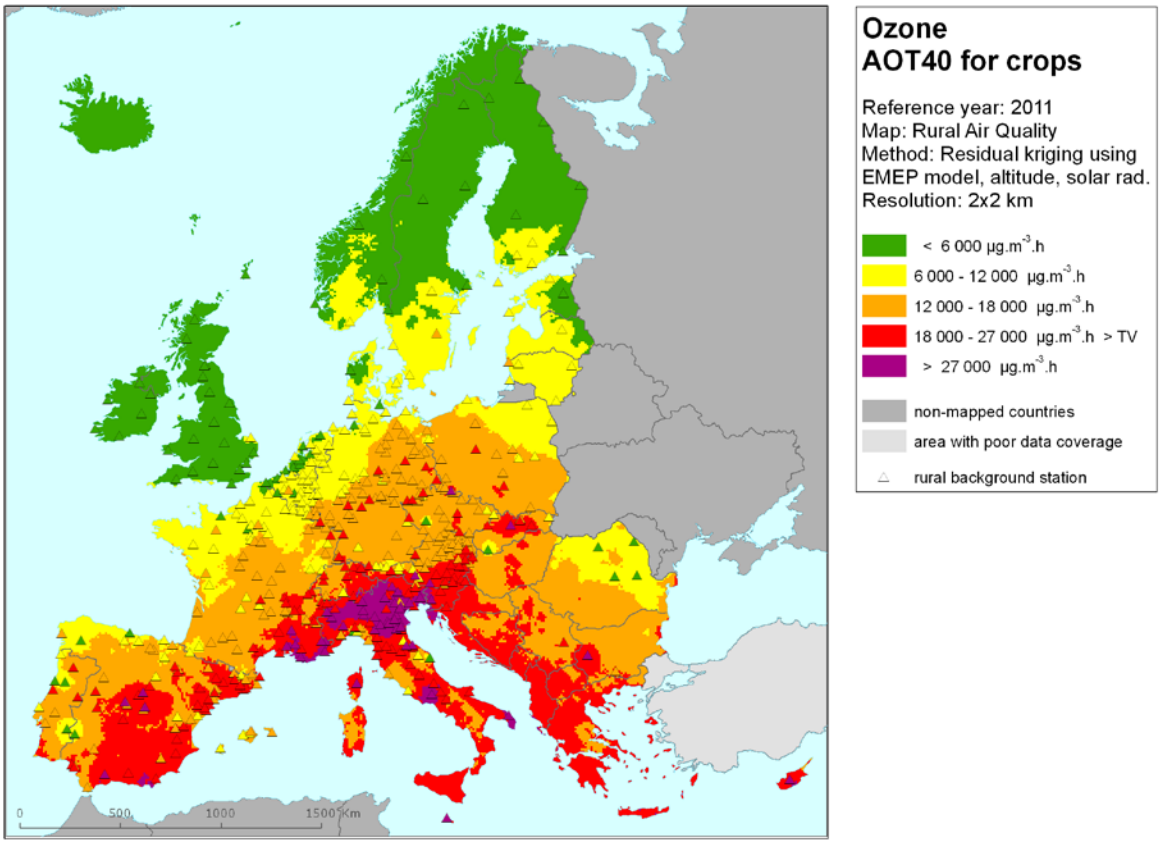

Figure 6.8 Rural concentration map of ozone vegetation indicator AOT40 for crops for the year 2011. Units: µg.m^{-3}.hours. Resolution: 2x2km.

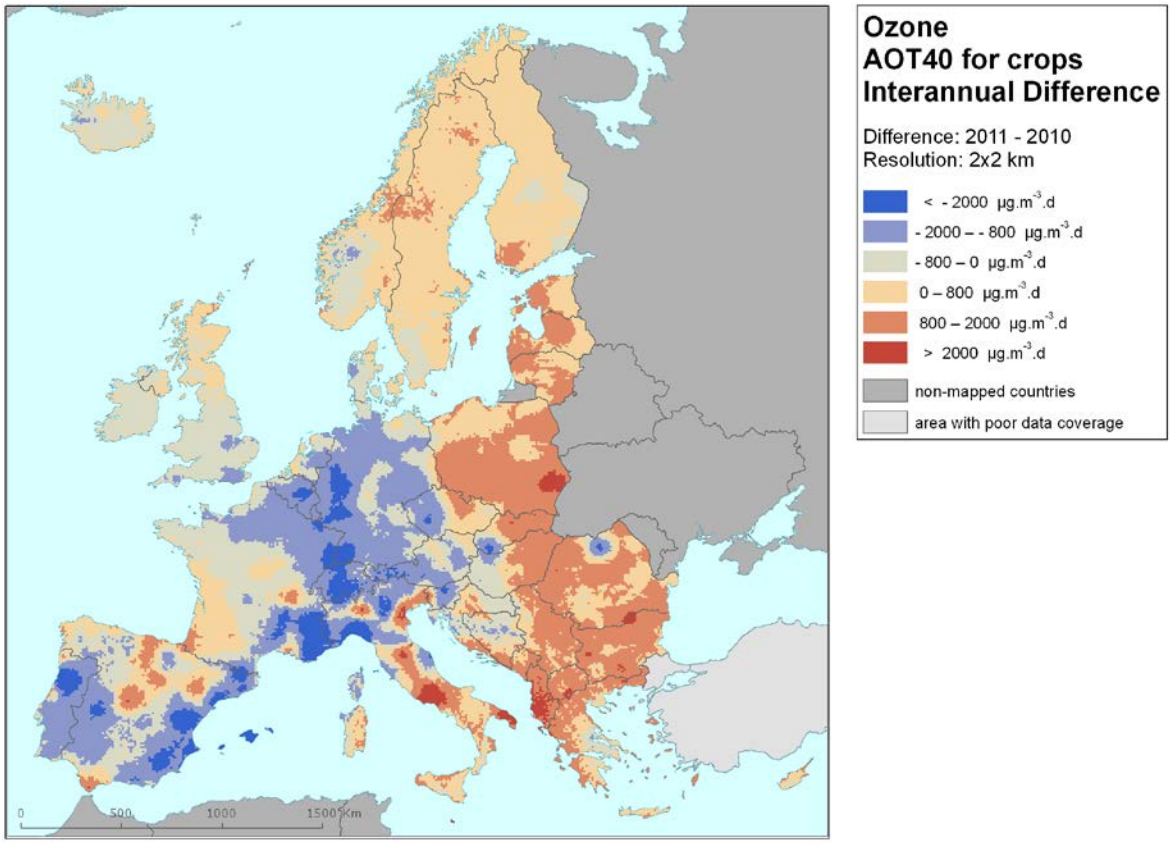

Figure 6.9 Interannual difference between mapped concentrations for 2011 and 2010 – ozone, AOT40 for crops. Units: µg.m^{-3}.hours.

Figure 6.9 presents the interannual difference between 2011 and 2010 for AOT40 for crops. Red areas show an increase of ozone concentration, while blue areas show a decrease. The highest decreases can be seen in Germany, Switzerland, south-eastern France, south-eastern Spain and Portugal. Contrary to that, considerable increases are visible in eastern and south-eastern Europe – especially in Poland, Romania, Bulgaria, Serbia, FYR of Macedonia, Montenegro, Albania, southern Italy. In the most of these areas, an inverse effect occurs here compared to what was observed between the years 2010 and 2009.

Figure 6.10 presents the final map of AOT40 for forests. Like Figure 6.8, it concerns a map for rural areas. It is based on rural background station observations only, representing an indicator for vegetation exposure to ozone. For AOT40 for forests there is no TV defined.

In Figure 6.11, the interannual difference between 2011 and 2010 for AOT40 for forests is shown. Again, the main increase is visible in south-eastern Europe (specifically in Romania, Bulgaria, Serbia, FYR of Macedonia, Montenegro, Greece, Albania, southern Italy and Cyprus). Next to this, a considerable increase is observed also in Po Valley in the northern Italy. The decrease is visible particularly in Portugal. Again, in most of the mentioned areas the inverse effects occur here compared to what was observed between the years 2010 and 2009. The limited number of measuring stations in the south-eastern Europe and in the southern Italy might influence the interannual difference shown.

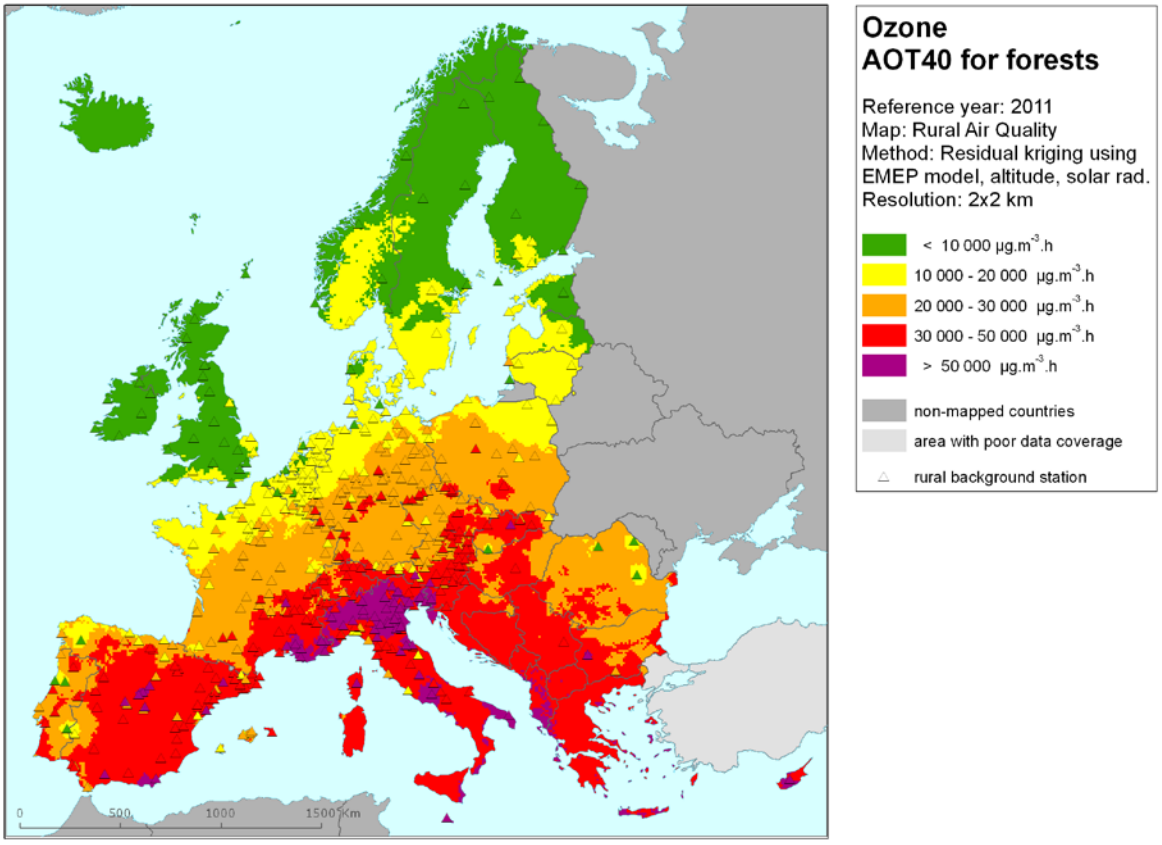

Figure 6.10 Rural concentration map of ozone vegetation indicator AOT40 for forests for the year 2011. Units: µg.m^{-3}.hours. Resolution: 2x2km.

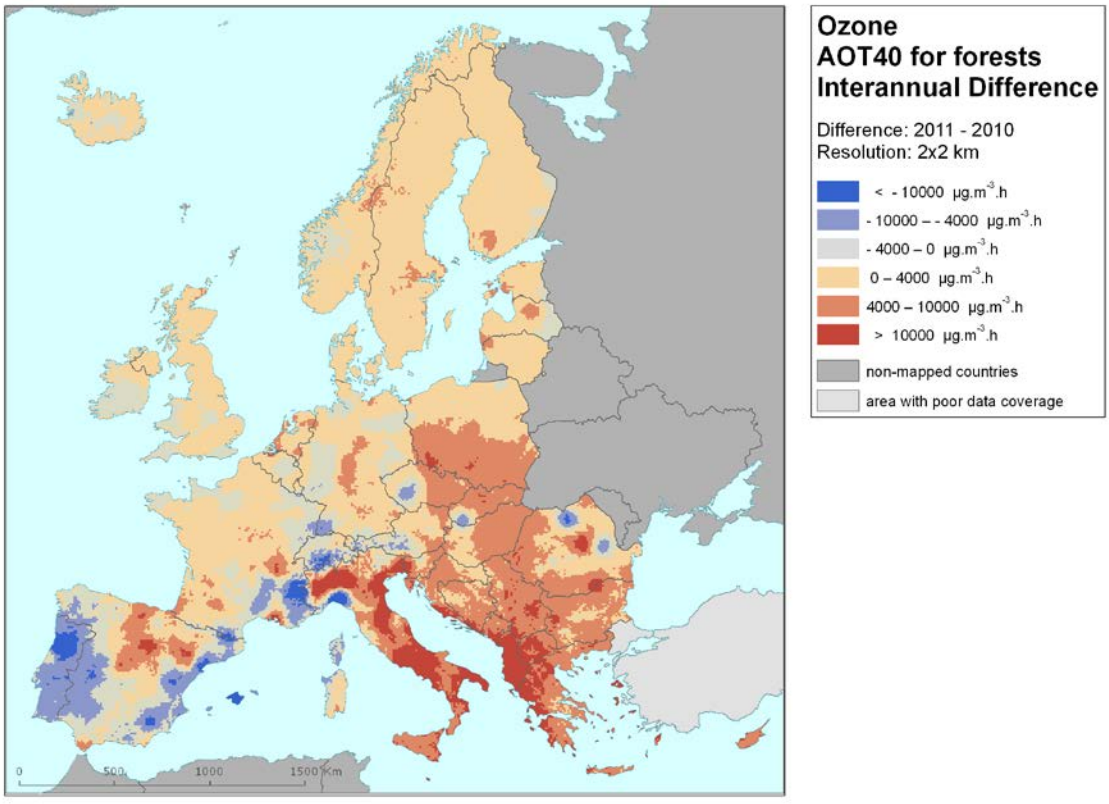

Figure 6.11 Interannual difference between mapped concentrations for 2011 and 2010 – ozone, AOT40 for crops. Units: µg.m^{-3}.hours. Resolution: 2x2km.

6.3.2 Vegetation exposure

Agricultural crops

The rural map with ozone indicator AOT40 for vegetation, i.e. agricultural crops, as given in Figure 6.8, has been combined with the land cover CLC2006 map. Following a similar procedure as described in Horálek et al. (2007) the exposure of agricultural areas, defined as the Corine Land Cover level-1 class *2 Agricultural areas* (encompassing the level-2 classes *2.1 Arable land, 2.2 Permanent crops, 2.3 Pastures* and *2.4 Heterogeneous agricultural areas)* has been calculated at the country-level.

Table 6.10 gives the absolute and relative agricultural area for each country and for four European regions where the target value (TV) and long-term objective (LTO) for ozone are exceeded. The frequency distribution of the agricultural area per country over the exposure classes is presented as well.

The table indicates the country grouping with corresponding colours of the region; *Northern Europe*: Sweden, Finland, Norway, Estonia, Lithuania, Latvia and Denmark. *North-western Europe*: United Kingdom, Ireland, Iceland, the Netherlands, Belgium, Luxembourg and France north of 45 degrees latitude. *Central and Eastern Europe*: Germany, Poland, Czech Republic, Slovakia, Hungary, Austria, Liechtenstein, Bulgaria and Romania. *Southern Europe*: Albania, Bosnia-Herzegovina, France south of 45 degrees latitude, Portugal, Spain, Italy, San Marino, Slovenia, Croatia, Greece, Cyprus, F.Y.R. of Macedonia, Montenegro, Serbia (including Kosovo) and Malta.

Table 6.10 illustrates that in 2011, some 19 % of all European agricultural land was exposed to ozone exceeding the target value (TV) of 18 $mg.m^{-3}.h$. This is a decrease in the total area with agricultural crops above the TV (and as such considered to suffer from adverse effects to ozone exposure) compared to 2010 (21 %) and 2009 (26 %). It is considerable lower than 2008 (38 %), 2007 (36 %) and well below that of 2006 (70 %), see Table 6.12 (and also below that of 2005 (49%), see Horálek et al., 2008). Considering the long-term objective (LTO, 6 $mg.m^{-3}.h$) the area in excess (almost 88 %) was higher than in 2010 (85 %), 2009 (81%) and 2007 (78 %), but lower than in 2008 (96 %) and 2006 (98 %). Like in 2010 Ireland and Iceland did have ozone levels not being in excess of the LTO. In many countries of southern Europe, more than half of their total agricultural area experienced exposures above the less stringent TV.

Table 6.12 (left) presents for comparison the percentages of area in exceedance of the target value for the years 2006 – 2011. In southern Europe, about 54 % of the total agricultural area exceeded the target value in 2011. This is slightly less than in 2010 (57 %) and within the range of what it was in 2009 (60 %), 2008 (64 %) and 2007 (55 %) and substantially below the amounts of 2006 (94 %). For 2011 – 2007 (and also for 2005) no area was mapped in excess of the target value in northern Europe; only in 2006 almost 4 % of its area was in excess. In the north-western region the area exceeding the target value is back to its low percentage of 1.1 %, comparable to levels of 2007-2009 and quite a reduction compared to 2010 (33 %) and 2006 (50 %). For the central and eastern region, the total area where ozone exceeds the target value decreased considerably from 2006 to 2007: from 77 % to 50 % (after an initial increase from 44% in 2005). From that time, it has further reduced to 47 % in 2008, 17 % in 2009, 11 % in 2010 and to its lowest level of 5 % in 2011.

Compared to 2006, the frequency distribution of agricultural area over the exposure classes showed a clear shift towards lower exposures in 2007 leading to a decreased total area exceeded (to a distribution more similar to that of 2005, see Horálek et al., 2008). In 2008, this tendency continued with an approximately similar area percentage in excess of the TV, however, a shift in area percentages with lower exposure levels in 2007 to somewhat higher levels in 2008 (but still below the target value) also occurred. Compared to 2007 – 2008, we observed in 2009 – 2010 an increased area with lower exposure level, leading to a lower TV exceedance. In 2011 this tendency seems to continue for most regions except for the southern European region where the areas with more elevated levels or areas in exceedances of the TV continue to exist or extended (Table 6.10).

Table 6.10 Agricultural area exposure and exceedance (Long Term Objective, LTO and Target Value, TV) for ozone, AOT40 for crops, year 2011.

Country	Agricultural Area, 2011					Percentage of agricultural area, 2011 [%]				
	total area	> LTO (6 mg.m^{-3}.h)		> TV (18 mg.m^{-3}.h)		< 6	6 - 12	12 - 18	18 - 27	> 27
	[km^2]	[km^2]	[%]	[km^2]	[%]	mg.m^{-3}.h	mg.m^{-3}.h	mg.m^{-3}.h	mg.m^{-3}.h	mg.m^{-3}.h
Albania	7877	7877	100	7877	100.0	0.0	0.0	0.0	99.8	0.2
Austria	27220	27220	100	8851	32.5	0.0	0.2	67.2	32.5	0.0
Belgium	17597	15194	86.3	0	0	13.7	83.4	2.9	0.0	0.0
Bosnia-Herzegovina	18837	18837	100	9649	51.2	0.0	0.0	48.8	51.2	0.0
Bulgaria	57399	57399	100	6024	10.5	0.0	0.6	88.9	10.3	0.2
Croatia	22502	22502	100	15445	68.6	0.0	0.0	31.4	64.5	4.1
Cyprus	4289	4289	100	3887	90.6	0.0	0.0	9.4	85.6	5.0
Czech Republic	45116	45116	100	2173	4.8	0.0	3.1	92.1	4.8	0.0
Denmark (no Faroes)	32045	24051	75.1	0	0.0	24.9	73.5	1.6	0.0	0.0
Estonia	14645	6913	47.2	0	0	52.8	47.2	0.0	0.0	0.0
Finland	29023	10630	36.6	0	0	63.4	36.6	0.0	0.0	0.0
France	327709	325886	99.4	21408	6.5	0.6	45.5	47.4	5.8	0.7
Germany	212175	212026	99.9	730	0.3	0.1	32.1	67.5	0.3	0.0
Greece (CLC2000)	51576	51576	100	40028	77.6	0.0	0.0	22.4	76.8	0.8
Hungary	62222	62222	100	9502	15.3	0.0	1.7	83.0	15.3	0.0
Iceland	2379	0	0	0	0.0	100.0	0.0	0.0	0.0	0.0
Ireland	46138	0	0	0	0.0	100.0	0.0	0.0	0.0	0.0
Italy	156493	156493	100	126270	80.7	0.0	0.6	18.7	53.5	27.2
Latvia	28258	22037	78.0	0	0	22.0	77.6	0.4	0.0	0.0
Liechtenstein	40	40	100	40	100	0.0	0.0	0.0	100.0	0.0
Lithuania	39812	39812	100.0	0	0	0.0	99.8	0.2	0.0	0.0
Luxembourg	1389	1389	100	0	0	0.0	15.7	84.3	0.0	0.0
Macedonia	9316	9316	100	6720	72	0.0	0.0	27.9	72.1	0.0
Malta	124	124	100	124	100.0	0.0	0.0	0.0	76.1	23.9
Monaco	0.00	0.00		0.00						
Montenegro	2297	2297	100	1914	83	0.0	0.0	16.7	83.3	0.0
Netherlands	24243	18392	75.9	0	0	24.1	75.9	0.0	0.0	0.0
Norway	15673	1793	11.4	0	0	88.6	11.4	0.0	0.0	0.0
Poland	195799	195799	100	1162	0.6	0.0	30.0	69.4	0.6	0.0
Portugal	41908	41908	100.0	1751	4	0.0	23.2	72.6	4.2	0.0
Romania	135291	135209	100	36	0.0	0.1	51.4	48.5	0.0	0.0
San Marino	42	42	100	42	100	0.0	0.0	0.0	100.0	0.0
Serbia (incl. Kosovo)	48636	48503	100	1411	3	0.0	8.9	88.2	2.9	0.0
Slovakia	23662	23662	100	6016	25	0.0	15.6	58.9	25.4	0.0
Slovenia	7104	7104	100	7104	100	0.0	0.0	0.0	91.6	8.4
Spain	251580	251516	100.0	121651	48.4	0.0	8.5	43.1	48.1	0.2
Sweden	38650	26992	69.8	0	0	30.2	69.7	0.1	0.0	0.0
Switzerland	11804	11804	100.0	3445	29	0.0	1.5	69.3	28.7	0.5
United Kingd.(+ Man)	138864	3179	2.3	0	0	97.7	2.3	0.0	0.0	0.0
Total	**2149731**	**1889149**	**87.9**	**413550**	**19.2**	**12.1**	**25.7**	**43.0**	**17.0**	**2.2**
France over 45N	259935	258113	99.3	5472	2.1	0.7	56.1	41.1	2.1	0.0
France below 45N	67774	67774	100.0	15936	23.5	89.0	11.0	0.0	0.0	0.0
Kosovo	4445	4438	99.8	2798	63	0.0	0.0	36.9	62.9	0.0
Serbia (excl. Kosovo)	44058	44197	100.3	8904	20	0.0	0.0	80.1	20.2	0.0
Northern	198105	132228	66.7	0	0					
North-western	490545	296267	60.4	5472	1.1					
Central & Eastern	770729	770498	100.0	37980	4.9					
Southern	690353	690157	100.0	359808	52.1					
Total	**2149731**	**1889149**	**87.9**	**403260**	**18.8**					

Note1: Countries not included due to lack of land cover data: Andorra, Turkey.
Note2: The percentage value "0.0" indicates an exposured population exists, but is small and estimated less than 0.05 %.
Empty cells mean: no population in exposure.

Forests

The rural map with ozone indicator AOT40 for forests, as given in Figure 6.9, was combined with the land cover CLC2000 map as done for crops. Following a similar procedure as described in Horálek et al. (2007) the exposure of forest areas, defined as CORINE Land Cover level-2 class *3.1 Forests* has been calculated at the country-level.

Table 6.11 gives the absolute and relative forest area where the *Reporting Value* (RV of 20 $mg.m^{-3}.h$, as Annex III of the ozone directive defines it) in combination with the *Critical Level* (*CL* of 10 $mg.m^{-3}.h$, as defined in the UNECE Mapping Manual) are exceeded. This is done for each country, for four European regions and for Europe as a whole. The table presents the frequency distribution of the forest area per country and over the exposure classes. The Reporting Value of the ozone directive was exceeded in 2011 at 53 % of the total European forest area. Table 6.12 (right) presents for comparison the percentages of area that exceed the Reporting Value for the years 2006 – 2011. The RV for 2011 is slightly higher than in 2010 and 2009 (both 49%), 2008 (50 %) and 2007 (48 %), while in 2006 it was almost 70 % (and in 2005 about 60 %, see Horálek et al., 2008). This means that the area of forest exposed to levels above the accumulated ozone RV diminished and stabilises in the period 2007 – 2011 to an area of around 20 percentage points below that of 2006 (and 10 percentage points below that of 2005).

In 2006 about all of the European forest areas were exposed to exceedances of the Critical Level (CL) of 10 $mg.m^{-3}.h$ (while in 2005 it was the case for three-quarters of the forest areas). This extensive portion shrank in 2007 to 62 %, but in 2008 it increased to 80 %. In 2009, the area reduced to a level of 67 % and in 2010 to a level of 63%. In 2011 a slight increase to 69 % occurred (Table 6.11).

Like in 2010, in 2011 almost all European countries had their forests exposed to accumulated ozone concentrations above the CL and many of those had forests experiencing exposures in excess of the less stringent RV. About the same set of countries do show in 2011 no RV exceedances like in 2010, however, most of them have increased forest areas exposed to concentrations above the CL compared to 2010, such as Estonia, Finland, Netherlands, Norway and Sweden. As in previous years, in 2011 the southern European region continued to have AOT40 levels such that all forested areas were exposed to exceedances of the CL and approximately all of the RV. In 2011, all forests of central and eastern regions are above the CL, of which 90 % also above the RV.

The central and eastern regions show, for the period of 2005 – 2011, a continued 100 % exceedance of the CL. The area with exceedances of the RV (Table 6.12) showed a peak of 100 % in 2006, followed by a reduction to about 86 % in 2007 and a subsequent increase of about 10 % in 2008 to 95 % (which comes close to the 96 % of 2005, see Horálek et al., 2008). In 2009, the area in excess of the RV was 88 %. In 2010 it is 76 % and in 2011 it increases to 90%. In the north-western region, the area exceeding the CL increased from 84 % in 2005 to practically the whole area (98 %) in 2006. In 2007, it dropped again to 78 %, but in 2008 it increased to almost all forested area (94 %). In 2009, it was 81 % and in 2010 and 2011 it is 82 %, close to the excess of 2007. Concerning the north-western European forested area above the RV, there was a prominent drop from 80% in 2006 to 28% in 2007 (after an increase from 69% in 2005) that continued in 2008 to 23 %, but increased again in 2009 to 30 % and to 60 % in 2010 and 2011. Specifically in the northern region of Europe, the area in exceedance peaked considerably in 2006: the area above the CL enlarged from 40 % in 2005 to 100 % in 2006 and reduced thereafter to 12 % in 2007 and increased in 2008 to 51 %. In 2009, some 23 % of the northern European forest area exceeded the CL. In 2010 it was about 13 % which increased in 2011 back to some 25 %. The RV (Table 6.12) decreases in northern Europe from 23 % in 2006 (after an increase from none in 2005) to none in 2007 – 2011. In comparison with 2006, the frequency distribution of the whole European forested area over the exposure classes shows for 2007 a clear shift to lower exposures. In 2008 a shift was observed of areas exposed in 2007 to the highest exposure class to its neighbouring lower class interval and for the areas exposed in 2007 to the lowest exposure class to its neighbouring higher class interval. In 2009 and 2010 the distribution showed similarity with that of 2007. In 2011 a light shift to the higher classes is observed, most prominently in the central and eastern European regions.

Table 6.11 Forest area exposure and exceedance (critical level, CL and reporting value, RV) for ozone, AOT40 for forests, year 2011.

Country	Forested area, 2011					Percentage of forested area, 2011 [%]				
	total area	> CL (10 mg.m^{-3}.h)		> RV (20 mg.m^{-3}.h)		< 10	10 - 20	20 - 30	30 - 50	> 50
	[km^2]	[km^2]	[%]	[km^2]	[%]	mg.m^{-3}.h	mg.m^{-3}.h	mg.m^{-3}.h	mg.m^{-3}.h	mg.m^{-3}.h
Albania	7587	7587	100	7587	100	0.0	0.0	0.0	58.3	41.7
Austria	37222	37222	100	37112	100	0.0	0.3	36.5	63.2	0.0
Belgium	6093	6059	99.4	2183	36	0.6	63.6	35.8	0.0	0.0
Bosnia-Herzegovina	22805	22805	100	22805	100	0.0	0.0	0.1	99.9	0.0
Bulgaria	34640	34640	100	34640	100	0.0	0.0	29.4	69.6	1.0
Croatia	20089	20089	100	20089	100	0.0	0.0	7.4	85.3	7.3
Cyprus	1535	1535	100	1535	100	0.0	0.0	0.0	24.1	75.9
Czech Republic	26094	26094	100	26008	100	0.0	0.3	72.1	27.6	0.0
Denmark (no Faroes)	3730	3214	86.2	35	1	13.8	85.2	0.9	0.0	0.0
Estonia	20561	6627	32.2	0	0	67.8	32.2	0.0	0.0	0.0
Finland	194000	11149	5.7	0	0	94.3	5.7	0.0	0.0	0.0
France	144848	144796	100	123535	85	0.0	14.7	54.0	23.9	7.4
Germany	104149	104149	100	88676	85	0.0	14.9	79.8	5.4	0.0
Greece (CLC2000)	23553	23553	100	23553	100	0.0	0.0	0.2	92.1	7.8
Hungary	17519	17519	100	17510	100	0.0	0.0	32.4	67.6	0.0
Iceland	318	0	0	0	0	100.0	0.0	0.0	0.0	0.0
Ireland	2835	0	0	0	0	100.0	0.0	0.0	0.0	0.0
Italy	78244	78244	100	78244	100	0.0	0.0	0.8	69.0	30.2
Latvia	26157	19692	75.3	64	0	24.7	75.0	0.2	0.0	0.0
Liechtenstein	85	85	100	85	100	0.0	0.0	0.0	100.0	0.0
Lithuania	18728	18728	100	80	0	0.0	99.6	0.4	0.0	0.0
Luxembourg	930	930	100	763	82	0.0	18.0	82.0	0.0	0.0
Macedonia	8231	8231	100	8231	100	0.0	0.0	0.0	97.5	2.5
Malta	2	2	100	2	100	0.0	0.0	0.0	0.0	100.0
Monaco	0.41	0.41	100	0.41	100	0.0	0.0	0.0	0.0	100.0
Montenegro	5737	5737	100	5737	100	0.0	0.0	0.0	95.6	4.4
Netherlands	3101	2861	92.3	0	0	7.7	92.3	0.0	0.0	0.0
Norway	103844	34124	32.9	0	0	67.1	32.9	0.0	0.0	0.0
Poland	93923	93923	100	68766	73	0.0	26.8	68.3	4.9	0.0
Portugal	20133	20133	100	17933	89	0.0	10.9	61.7	27.4	0.0
Romania	69987	69987	100	67183	96	0.0	4.0	79.2	16.8	0.0
San Marino	6	6	100	6	100	0.0	0.0	0.0	0.0	100.0
Serbia (incl. Kosovo)	26878	26878	100	26878	100	0.0	0.0	1.4	98.6	0.0
Slovakia	19680	19680	100	19645	100	0.0	0.2	23.3	76.6	0.0
Slovenia	11471	11471	100	11471	100	0.0	0.0	0.0	76.3	23.7
Spain	90270	90270	100	84043	93.1	0.0	6.9	22.1	70.3	0.7
Sweden	243521	61544	25.3	0	0	74.7	25.3	0.0	0.0	0.0
Switzerland	12529	12529	100	12529	100	0.0	0.0	23.9	70.9	5.2
United Kingd. (+ Man)	20054	1647	8.2	0	0	89.0	11.0	0.0	0.0	0.0
Total	**1521089**	**1043740**	**68.6**	**806928**	**53.0**	**31.4**	**15.6**	**24.6**	**25.3**	**3.1**
France over 45N	89502	89450	99.9	70257	78.5	0.1	21.4	66.0	12.2	0.3
France below 45N	55346	55346	100.0	53278	96.3	89.0	11.0	0.0	0.0	0.0
Kosovo	4291	4291	100	4291	100	0.0	0.0	0.0	100.0	0.0
Serbia (excl.Kosovo)	22587	22587	100	22587	100	0.0	0.0	1.7	98.3	0.0
Northern	610542	155079	25.4	179	0.0					
North-western	122834	100948	82.2	73203	59.6					
Central & Eastern	415826	415826	100.0	372154	89.5					
Southern	371887	371887	100.0	361392	97.2					
Total	**1521089**	**1043740**	**68.6**	**806928**	**53.0**					

Note1: Countries not included due to lack of land cover data: Andorra, Turkey.
Note2: The percentage value "0.0" indicates an exposured population exists, but is small and estimated less than 0.05 %.
Empty cells mean: no population in exposure.

Table 6.12 Evolution of percentage agricultural area above target value for AOT40 for crops (left) and percentage forested area above reporting value for AOT40 for forests (right) in the years 2006-2011.

Country		AOT40 for crops							AOT40 for forests						
		Agricultural area above TV [%]							Forested area above RV [%]						
		2006	2007	2008	2009	2010	2011	diff. '11 - '10	2006	2007	2008	2009	2010	2011	diff. '11 - '10
Albania	AL	100	100	87.3	100	4.0	100	96.0	100	100	100	100	100	100	0.0
Austria	AT	100	81.8	67.3	4.0	40.9	32.5	-8.4	100	100	100	100	99.7	99.7	0.0
Belgium	BE	98.0	0	0	0	0	0.0	0.0	99.8	7.9	0	0	33.7	36	2.1
Bosnia-Herzegovina	BA	62.7	100	80.0	90.3	46.2	51.2	5.0	100	100	100	100	100	100	0.0
Bulgaria	BG	44.5	99.6	2.4	64.4	4.6	10.5	5.9	100	100	100	100	98.1	100	1.9
Croatia	HR	82.2	100	95.8	85.5	62.0	68.6	6.6	100	100	100	100	100	100	0.0
Cyprus	CY	99.0	100	0.0	100	87.2	90.6	3.4	100	100	100	100	100	100	0.0
Czech Republic	CZ	100	83.0	99.0	0.0	8.0	4.8	-3.2	100	100	100	100	96.4	99.7	3.3
Denmark	DK	5	0	0	0	0	0.0	0.0	91.7	0.9	1.7	1.7	0	0.9	0.9
Estonia	EE	0	0	0	0	0	0.0	0.0	52.6	0	0	0	0	0	0.0
Finland	FI	0	0	0	0	0	0.0	0.0	2.1	0	0	0	0	0	0.0
France	FR	78.0	3.4	10.2	10.2	11.9	6.5	-5.4	97.0	50.9	48.0	52.2	85.3	85.3	0.0
Germany	DE	94.7	3.6	62	0.0	24.4	0.3	-24.1	99.8	76.9	92.8	81.0	84.0	85.1	1.2
Greece	GR	95.2	97.4	79.0	95.2	44.1	77.6	33.5	100	100	100	100	100	100	0.0
Hungary	HU	93.4	100	82.8	83.6	7.2	15.3	8.1	100	100	100	100	92.6	100	7.3
Iceland	IS	*no d.*	0	0	0	0	0.0	0.0	*no d.*	0	0	0	0	0.0	0.0
Ireland	IE	0	0	0	0	0	0.0	0.0	0	0	0	0	0	0.0	0.0
Italy	IT	100.0	84.0	83.8	91.2	67.9	80.7	12.8	100	100	100	100	100	100	0.0
Latvia	LV	0	0	0	0	0	0.0	0.0	39.9	0	0	0	0	0	0.2
Liechtenstein	LI	100	7.7	100	0	100	100.0	0.0	100	100	100	100	100	100	0.0
Lithuania	LT	0	0	0	0	0	0.0	0.0	55.1	0	0	0	0	0	0.4
Luxembourg	LU	100	0	0	0	26.8	0.0	-26.8	100	64.8	7.4	100	94.9	82	-12.9
Macedonia, FYR of	MK	100	100	99.8	100	1.3	72.1	70.8	100	100	100	100	100	100	0.0
Malta	MT	99	99.1	100	100	100	100.0	0.0	100	100	100	100	100	100	0.0
Monaco	MC	100	92.3	0	100	100		-100.0	100	100	100	100	100	100	0.0
Montenegro	ME	*no d.*	100	94.2	100	26.4	83.3	56.9	*no d.*	100	100	100	100	100	0.0
Netherlands	NL	53.3	0	0	0	0	0.0	0.0	87.7	0	0	0	0	0	0.0
Norway	NO	*no d.*	0	0	0	0	0.0	0.0	*no d.*	0.2	0.0	0	0	0	0.0
Poland	PL	94.4	21.2	38.9	0	0	0.6	0.6	100	65.3	81.7	70.0	27.3	73.2	45.9
Portugal	PT	87.7	0	2	0	41.5	4.2	-37.3	100	91.1	89.1	95.7	99.7	89	-10.6
Romania	RO	10.4	97.0	9.9	21.5	0	0.0	0.0	98.8	100	99.6	100	80.8	96.0	15.2
San Marino	SM	100	100	100	100	100	100.0	0.0	100	100	100	100	100	100	0.0
Serbia (inc.Kosovo)	RS	*no d.*	100	67.4	100	2.9	24.1	21.2	*no d.*	100	100	100	100	100	0.0
Slovakia	SK	99.1	99.7	78.7	58.4	0.2	25.4	25.2	100	100	100	100	90.8	100	9.0
Slovenia	SI	100	100	95.6	73.1	100	100.0	0.0	100	100	100	100	100	100	0.0
Spain	ES	93.3	27.2	58.5	35.1	60.7	48.4	-12.3	99.4	94.3	89.8	88.4	93.3	93.1	-0.2
Sweden	SE	12.6	0	0	0	0	0.0	0.0	31.2	0.0	0	0	0	0	0.0
Switzerland	CH	*no data*		67.4	10.0	98.1	29.2	-68.9	*no data*		100	99.9	100	100	0.0
United Kingdom	UK	14.4	0	0	0	0	0.0	0.0	11.0	0	0	0	0	0	0.0
Total		**69.1**	**35.7**	**37.8**	**26.0**	**21.3**	**19.2**	**-2.1**	**69.4**	**48.4**	**50.2**	**49.2**	**49.3**	**53.0**	3.8
Northern		3.6	0	0	0	0	0	0.0	22.9	0.0	0	0.0	0	0	0.0
North-western		49.4	0.1	2.0	2.0	33.0	1.1	-31.9	79.8	27.8	23.3	29.9	59.7	59.6	-0.1
Central & eastern		76.8	50.3	47.2	17.4	11.0	4.9	-6.1	99.7	86.1	94.0	88.5	75.4	89.5	14.1
Southern		93.9	55.3	63.5	60.4	56.8	53.6	-3.2	99.7	94.2	93.1	92.8	97.8	97.2	-0.6

Note: Lack of land cover data in 2006: CH, IS, ME, NO, RS; in 2007: CH.

The total area with AOT40 levels below the CL diminished by 18 % in 2008 (20 %) compared to 2007 (38 %) but increased again in 2009 up to 33 % and in 2010 to 37 %. In 2011 it is with 32% about the

same as in 2009. The total forested area exposed to levels below the RV stabilised in the period 2007 – 2011 around a value of 50 %.

6.3.3 Uncertainties

Uncertainty estimated by cross-validation

In Table 6.9 the absolute mean uncertainty (RMSE) obtained by cross-validation is 5263 µg.m^{-3}.h for the AOT40 for crops and 9341µg.m^{-3}.h for the AOT40 for forests. It indicates that the year 2011 has slightly higher absolute mean uncertainties for the crops than in 2010 (5198 µg.m^{-3}.h) and 2009 (5138 µg.m^{-3}.h), while similar as in the year 2008 (5283 µg.m^{-3}.h) and lower than in the previous years, 5876 µg.m^{-3}.h (2007), 7674 µg.m^{-3}.h (2006) and 7700 µg.m^{-3}.h (2005). For forests, it is higher than the values 8384 µg.m^{-3}.h (2010) and 8750 µg.m^{-3}.h (2008), similar to 9311 µg.m^{-3}.h (2009) and lower than the values 10190 µg.m^{-3}.h (2007), 11990 µg.m^{-3}.h (2006) and 12500 µg.m^{-3}.h (2005). The relative mean uncertainties of the 2010 maps of ozone indicator AOT40 for crops is 35 %, while in the case of AOT40 for forests it is about 33%. For crops, that is higher than in 2010 (31%), 2008 (31 %) and 2006 (30%), while lower than in 2009 (38 %), 2007 (40 %) and 2005 (41 %). For forests, the relative RMSE is more than in 2010 (31%) and less than all previous years 2009 (34 %), 2008 (34 %), 2007 (37 %), 2006 (34 %) and 2005 (41%). Table 7.7 summarises both the absolute and the relative uncertainties over these past seven years.

Figure 6.12 shows the cross-validation scatter plots of the AOT40 for both crops and forests. R^2 indicates that for AOT40 for crops about 62 % and for AOT40 for forests about 67 % of the variability is attributable to the interpolation. The corresponding values for the 2010 maps (67 % and 69 %), 2009 maps (69 % and 68 %), 2008 maps (53 % and 56 %), 2007 maps (63 % and 67 %), the 2006 maps (47 % and 49 %) and 2005 maps (55 % and 58 %), indicate a somewhat increased level of interpolation performance at the 2009, 2010 and 2011 maps compared to those of previous years.

The cross-validation scatter plots show again that in areas with higher accumulated ozone concentrations the interpolation methods tend to deliver underestimated predicted values. For example, in agricultural areas (Figure 6.12, left panel) an observed value of 30 000 µg.m^{-3}.h is estimated in the interpolation as about 24 400 µg.m^{-3}.h, i.e. an underestimation of about 18 %. In addition, an overestimation at the lower end of predicted values occurred. One could reduce this under- and overestimation by extending the number of measurement stations and by optimising the spatial distribution of those stations, specifically in areas with elevated values.

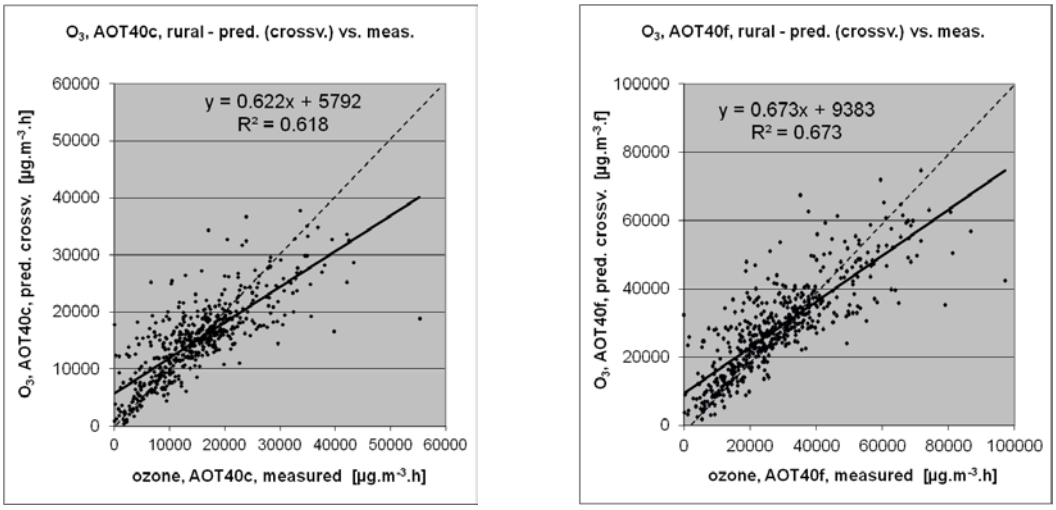

Figure 6.12 Correlation between cross-validation predicted values (y-axis) and measurements (x-axis) for the ozone indicators AOT40 for crops (left) and AOT40 for forests (right) for rural areas in 2011.

Comparison of point measurement values with the predicted grid value

In addition to the point observation – point prediction cross-validation, a simple comparison was made between the point measurements and interpolated predicted grid values on the grid of 2 km^2 resolution. The results of the cross-validation compared to the gridded validation are summarised in Table 6.13. The table shows for both receptors a better correlation between the station measurements and the averaged interpolated predicted values of the corresponding grid cells (case ii) than it does at the point cross-validation predictions (case i) of Figure 6.12. Case ii) represents the uncertainty in the predicted gridded interpolation map at the actual station locations (points) itself, whereas the point observation – point prediction cross-validation of case i) simulates the behaviour of the interpolation at point positions without actual measurements within the area covered by measurements. The uncertainty at measurement locations has partly its cause in the smoothing effect of interpolation and partly in the spatial averaging of the values in the 2x2 km grid cells. In such situations the degree of smoothing leading to underestimation at areas with high values is smaller than it is in case no measurement is present in such areas. For example, in agricultural areas a predicted interpolation grid value will be about 27 000 $\mu g.m^{-3}.h$ at a corresponding station point with an observed value of 30 000 $\mu g.m^{-3}.h$, i.e. an underestimation of about 10 %. This is lower than the likely underestimation of about 18% in areas where no measurements exist, as discussed in the previous subsection.

Table 6.13 Linear regression equation and coefficient of determination R^2 from the scatter plots of (i) the predicted point values based on cross-validation and (ii) aggregation into 2x2 km grid cells versus the measured point values for ozone indicators AOT40 for crops (left) and AOT40 for forests (right) for rural areas in 2011.

	AOT40 for crops		AOT40 for forests	
	equation	R^2	equation	R^2
i) cross-validation prediction (Fig 6.12)	y = 0.622x + 5792	0.618	y = 0.673x + 9383	0.673
ii) 2x2 km grid prediction	y = 0.796x + 3095	0.884	y = 0.819x + 5145	0.891

The AOT40 for crops with a target value of 18 000 $\mu g.m^{-3}.h$ would allow us to prepare a probability of exceedance map. However, we limited the preparation of such maps to the human health related indicators, thus not involving the accumulative ozone indicators used in the EEA CSI005 (itself not demanding such maps).

7 Concluding exposure and uncertainty estimates

Mapping and exposure results

This paper presents the interpolated maps for 2011 on the PM_{10}, $PM_{2.5}$ and ozone human health related air pollution indicators, together with their frequency distribution of the estimated population exposures and exceedances. It concerns the annual average and the 36th highest daily mean for PM_{10}, annual average for $PM_{2.5}$, and the 26th highest daily maximum 8-hour value and the SOMO35 for ozone. Interpolated maps on the vegetation/ecosystem based ozone indicators AOT40 for crops and AOT40 for forests are additionally presented, including their frequency distribution of estimated land area exposures and exceedances. A mapping approach similar to previous years (De Smet et al. 2011 and references cited therein, Denby et al. 2011c) on observational data was used. For the second time, interannual difference maps are presented.

Human health PM_{10} indicators

Table 7.1 summarises for both *human health PM_{10} indicators* the average concentration the European inhabitant is exposed to, i.e. the population-weighted concentration and the number of Europeans exposed to PM_{10} concentrations above their limit values (LV) for the years 2005 to 2011. The table presents the results obtained from both the 10x10 km resolution fields, as used in previous data years up to 2007 and the 1x1 km resolution grid as tested with the 2006 data in Horálek et al (2010), recomputed for 2007 and implemented fully on the 2008 data and onwards. This indicates that the underestimated predictions of PM_{10} values caused by merging rural and urban predictions at 10x10 km resolution have been resolved better when using the higher 1x1 km grid resolution. In other words, an increased merging resolution contributes to a quantitatively better population exposure estimate due to better-resolved spatially smaller urbanised patterns in the map.

Table 7.1 Percentage of the total European population exposed to PM_{10} concentrations above the limit values (LV) and the population-weighted concentration for the human health PM_{10} indicators annual average and 36th highest daily average for 2005 to 2011.

PM10			2005	2006	2007	2008	2009	2010	2011
Annual average									
Population-weighted concentration	($\mu g.m^{-3}$)	10x10 merger	26.3	27.1	25.3				
		1x1 merger		28.5	26.2	24.8	24.6	24.3	22.1
Population exposed > LV (40 $\mu g.m^{-3}$)	(% of total)	10x10 merger	9.3	7.7	5.7				
		1x1 merger		10.32	6.796	5.8	6.0	5.2	2.5
36th max. daily average									
Population-weighted concentration	($\mu g.m^{-3}$)	10x10 merger	43.8	45.4	42.4				
		1x1 merger		47.8	44.11	41.3	41.2	41.87	39.0
Population exposed > LV (50 $\mu g.m^{-3}$)	(% of total)	10x10 merger	28.1	28.5	22.0				
		1x1 merger		35.7	26.19	19.4	16.5	20.64	15.76

The population exposed to *annual mean* concentrations of PM_{10} above the limit value of 40 $\mu g.m^{-3}$ is at least 2.5 % of the total population in 2011, slightly less than in 2010. Furthermore, it is estimated that European inhabitants living in background (neither hot-spot nor industrial) areas – without regard to urban or rural – are exposed on average to the annual mean PM_{10} concentration of about 22 $\mu g.m^{-3}$. In comparison with the previous three years, the number of people living in the areas above the LV tends to go down slightly. It is not possible to talk about a trend when taking into account (i) the meteorologically induced variations and (ii) the uncertainties involved in the interpolation. Longer time series and reduced uncertainties will be needed before any conclusions on a possible trend can be drawn.

In 2011 about 16 % of the European population lived in areas where the PM_{10} limit value of 50 $\mu g.m^{-3}$ for the *36th highest daily mean* is exceeded, being some 5 % lower than in 2010, 1 % lower than in 2009, 3 % lower than in 2008, 10 % lower than in 2007, and 20 % lower than in 2006. The overall European population-weighted concentration of the 36th highest daily mean for the background areas is estimated at about 39 $\mu g.m^{-3}$, which is of about 2 - 3 $\mu g.m^{-3}$ less than in 2008 – 2010. Comparing the observed (and also predicted) exceedances for both PM_{10} indicators, one can conclude that the daily limit value is the most stringent throughout the years.

Human health $PM_{2.5}$ indicator

Table 7.2 summarises for *human health $PM_{2.5}$ indicator* (annual average) the population-weighted concentration and the number of Europeans exposed to $PM_{2.5}$ concentrations above its target value (TV) for the years 2007 to 2011 (without 2009, for which nor the map nor the population exposure were prepared).

Table 7.2 Percentage of the total European population exposed to $PM_{2.5}$ concentrations above the target value (TV) and the population-weighted concentration for the human health $PM_{2.5}$ indicator annual average for 2007 to 2011.

PM2.5			2007	2008	2009	2010	2011
Annual average							
Population-weighted concentration	($\mu g.m^{-3}$)	10x10 merger	15.5	15.6	not		
		1x1 merger	16.3	16.3	mapped	16.8	15.9
Population exposed > TV (25 $\mu g.m^{-3}$)	(% of total)	10x10 merger	6.2	6.2	not		
		1x1 merger	7.8	7.6	mapped	8.3	6.2

The proportion exposed to annual mean concentrations of $PM_{2.5}$ above the target value of 25 $\mu g.m^{-3}$ is at least 6 % of the total population in 2011, which is slightly less than in 2007, 2008 and 2010. Furthermore, it is estimated that European inhabitants living in background (neither hot-spot nor industrial) areas – without regard to urban or rural – are exposed on average to the annual mean $PM_{2.5}$ concentration of about 16 $\mu g.m^{-3}$. In comparison with the previous years, the number of people living in the areas above the TV seems to decrease slightly.

Human health ozone indicators

Table 7.3 summarises the levels of both *human health ozone indicators* that European inhabitants are exposed to, i.e. population-weighted concentrations. Furthermore, it presents the number of Europeans exposed to concentrations above the target value (TV) of the 26th highest daily maximum 8-hour mean and above a level of 6 $mg.m^{-3}.d$ for the SOMO35 for the years 2005 to 2011.

Table 7.3 Percentage of the total European population exposed to ozone concentrations above the target value (TV) for the 26th highest daily maximum 8-hour average and an indicative chosen threshold for SOMO35, including their population-weighted concentrations for2005 to 2011.

Ozone			2005	2006	2007	2008	2009	2010	2011
26th highest daily max. 8-hr average									
Population-weighted concentration	($\mu g.m^{-3}$)	10x10 merger	112.9	119.6	112.1				
		1x1 merger		118.2	110.7	109.8	108.1	106.8	108.9
Population exposed > TV (120 $\mu g.m^{-3}.h$)	(% of total)	10x10 merger	37.8	55.5	33.5				
		1x1 merger		51.4	27.1	15.0	16.0	16.3	16.5
SOMO35									
Population-weighted concentration	($\mu g.m^{-3}$)	10x10 merger	5047	5485	4679				
		1x1 merger		5167	4411	4275	4275	3917	4414
Population exposed > 6 $mg.m^{-3}.d$	(% of total)	10x10 merger	33.9	37.4	32.6				
		1x1 merger		29.5	28.07	19.6	24.6	16.64	23.55

The table presents the results obtained with the merging resolution of 10x10 km, as used at previous data years up to 2007, and the 1x1 km merging resolution as tested on the 2006 data in Horálek et al (2010) and implemented fully on the 2008 data and onwards. It provides an indication that the underestimation of ozone values when merged with the 10x10 km grid resolution has been resolved better when using a higher 1x1 km grid resolution. In other words, an increased merging resolution contributes to a quantitatively better population exposure estimate due to better-resolved spatially smaller urbanised patterns in the map.

For the ozone indicator *26th highest daily maximum 8-hour mean* it is estimated that at least 16 % of the population lived in 2011 in areas above the ozone target value (TV) of 120 µg.m^{-3}, which was similar to that of 2010. The overall European population-weighted ozone concentration in terms of the 26th highest daily maximum 8-hour mean in the background areas is estimated at almost 109 µg.m^{-3} which is slightly higher than that of 2010 (107 µg.m^{-3}). Compared to the previous years 2005 – 2009, one could conclude that 2006 is a year with elevated ozone concentrations, leading to increased exposure levels compared to the other five years. Additionally, the population exposed to ozone level above the target value is in 2008 – 2011 substantially lower than in the preceding period 2007 – 2005.

A similar tendency is observed for the *SOMO35*: In 2006 – 2007 almost one-third of the population lived in areas where a level of 6 mg.m^{-3}.d$^{(*)}$ was exceeded, with the highest level in 2006. In 2008 it concerns only one-fifth of the population, a quarter in 2009, one-sixth in 2010 and a quarter in 2011. The population-weighted SOMO35 concentrations shows quite a similar pattern in time.

(*) Note that the 6 mg.m^{-3}.d does not represent a health-related legally binding 'threshold'. In this and previous papers it concerns a somewhat arbitrarily chosen threshold to facilitate the discussion of the observed distributions of SOMO35 levels in their spatial and temporal context. For motivation of this choice, see Section 6.2.2.

Agricultural and forest ozone indicators

Exposure indicators describing the *agricultural and forest areas exposed to accumulated ozone* concentrations above defined thresholds are summarised in Table 7.4. Those thresholds are the target value (TV) of 18 mg.m^{-3}.h and the long-term objective (LTO) of 6 mg.m^{-3}.h for the AOT40 for crops, and the Reporting Value (RV) of 20 mg.m^{-3}.h and the Critical Level (CL) of 10 mg.m^{-3}.h for the AOT40 for forests.

Table 7.4 Percentages of the total European agricultural and forest area exposed to ozone concentrations above their thresholds: target value (TV) and long-term objective (LTO) for AOT40 for crops, and Critical Level (CL) and Reporting Value (RV) for AOT40 for forests for2005 to 2011.

Ozone		2005	2006	2007	2008	2009	2010	2011
AOT40 for crops								
Agricultural area % > TV (18 mg.m^{-3}.h)	(% of total)	48.5	69.1	35.7	37.8	26.0	21.3	19.2
Agricultural area % > LTO (6 mg.m^{-3}.h)	(% of total)	88.8	97.6	77.5	95.5	81.0	85.4	87.9
AOT40 for forests								
Forest area exposed > RV (20 mg.m^{-3}.h)	(% of total)	59.1	69.4	48.4	50.2	49.2	49.3	53.0
Forest area exposed > CL (10 mg.m^{-3}.h)	(% of total)	76.4	99.8	62.1	79.6	67.4	63.4	68.6

In 2011, 19% of all agricultural land (*crops*) was exposed to accumulated ozone concentrations exceeding the target value (TV) and 88 % was exposed to levels in excess of the long-term objective (LTO). Compared to the previous five years one could conclude that 2006 was a year with elevated ozone concentrations, leading to increased exposure levels above the target value and that they subsided in the period 2007 – 2011 to levels clearly below those of 2005. On the other hand, the percentage of the total area exposed to levels above the long-term objective (LTO) is in 2007 lowest compared to all the other years.

For the ozone indicator AOT40 for *forests* the level of 20 mg.m^{-3}.h (Reporting Value, RV) was in 2011 exceeded in about 53 % of the European forest area, which is slightly more than in the years 2007 – 2010 and clearly below the percentages of the years 2005 and 2006. The forest area exceeding

the Critical Level was in 2011 about 69 %, which is slightly more than in the years 2009, 2010 and 2007 (with 62 – 67 % exceedance) and well below 2008 and 2005 (with 76 – 80 % exceedance), and 2006 when all forest area was exceeded.

The temporal pattern of the AOT40 for forests exceedances shows some similarity with those of the AOT40 for crops, despite their different definitions. This annual variability is heavily dependent on meteorological variability.

Uncertainty results

Next to the creation of European wide interpolated air pollutant maps and exposure tables, we evaluated the uncertainty of the presented concentration maps and maps with estimated probability of threshold exceedance for the human health indicators. As exactly the same method and data sources have been applied over the years 2005 to 2011, a change in uncertainty is in principle related to the data content itself. However, for the 2008 data we implemented for the first time an increased resolution (from a 10x10 km into 1x1 km grid field) at the merging of the separate human health indicator interpolated maps (on 10x10 km grid) into one combined final 1x1 km gridded indicator map. The merging made use of the 1x1 km population density map. (The subsequent exposure estimates however, have been based on the 10x10 km grid fields aggregated from the 1x1 km grids of the merging result). The increased merging resolution should in principle improve the accuracy in the concentration maps, including the subsequent exposure estimates. Denby et al. (2009) discusses a diversity of uncertainty factors potentially involved, including their possible levels of influence. More background information on causes of uncertainties and their assessment can be found in Malherbe et al (2012). The paper recommends options to reduce uncertainties systematically. Horálek et al. (2010) explored specific options to reduce interpolation uncertainty related to the spatial resolutions applied at the different process steps of the mapping method. This paper concludes and justifies the implementation of the increased merging grid as the most significant uncertainty reduction measure, against the least additional computational demands. For further reading on the sub-grid variability and its influence to the exposure estimates, see Denby et al. (2011a).

Table 7.5 summarises the absolute and relative mean interpolation uncertainties of the PM_{10} maps for the seven-year sequence. The higher uncertainty levels for urban areas in the years 2008 - 2011, compared to the years 2007 – 2005, are caused specifically by addition of Turkish urban background stations reported only since 2008.

Table 7.5 Absolute mean uncertainty (RMSE, $\mu g.m^{-3}$) and relative mean uncertainty (RMSE relative to mean indicator value, in %) for the total European rural and urban areas for PM_{10} annual average and the 36th highest daily average for the years 2005 – 2011.

PM10			2005	2006	2007	2008	2009	2010	2011
Annual average									
rural areas	abs. mean uncertainty	RMSE ($\mu g.m^{-3}$)	5.5	5.8	4.6	5.0	4.6	4.5	4.1
	rel. mean uncertainty	(%)	*25.9*	*26.6*	*23.5*	*27.2*	*23.9*	*22.7*	*21.1*
urban areas	abs. mean uncertainty	RMSE ($\mu g.m^{-3}$)	5.5	6.1	5.0	6.3	6.7	6.6	6.1
	rel. mean uncertainty	(%)	*20.0*	*20.9*	*18.4*	*22.4*	*23.0*	*22.5*	*20.7*
36th max. daily average									
rural areas	abs. mean uncertainty	RMSE ($\mu g.m^{-3}$)	9.7	9.9	8.0	8.8	8.0	8.6	8.4
	rel. mean uncertainty	(%)	*26.3*	*26.6*	*23.5*	*28.2*	*24.1*	*24.4*	*23.5*
urban areas	abs. mean uncertainty	RMSE ($\mu g.m^{-3}$)	9.9	11.7	9.1	12.7	13.2	12.2	13.0
	rel. mean uncertainty	(%)	*21.4*	*23.5*	*19.6*	*24.4*	*26.7*	*23.7*	*24.3*

Table 7.6 presents the uncertainty results for $PM_{2.5}$ maps for the years 2007 – 2011 (excluding the 'non-mapped' year 2009). Both absolute and relative uncertainties show a decrease in 2011 in rural areas, in comparison with the previous years. The results for the urban areas are the similar as in 2010.

Table 7.6 Absolute and relative mean uncertainty for the total European rural and urban areas for $PM_{2.5}$ annual average, for the years 2007 – 2011.

PM2.5			2007	2008	2009	2010	2011
Annual average							
rural areas	abs. mean uncertainty	RMSE ($\mu g.m^{-3}$)	3.3	3.5	not	3.4	2.8
	rel. mean uncertainty	(%)	*27.4*	*29.8*	mapped	*25.0*	*16.8*
urban areas	abs. mean uncertainty	RMSE ($\mu g.m^{-3}$)	4.1	3.6	not	3.1	3.2
	rel. mean uncertainty	(%)	*23.7*	*20.0*	mapped	*16.8*	*16.7*

The relative mean interpolation uncertainty of the ozone maps in Table 7.7 at the rural areas increased slightly for the majority of the indicators in 2011, compared to previous year 2010. The exception is the 26th highest daily maximum 8-hour average with a slight decrease in relative uncertainty. The uncertainties of the maps for the urban areas decreased in 2011 somewhat compared to previous years in the case of the 26th highest daily maximum 8-hour average, while SOMO35 shows comparable results.

Table 7.7 Absolute and relative mean uncertainty for the total European areas for ozone the 26th highest daily maximum 8-hour average, SOMO35, AOT40 for crops and for forests, for the years 2005 – 2011.

Ozone			2005	2006	2007	2008	2009	2010	2011
26th highest daily max. 8-hr average									
rural areas	abs. mean uncertainty	RMSE ($\mu g.m^{-3}$)	12.3	11.2	8.8	8.7	8.2	8.9	8.4
	rel. mean uncertainty	(%)	*10.3*	*8.9*	*7.5*	*7.6*	*7.2*	*7.7*	*7.2*
urban areas	abs. mean uncertainty	RMSE ($\mu g.m^{-3}$)	10.0	10.2	8.9	8.8	9.3	9.2	9.1
	rel. mean uncertainty	(%)	*8.9*	*8.4*	*7.9*	*7.9*	*8.4*	*8.2*	*8.1*
SOMO35									
rural areas	abs. mean uncertainty	RMSE ($\mu g.m^{-3}.d$)	2173	2077	1801	1609	1635	1608	1747
	rel. mean uncertainty	(%)	*35.5*	*31.6*	*33.3*	*30.7*	*29.7*	*29.6*	*29.6*
urban areas	abs. mean uncertainty	RMSE ($\mu g.m^{-3}.d$)	1459	1472	1260	1293	1475	1278	1374
	rel. mean uncertainty	(%)	*32.0*	*29.2*	*29.5*	*31.3*	*33.1*	*29.6*	*29.7*
AOT40 for crops									
rural areas	abs. mean uncertainty	RMSE ($\mu g.m^{-3}.h$)	7677	7674	5876	5283	5138	5198	5263
	rel. mean uncertainty	(%)	*40.7*	*29.6*	*39.6*	*31.3*	*37.7*	*30.8*	*34.9*
AOT40 for forests									
rural areas	abs. mean uncertainty	RMSE ($\mu g.m^{-3}.h$)	12474	11990	10190	8750	9304	8384	9341
	rel. mean uncertainty	(%)	*41.5*	*33.6*	*37.1*	*34.0*	*33.9*	*31.4*	*32.7*

The scatter plots of the interpolation results versus the measurements show that for both the PM_{10} and the ozone indicators, in areas with high values, an underestimation of the predicted values occurs. This also leads to a considerable underestimation at locations without measurements and at areas with the higher concentrations. This effect occurs most prominently for the ozone indicators. We expect that the underestimation would reduce when an improved fit of the linear regression with (other) supplementary data could be obtained. For example, in the near future more contributions from satellite imagery data and interpretation techniques could be expected. An option is to extend the number of measurement stations and/or using additional mobile stations (e.g. in measurement campaigns). For further reading on this subject, we refer to Denby et al. (2009), Gräler et al. (2012, 2013), Schneider et al. (2012), Castell et al (2013) and Tarrasón et al (2014).

Probability of exceedance

Maps with the probability of exceedance of Limit Values and Target Value have been prepared for the human health indicators of PM_{10}, $PM_{2.5}$, and ozone, respectively. These probability maps, with a class distribution as defined in Table 4.5, are derived from combining the indicator map and its uncertainty map following the same method throughout the years 2005 to 2011. The differences in the maps

between years depend on annual fluctuations in concentration levels, supplementary data and their involved uncertainties (Denby et al. 2009, Gerharz et al. 2011, and Gräler et al. 2012, 2013). Some disruption or 'jump' could be expected between the data of 2005 – 2007 and 2008 – 2010. This would be caused by the increased merging resolution applied for the first time on the 2008 data. As Horálek et al. (2010) indicated, it should improve the population exposure estimates, specifically for population living in urban areas (that profit most of this methodological refinement). Nevertheless, as the maps are spatially merged into 10x10 km grid resolution, the influence of the urban pollution into the final map is smaller than was in the methodology used until 2007. Thus, it is needed to bear in mind that the spatial average of a 10x10 km grid cell can show low probability of exceedance even though some smaller (e.g. urban) areas inside such a grid cell would show high probability of exceedance (in case of using a finer grid cell resolution).

In 2011 for the annual average PM_{10}, the patterns in the spatial distribution of the different probability of exceedance (PoE) classes over Europe were quite similar to those of 2010. However, the region of southern Poland – north-eastern Czech Republic with the industrial zones of Katowice and Ostrava showed a smaller area with high PoE values in comparison with 2010. Contrary to that, the Po Valley in Italy showed a higher probability of exceedance, in comparison with 2010.

The 36^{th} highest daily means of PM_{10} do show a decrease in the spatial extents and PoE levels throughout south-eastern Europe, in comparison with PoE in 2010. In particular, large areas of Greece and Cyprus have decreased PoE. The Po Valley in northern Italy has quite a similar PoE pattern to 2009 and 2010. Western Belgium and north-western France have increased levels of PoE. Hungary, northern Serbia and eastern and southern Romania show larger areas with high PoE levels, comparing with 2010. The areas with the increased PoE levels in southern Poland and north-eastern Czech Republic are smaller than in 2010.

PoE map for $PM_{2.5}$ is presented for the second time. In comparison with 2010, larger area in the Po Valley with the increased levels of PoE does occur. Next to this, more elevated PoE than in 2010 is visible in larger areas and some agglomerations of Hungary, Serbia, Romania and Bulgaria. Contrary to that, the reduction of the areas with elevated levels of PoE in Poland took place.

Interpreting 2011 and its preceding six years, one can conclude for ozone that in 2006 the probability of exceedance (PoE) increased temporarily in most parts of Europe. In 2007 – 2011, a decrease took place in the levels of PoE, to levels in many areas well below those of 2005. In 2011, most of the areas with large PoE in the northern Italy, southern France and Slovenia did not change compared to 2010. In south-eastern Europe and in southern Italy there were clear increase of the areas with elevated PoE. On the Iberian Peninsula reduced areas were estimated with large PoE, a minor decrease was visible also in some areas of central Europe.

References

AirBase, European air quality database, http://acm.eionet.europa.eu/databases/airbase/index_html

Castell N, Viana M, Minguillón M C, Guerreiro C, Querol X (2013). Real-world application of new sensor technologies for air quality monitoring. ETC/ACM Technical Paper 2013/16. http://acm.eionet.europa.eu/reports/ETCACM_TP_2013_16_new_AQ_SensorTechn

Cressie N (1993). Statistics for spatial data. Wiley series, New York.

De Leeuw F (2012). AirBase: a valuable tool in air quality assessments at a European and local level. ETC/ACM Technical Paper 2012/4. http://acm.eionet.europa.eu/reports/ETCACM_TP_2012_4_AirBase_AQassessment

Denby B, Schaap M, Segers A, Builtjes P, Horálek J (2008). Comparison of two data assimilation methods for assessing PM_{10} exceedances on the European scale. Atmospheric Environment 42, 7122–7134.

Denby B, De Leeuw F, De Smet P, Horálek J (2009). Sources of uncertainty and their assessment in spatial mapping. ETC/ACC Technical Paper 2008/20. http://acm.eionet.europa.eu/reports/ETCACC_TP_2008_20_spatialAQ_uncertainties

Denby B, Cassiani M, de Smet P, de Leeuw F, Horálek J (2011a). Sub-grid variability and its impact on European wide air quality exposure assessment. Atmospheric Environment 45, 4220-4229.

Denby B, Gola G, De Leeuw F, De Smet P, Horálek J (2011b). Calculation of pseudo $PM_{2.5}$ annual mean concentrations in Europe based on annual mean PM10 concentrations and other supplementary data. ETC/ACC Technical Paper 2010/9. http://acm.eionet.europa.eu/reports/ETCACC_TP_2010_9_pseudo_PM2.5_stations

Denby B, Horálek J, de Smet P, de Leeuw F (2011c). Mapping annual mean $PM_{2.5}$ concentrations in Europe: application of pseudo $PM_{2.5}$ station data. ETC/ACM Technical Paper 2011/5. http://acm.eionet.europa.eu/reports/ETCACM_TP_2011_5_spatialPM2.5mapping

De Smet P, Horálek J, Coňková M, Kurfürst P, de Leeuw F, Denby B (2009). European air quality maps of ozone and PM_{10} for 2006 and their uncertainty analysis. ETC/ACC Technical Paper 2008/8. http://acm.eionet.europa.eu/reports/ETCACC_TP_2008_8_spatAQmaps_2006

De Smet P, Horálek J, Coňková M, Kurfürst P, de Leeuw F, Denby B (2010). European air quality maps of ozone and PM_{10} for 2007 and their uncertainty analysis. ETC/ACC Technical Paper 2009/9. http://acm.eionet.europa.eu/reports/ETCACC_TP_2009_9_spatAQmaps_2007

De Smet P, Horálek J, Coňková M, Kurfürst P, de Leeuw F, Denby B (2011). European air quality maps of ozone and PM_{10} for 2008 and their uncertainty analysis. ETC/ACC Technical Paper 2010/10. http://acm.eionet.europa.eu/reports/ETCACC_TP_2010_10_spatAQmaps_2008

De Smet P, Horálek J, Schreiberová M, Kurfürst P, de Leeuw F (2012). European air quality maps of ozone and PM_{10} for 2009 and their uncertainty analysis. ETC/ACM Technical Paper 2011/11. http://acm.eionet.europa.eu/reports/ETCACM_TP_2011_11_spatAQmaps_2009

EC (2008). Directive 2008/50/EC of the European Parliament and of the Council of 21 May 2008 on ambient air quality and cleaner air for Europe. OJ L 152, 11.06.2008, 1-44. http://eur-lex.europa.eu/LexUriServ/LexUriServ.do?uri=OJ:L:2008:152:0001:0044:EN:PDF

ECMWF: Meteorological Archival and Retrieval System (MARS). http://www.ecmwf.int/

EEA (2008). ORNL Landscan 2008 Global Population Data conversion into EEA ETRS89-LAEA5210 1km grid (eea_r_3035_1_km_landscan-eurmed_2008, by Hermann Peifer of EEA).

EEA (2011). Guide for EEA map layout. EEA operational guidelines. August 2011, version 4. http://www.eionet.europa.eu/gis/docs/GISguide_v4_EEA_Layout_for_map_production.pdf

EEA (2012). Corine land cover 2006 (CLC2006) raster data. 100x100m gridded version 16 (04/2012). http://www.eea.europa.eu/data-and-maps/data/corine-land-cover-2006-raster-2

EEA (2013). Air quality in Europe – 2013 report. EEA Report 9/2013. http://acm.eionet.europa.eu/reports/EEA_TR_9_2013_AQinEurope

Eurostat (2013). Total population for European states for 2011. http://epp.eurostat.ec.europa.eu/tgm/table.do?tab=table&language=en&pcode=tps00001&tableSelection=1&footnotes=yes&labeling=labels&plugin=1

EMEP (2013). Transboundary acidification, eutrophication and ground level ozone in Europe in 2011. EMEP Report 1/2013. http://emep.int/publ/reports/2013/EMEP_status_report_1_2013.pdf
Gerharz L, Gräler B, Pebesma E (2011). Measurement artefacts and inhomogeneity detection, ETC/ACM Technical Paper 2011/8. http://acm.eionet.europa.eu/reports/ETCACM_TP_2011_8_artefacts_inhom_detection
Gräler B, Gerharz L, Pebesma E (2012). Spatio-temporal analysis and interpolation of PM_{10} measurements in Europe. ETC/ACM Technical Paper 2011/10. http://acm.eionet.europa.eu/reports/ETCACM_TP_2011_10_spatio-temp_AQinterpolation
Gräler B, Rehr M, Gerharz L, Pebesma E (2013). Spatio-temporal analysis and interpolation of PM10 measurements in Europe for 2009. ETC/ACM Technical Paper 2012/8. http://acm.eionet.europa.eu/reports/ETCACM_2012_8_spatio-temp_PM10analyses
Horálek J, Kurfürst P, Denby B, de Smet P, de Leeuw F, Brabec M, Fiala J (2005). Interpolation and assimilation methods for European scale air quality assessment and mapping. Part II: Development and testing new methodologies. ETC/ACC Technical paper 2005/8. http://acm.eionet.europa.eu/docs/ETCACC_TechnPaper_2005_8_SpatAQ_Part_II.pdf
Horálek J, Denby B, de Smet P, de Leeuw F, Kurfürst P, Swart R, van Noije T (2007). Spatial mapping of air quality for European scale assessment. ETC/ACC Technical paper 2006/6. http://acm.eionet.europa.eu/reports/ETCACC_TechnPaper_2006_6_Spat_AQ
Horálek J, de Smet P, de Leeuw F, Denby B, Kurfürst P, Swart R, (2008). European air quality maps including uncertainty analysis. ETC/ACC Technical paper 2007/7. http://acm.eionet.europa.eu/reports/ETCACC_TP_2007_7_spatAQmaps_ann_interpol
Horálek J, de Smet P, de Leeuw F, Coňková M, Denby B, Kurfürst P (2010). Methodological improvements on interpolating European air quality maps. ETC/ACC Technical Paper 2009/16. http://acm.eionet.europa.eu/reports/ETCACC_TP_2009_16_Improv_SpatAQmapping
Horálek J, de Smet P, Corbet L, Kurfürst P, de Leeuw F (2013). European air quality maps of PM and ozone for 2010 and their uncertainty. ETC/ACM Technical Paper 2012/12. http://acm.eionet.europa.eu/reports/ETCACM_TP_2012_12_spatAQmaps_2010
JRC (2009). Population density disaggregated with Corine land cover 2000. 100x100 m grid resolution, EEA version pop01clcv5.tif of 24 Sep 2009. http://www.eea.europa.eu/data-and-maps/data/population-density-disaggregated-with-corine-land-cover-2000-2
Malherbe L, Ung A, Colette A, Debry E (2012). Formulation and quantification of uncertainties in air quality mapping. ETC/ACM Technical Paper 2001/9. http://air-climate.eionet.europa.eu/reports/ETCACM_TP_2011_9_AQmapping_uncertainties
Mareckova K, Wankmüller R, Moosman L, Pinterits M (2013). Inventory Review 2013. Review of emission data reported under the LRTAP Convention and NEC Directive. Stage 1 and 2 review and review of gridded data. EEA/CEIP Technical Report. http://www.ceip.at/fileadmin/inhalte/emep/pdf/2013/InventoryReport2013_forWeb.pdf
Mol W, van Hooydonk P (2013). The European exchange of information in 2012. ETC/ACM Technical Paper 2013/1. http://acm.eionet.europa.eu/reports/ETCACM_TP_2013_1_EoI_AQ_meta_info2011
NILU (2013). EBAS, database of atmospheric chemical composition and physical properties (NILU, Norway). http://ebas.nilu.no/
ORNL (2008). ORNL LandScan high resolution global population data set. http://www.ornl.gov/sci/landscan/landscan_documentation.shtml
Schneider P, Tarrasón L, Guerreiro C, (2012), The potential of GMES satellite data for mapping nitrogen dioxide at the European scale, ETC/ACM Technical Paper 2012/9. acm.eionet.europa.eu/reports/ETCACM_TP_2012_9_GMESsatdata_NOx_Euromap
Simpson D, Benedictow A, Berge H, Bergstrom R, Emberson LD, Fagerli H, Hayman GD, Gauss M, Jonson JE, Jenkin ME, Nyíri A, Richter C, Semeena VS, Tsyro S, Tuovinen J-P, Valdebenito A, Wind P (2012). The EMEP MSC-W chemical transport model – technical description. Atmospheric Chemistry and Physics, 12, 7825–7865, doi:10.5194/acp-12-7825-2012.
Simpson D, Schulz M, Semeena VS, Tsyro S, Valdebenito Á, Wind P, Steensen BM (2013). Part II Model System Development. In: Transboundary acidification, eutrophication and ground level ozone in Europe in 2011, EMEP Report 1/2013. http://emep.int/publ/reports/2013/EMEP_status_report_1_2013.pdf

Tarrasón L, Horálek J, Malherbe L, Schneider P, Ung A, Denby B, Corbet L, de Smet P (2014). Capabilities of ETC/ACM spatial air quality mapping with the use of Copernicus MACC-II ensemble products *(working title)*. ETC/ACM Technical Paper 2013/9 *(in prep.)*. http://acm.eionet.europa.eu/reports

UNECE (2004). Manual on methodologies and criteria for modelling and mapping critical loads and levels and air pollution effects, risks and trends. UNECE Convention on Long-range Transboundary Air Pollution. http://www.icpmapping.org/Mapping_Manual

UN (2010). World Population Prospects – The 2010 Revision, Highlights. United Nations. Department of Economic and Social Affairs, Population Division. http://esa.un.org/unpd/wpp/index.htm

WHO (2005). WHO Air quality guidelines for particulate matters, ozone, nitrogen dioxide and sulphur dioxide. Global update 2005. http://www.who.int/phe/health_topics/outdoorair/outdoorair_aqg/en/index.html

Annex Recalculated maps of ozone health-related indicators for 2010

During the analysis, it was discovered that during the last year's analysis, the temporal aggregation of the EMEP model data for 2010 (see Horálek et al. 2013, Section 3.2) was not executed correctly in the case of ozone health related indicators. Subsequently, the maps created using these not-correctly aggregated EMEP data (and the exposure tables calculated based on them) were presented in the last year's report (Horálek et al., 2013, Section 6.2 and 6.3).

Therefore, the relevant 2010 maps and exposure tables are recomputed and presented in this Annex, using the correct aggregation of the EMEP modelling data. Next to the maps and tables, also their parameters and uncertainty analysis are included. These maps, tables and analysis are subsequently used for the interannual difference maps and tables presented in Sections 6.2 and 6.3 of this report. All the input data for these recomputed maps are just the same as referred in Horálek et al. (2013), Section 3.

26th highest daily maximum 8-hour average

Figure A.1 presents the recomputed final map for 26th highest daily maximum 8-hour average for 2010. Only small changes occur in comparison with the map shown in Figure 6.1 of Horálek et al. (2013). Some changes visible are in the south-eastern Europe (with a reduced influence of few extreme stations).

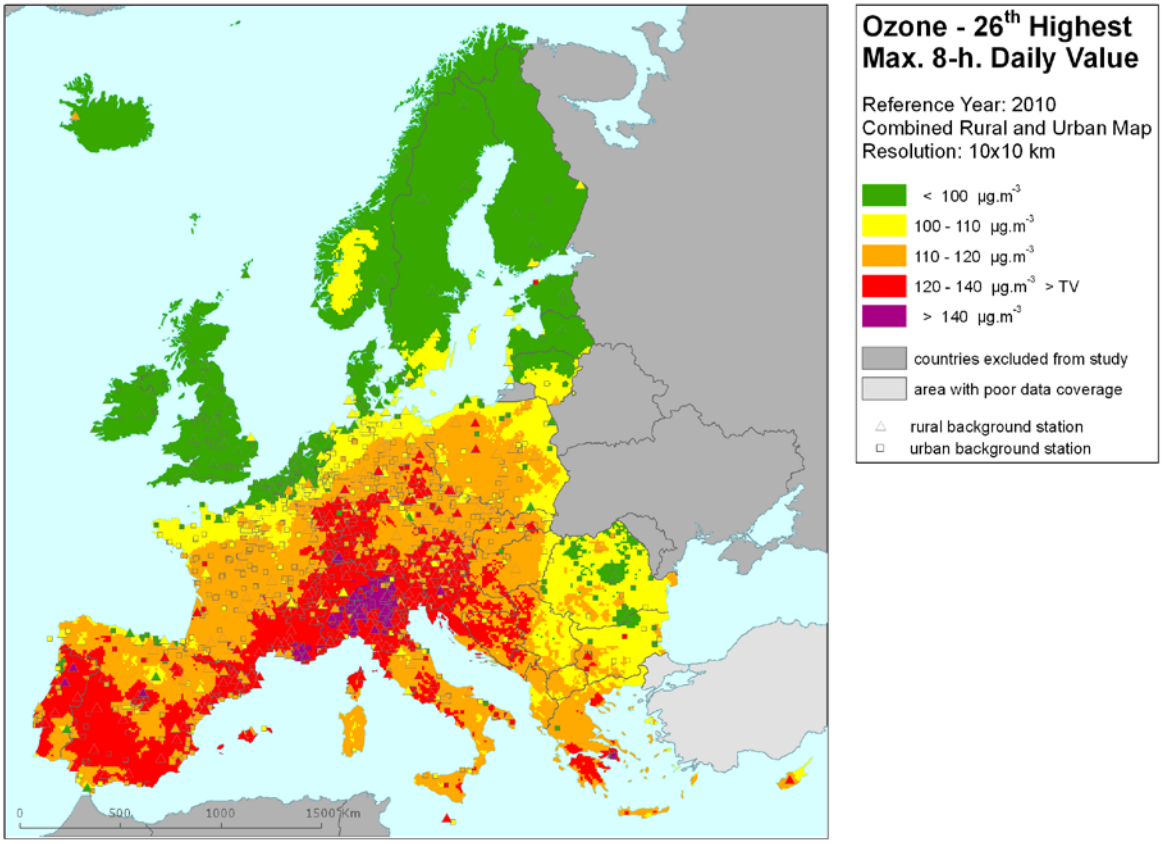

Figure A.1 Combined rural and urban concentration map of ozone health indicator 26th highest daily maximum 8-hour value in µg.m^{-3} for the year 2010. Its target value is 120 µg.m^{-3}. Resolution: 10x10 km. Recomputed map based on correctly aggregated EMEP model data.

Based on the recomputed map, the population frequency distribution for a limited number of exposure classes, as well as the population-weighted concentration for individual countries and for Europe as a whole is presented, see Table A.1.

Table A.1 Population exposure and population weighted concentration – ozone, 26th highest daily maximum 8-hour mean for the year 2010. Recomputed table based on correctly aggregated EMEP model data.

Country		Population	Ozone, 26th highest dmax. 8-h, exposed population [%]					Population-weighted conc.
			< TV			> TV		
		[inhbs . 1000]	< 100 µg.m-3	100 - 110 µg.m-3	110 - 120 µg.m-3	120 - 140 µg.m-3	> 140 µg.m-3	[µg.m-3]
Albania	AL	3 204		63.1	36.9	0.0		109.5
Andorra	AD	85				100		122.4
Austria	AT	8 375			73.2	26.8	0.0	118.4
Belgium	BE	10 840	66.7	30.5	2.9			97.7
Bosnia & Herzegovina	BA	3 760	29.0	32.5	22.0	16.5		107.4
Bulgaria	BG	7 564	17.0	76.9	5.8	0.3		103.8
Croatia	HR	4 426	8.4	13.1	58.2	20.3		114.3
Cyprus	CY	819		50.1	49.9			109.8
Czech Republic	CZ	10 507		3.5	95.6	0.9		114.1
Denmark	DK	5 535	97.3	2.7				91.4
Estonia	EE	1 340	67.2	32.8				97.2
Finland	FI	5 351	100.0	0.0				92.2
France	FR	64 694	10.6	32.4	35.1	21.8	0.1	111.6
Germany	DE	81 802	2.5	33.4	51.0	13.0	0.0	112.8
Greece	GR	11 305	0.1	10.9	45.8	43.2		119.4
Hungary	HU	10 014	6.0	27.2	63.3	3.5		110.9
Iceland	IS	318	100	0.1				78.3
Ireland	IE	4 468	100					85.6
Italy	IT	60 340	0.3	14.3	36.6	32.2	16.6	124.3
Latvia	LV	2 248	98.0	2.0				93.2
Liechtenstein	LI	36				100		123.3
Lithuania	LT	3 329	79.9	20.1				96.9
Luxembourg	LU	502		47.6	49.4	2.9		111.4
Macedonia, FYR of	MK	2 053		81.6	18.4			109.0
Malta	MT	414		82.3	17.0	0.7		109.4
Monaco	MC	35				100		124.0
Montenegro	ME	616	10.9	55.8	28.0	5.3		108.6
Netherlands	NL	16 575	91.1	8.9				90.7
Norway	NO	4 858	98.7	1.3	0.0			88.8
Poland	PL	38 167	15.2	53.0	31.7	0.0		106.6
Portugal	PT	10 638	17.2	16.8	42.8	23.2	0.1	112.0
Romania	RO	21 462	74.0	23.0	3.0	0.0		94.0
San Marino	SM	32			88.4	11.6		116.1
Serbia (incl. Kosovo)	RS	9 856	42.3	41.5	12.1	4.1		102.5
Slovakia	SK	5 425	0.4	20.5	78.1	1.1		112.8
Slovenia	SI	2 047			43.5	56.5	0.0	122.1
Spain	ES	45 989	7.1	11.5	50.6	30.7		115.4
Sweden	SE	9 341	95.5	4.5				91.2
Switzerland	CH	7 786			0.5	95.9	3.6	124.7
United Kingdom	UK	62 027	99.9	0.1	0.0			81.6
Total		**538 185**	**30.3**	**22.3**	**31.0**	**14.4**	**1.9**	**106.8**
			83.7			**16.3**		

Note1: Turkey is not included in the calculation due to lack of air quality data.
Note2: The percentage value "0.0" indicates an exposured population exists, but is small and estimated less than 0.05 %.
Empty cells mean: no population in exposure.

In comparison with the exposure table presented in Horálek et al. (2013), Table 6.1, the population-weighted concentration gives almost the same numbers for the most of the countries and for Europe as a whole. The difference for the whole Europe is 0.1 µg.m^{-3}. For individual countries, the difference does not exceed 0.6 µg.m^{-3}, apart from the countries of the south-eastern Europe and some microstates. (The major difference is 2.8 µg.m^{-3}, in the case of Malta.)

Based on the recomputed concentration map, the relevant uncertainty map (computed together with the concentration map) and the target value (TV) of 120 µg.m^{-3}, the probability of target value exceedance is constructed, see Figure A.2. (Section 4.1.3 explains the significance of the colour classes in the map.) In comparison with the relevant PoE map presented in Horálek et al. (2013), some shifts between the neighbouring classes in limited areas can be seen, namely in Poland (from yellow to green), Hungary (from yellow to orange), Bosnia-Herzegovina (from red to orange) and Greece (from orange to red, from yellow to orange).

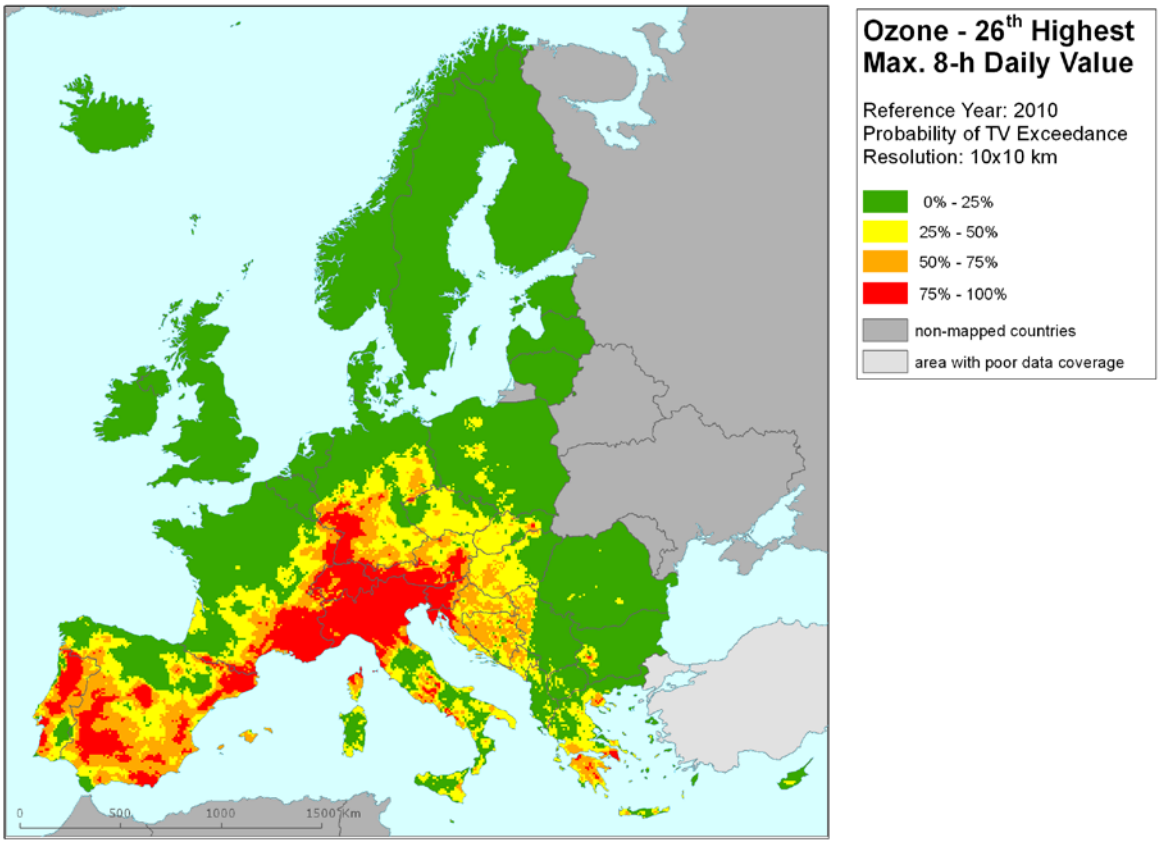

Figure A.2 Map with the probability of the target value exceedance for ozone indicator 26th highest daily maximum 8-hour average (µg.m^{-3}) for 2010 on European scale calculated on the 10 x 10 km grid resolution. Interpolation uncertainty is considered only, no other sources of uncertainty. Recomputed map based on correctly aggregated EMEP model data.

Table A.2 presents the estimated parameters of the linear regression models and of the residual kriging used in the map construction, and the statistical indicators of both the regression and the kriging. In comparison with the indicators presented in Horálek et al. (2013), Table 6.1, almost the same values of R^2 and standard error are shown in both the tables. (The difference does not exceed 0.01 for R^2 and 0.1 µg.m^{-3} for the standard error.)

In the mapping procedure, the same kriging setting as for the relevant maps for 2011 is used for the recomputed maps, which slightly differs from the setting used for the map constructed in Horálek et al. (2013). Namely, the minimum number of the station used for interpolation in rural areas is 15

(while it was 10 in Horálek et al., 2013). This slight change of the setting reduces the influence of the extreme values measured at the stations in the areas poorly covered by the station network. The changes of the concentration level in south-eastern Europe in Figure A.1 in comparison with the one presented in Figure 6.1 of Horálek et al. (2013) are probably related to just this change of the kriging setting.

Table A.2 Parameters of the linear regression models (Eq. 2.2) and of the ordinary kriging variograms (nugget, sill, range) – and their statistics – of ozone indicator 26th highest daily maximum 8-hour mean for 2010 in the rural (left) and urban (right) areas as used for final mapping. Recomputed based on correctly aggregated model.

linear regr. model + OK on its residuals	**rural areas (O.Ear-a)**	**urban areas (UO.Ewr-a)**
	coeff.	**coeff.**
c (constant)	9.8	31.4
a1 (EMEP model 2010)	0.79	0.68
a2 (altitude GTOPO)	0.0068	
a3 (wind speed 2010)		-2.83
a4 (s. solar radiation 2010)	0.99	0.86
adjusted R^2	**0.56**	**0.51**
standard error [µg.m^{-3}]	**10.42**	**11.86**
nugget	35	60
sill	95	93
range [km]	100	250
RMSE [µg.m^{-3}]	**8.92**	**9.18**
bias (MPE) [µg.m^{-3}]	**0.22**	**0.04**

The cross-validation uncertainty expressed by RMSE in µg.m^{-3} can be seen in Table A.2. The relevant relative mean uncertainty of the recomputed 2010 map is 7.7 % for rural areas and 8.2 % for urban areas. The differences with the values presented in Horálek et al. (2013), Section 6.1.3 do not exceed 0.1 µg.m^{-3} for absolute uncertainty (RMSE) and 0.1% for relative uncertainty.

Figure A.3 shows the cross-validation scatter plots for both the rural and urban areas of the 2010 recomputed map. In comparison with the scatterplots of Figure 6.3 in Horálek et al. (2013), the values of R^2 are very similar (the differences do not exceed 0.01).

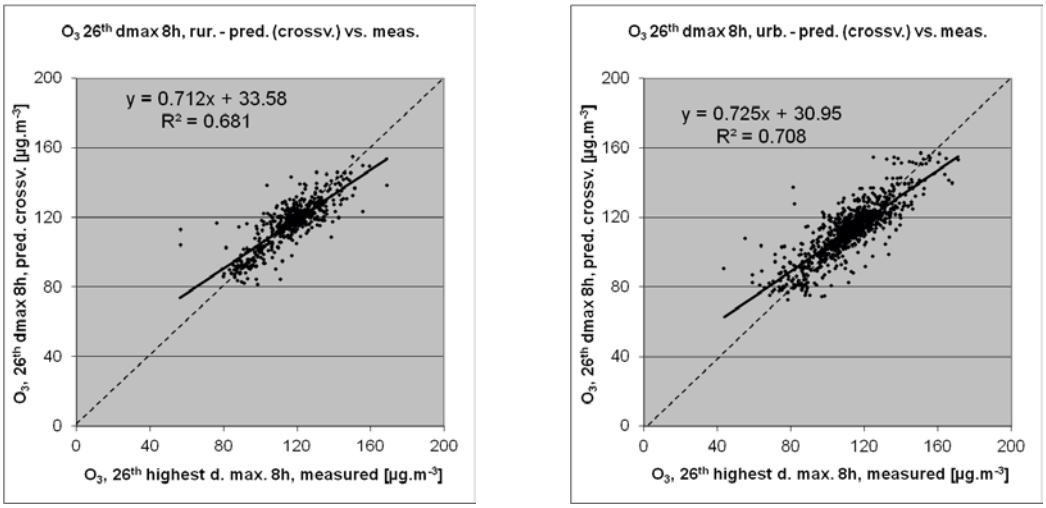

Figure A.3 Correlation between cross-validation predicted values (y-axis) and measurements (x-axis) for the ozone indicator 26th highest daily maximum 8-hour mean for rural (left) and urban (right) areas in 2010.

SOMO35

Figure A.4 presents the recomputed final map for SOMO35 for 2010. The changes in comparison with the map of Figure 6.5 in Horálek et al. (2013) are only minor, and less visible than in the case of 26th highest daily maximum 8-hour average.

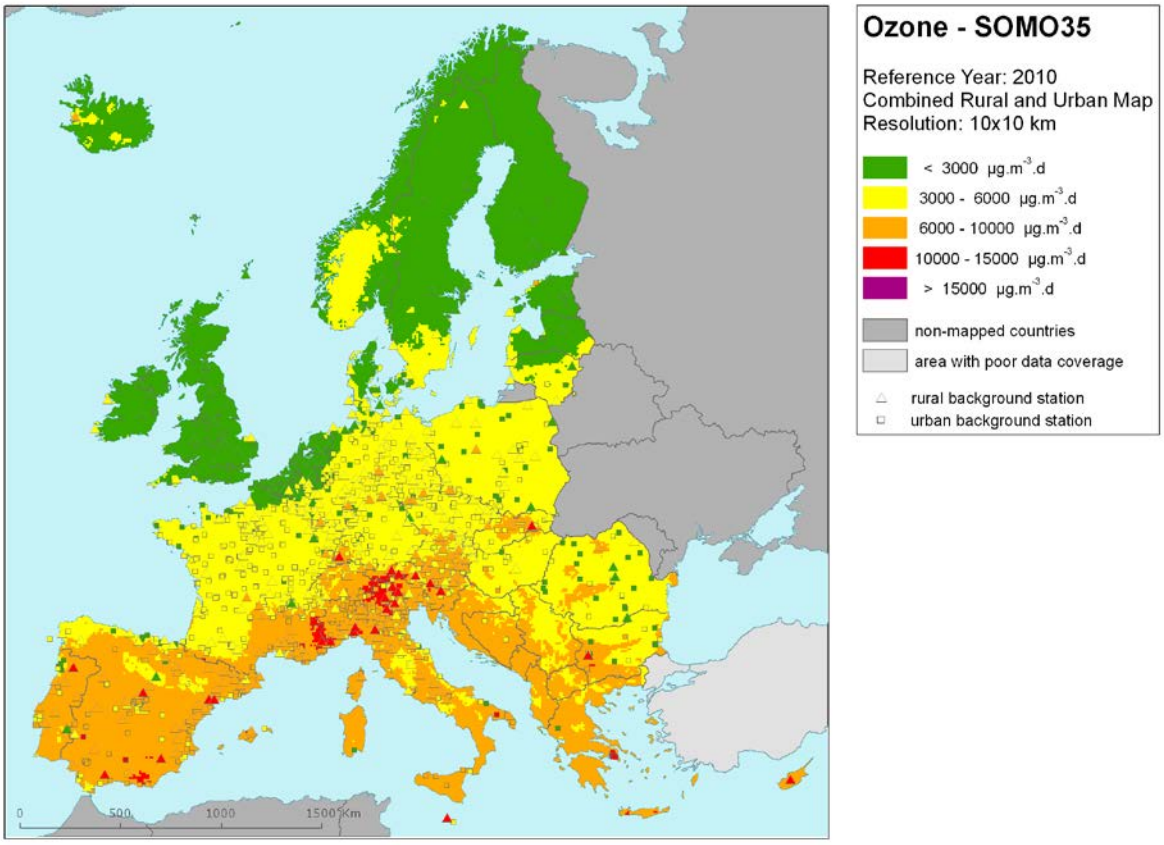

Figure A.4 Combined rural and urban concentration map of ozone indicators SOMO35 in µg.m^{-3}.days for the year 2010. Resolution: 10x10 km. Recomputed map based on correctly aggregated EMEP model data.

Based on the recomputed map, the population frequency distribution for a limited number of exposure classes, as well as the population-weighted concentration for individual countries and for Europe as a whole is presented, see Table A.3. In comparison with the exposure table presented in Horálek et al. (2013), Table 6.6, the population-weighted concentration gives very similar numbers for the most of the countries and for Europe as a whole. The difference for the whole Europe is 2 µg.m^{-3}.d. For individual countries, the difference does not exceed 100 µg.m^{-3}.d, apart from the countries of the south-eastern Europe and some microstates. (The major difference is 359 µg.m^{-3}.d, in the case of Cyprus.)

Table A.4 presents the estimated parameters of the linear regression models and of the residual kriging used in the map construction, and the statistical indicators of both the regression and the kriging. In comparison with the indicators presented in Horálek et al. (2013), Table 6.5, almost the same values of R^2 and standard error are shown in both the tables. (The difference does not exceed 0.05 for R^2 and 10 µg.m^{-3}.d for the standard error.)

In the mapping procedure, the same slight change of the kriging setting is applied at in the case of 26th highest daily maximum 8-hour average. Nevertheless, almost no influence to the concentration levels in visible in the relevant areas (i.e. in the areas poorly covered by the measuring stations).

Table A.3 Population exposure and population-weighted concentration – ozone, SOMO35, year 2010. Recomputed table based on correctly aggregated EMEP model data.

Country		Population	Ozone, SOMO35, exposed population [%]					Population-weighted conc.
			< 3000	3000 - 6000	6000 - 10000	10000 - 15000	> 15000	
		[inhbs.1000]	µg.m^{-3}.d	µg.m^{-3}.d	µg.m^{-3}.d	µg.m^{-3}.d	µg.m^{-3}.d	[µg.m^{-3}.d]
Albania	AL	3 204		67.9	32.1			5 617
Andorra	AD	85			100			7 282
Austria	AT	8 375		87.9	12.0	0.1		4 969
Belgium	BE	10 840	91.6	8.4				2 401
Bosnia & Herzegovina	BA	3 760	8.6	62.4	29.0			4 879
Bulgaria	BG	7 564	2.5	89.1	8.4	0.0		4 377
Croatia	HR	4 426		71.4	28.6			5 419
Cyprus	CY	819			100.0			7 374
Czech Republic	CZ	10 507		99.8	0.2			4 160
Denmark	DK	5 535	90.0	10.0				2 245
Estonia	EE	1 340	65.2	34.8				2 646
Finland	FI	5 351	99.8	0.2				1 925
France	FR	64 694	23.0	63.6	13.3	0.0		4 139
Germany	DE	81 802	14.1	85.6	0.3			3 652
Greece	GR	11 305		13.6	86.4	0.0		7 483
Hungary	HU	10 014	3.4	95.6	0.9			4 408
Iceland	IS	318	98.9	1.1				775
Ireland	IE	4 468	99.2	0.8				1 419
Italy	IT	60 340		38.3	61.4	0.3		6 302
Latvia	LV	2 248	90.9	9.1				2 304
Liechtenstein	LI	36		89.2	10.8			5 244
Lithuania	LT	3 329	71.5	28.5				2 608
Luxembourg	LU	502		100.0				3 505
Macedonia, FYR of	MK	2 053		86.4	13.6			5 081
Malta	MT	414			100.0			6 722
Monaco	MC	35			100			8 028
Montenegro	ME	616		66.9	33.1			5 653
Netherlands	NL	16 575	99.5	0.5				1 916
Norway	NO	4 858	94.7	5.3				1 803
Poland	PL	38 167	38.4	61.5	0.0			3 278
Portugal	PT	10 638	20.3	47.3	32.4	0.0		5 133
Romania	RO	21 462	59.4	39.5	1.1			3 033
San Marino	SM	32		88.4	11.6			5 331
Serbia	RS	9 856	33.7	56.8	9.4			4 001
Slovakia	SK	5 425		93.8	6.2			4 748
Slovenia	SI	2 047		62.5	37.5	0.0		5 998
Spain	ES	45 989	3.4	46.5	50.0	0.1		6 088
Sweden	SE	9 341	92.8	7.2				2 025
Switzerland	CH	7 786		87.1	12.7	0.2		5 127
United Kingdom	UK	62 027	99.3	0.7				1 072
Total		**538 185**	**34.2**	**49.2**	**16.6**	**0.1**	**0**	**3 917**
			83.4		**16.6**			

Note1: Turkey is not included in the calculation due to lacking air quality data.
Note2: The percentage value "0.0" indicates an exposured population exists, but is small and estimated less than 0.05 %. Empty cells mean: no population in exposure.

The cross-validation uncertainty expressed by RMSE in µg.m^{-3} can be seen in Table A.4. The relevant relative mean uncertainty of the recomputed 2010 map is 29.6 % for both rural and urban areas. The differences with the values presented in Horálek et al. (2013), Section 6.2.3 does not exceed 10 µg.m^{-3}.d for absolute uncertainty (RMSE); for relative uncertainty the difference is about 0.1, both for rural and urban areas.

Table A.4 Parameters of the linear regression models (Eq. 2.2) and of the ordinary kriging variograms (nugget, sill, range) - and their statistics - of ozone indicator SOMO35 for 2010 in the rural (left) and urban (right) areas as used for final mapping.

linear regr. model + OK on its residuals	rural areas (O.Ear-a) coeff.	urban areas (UO.Ewr-a) coeff.
c (constant)	-2163	-1912
a1 (EMEP model 2010)	0.46	0.43
a2 (altitude GTOPO)	1.48	
a3 (wind speed 2010)		-18.60
a4 (s. solar radiation 2010)	359.31	288.39
adjusted R^2	**0.59**	**0.54**
standard error [µg.m^{-3}.d]	**1660**	**1459**
nugget	1.6E+06	9.0E+05
sill	2.6E+06	1.4E+06
range [km]	140	210
RMSE [µg.m^{-3}.d]	**1608**	**1278**
bias (MPE) [µg.m^{-3}.d]	**8**	**4**

Figure A.5 shows the cross-validation scatter plots for both the rural and urban areas of the 2010 recomputed map. In comparison with the scatterplots of Figure 6.7 in Horálek et al. (2013), the values of R^2 are very similar (the differences do not exceed 0.005).

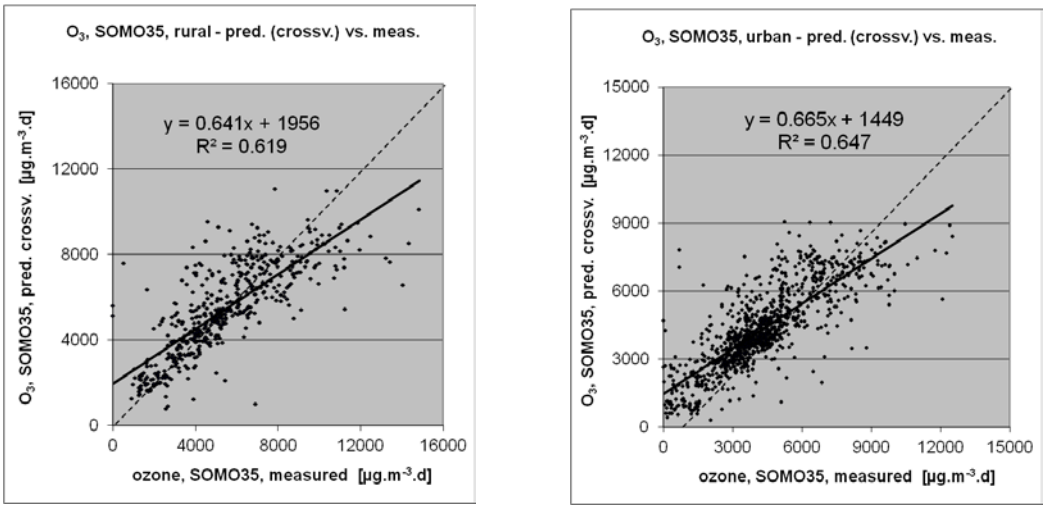

Figure A.5 Correlation between cross-validation predicted values (y-axis) and measurements (x-axis) for the ozone indicator SOMO35 for rural (left) and urban (right) areas in 2010.